UNIVERSITY OF CALIFORNIA, SAN DIEGO

Interactions of p53 and p73 with Human Promoters

A dissertation submitted in partial satisfaction of the requirements for the degree

Doctor of Philosophy

in

Biology

by

Vera Huang

Committee in charge:

Professor Jean Y.J. Wang, Chair
Professor Michael David, Co-Chair
Professor Xiang-Dong Fu
Professor Trey Ideker
Professor Michael G. Rosenfeld
Professor Yang Xu

2007

The Dissertation of Vera Huang is approved, and it is acceptable in quality and form for publication on microfilm:

_____

_____

_____

_____

_____

Co-Chair

_____

Chair

University of California, San Diego

2007

To
My parents, Warren and Juliet Huang,
for their unwavering love and support.

TABLE OF CONTENTS

LIST OF FIGURES

Chapter 1

Chapter2

Chapter 3

LIST OF TABLES

Chapter 2

Chapter 3

ACKNOWLEDGEMENTS

My deepest gratitude to my thesis advisor and mentor, Prof. Jean Wang, for her guidance throughout my graduate career. Special thanks to my bioinformatics mentor and collaborator, Prof. Xin Lu, for sharing his expertise in biostatistics and bioinformatics. This work would be impossible without his contribution. I also thank Prof. Bing Ren for his generous help for getting me started on ChIP-chip.

I would also like to thank my thesis committee members, Prof. Michael David, Prof. Xiang-Dong Fu, Prof. Trey Ideker, Prof. Michael Geof Rosenfeld, and Prof. Yang Xu, for providing helpful suggestions for my thesis project.

Many thanks to my previous undergraduate mentors-Prof. Astar Winoto and Prof. Terry Machen at UC Berkeley, for developing my interests in biological sciences and for giving me the opportunity to conduct undergraduate research.

I thank members of the Wang lab, both past and present, for providing a productive and friendly environment. Thanks to Dr. Yong Jiang, who assisted me with the motif analysis and for performing the gene chip analyses. I also thank all my friends and classmates in San Diego for all their support and friendship. Thanks to my best friend and lab buddy, Hua Jin, for accompanying me through this challenging journey. Special thanks to the elders from El Cerrito Chinese Christian Church and Torrey Pines Christian Church, especially Mr. and Mrs. Chien, and Rev. Mann and Mrs. Mann, for their kindness, caring, and prayers.

I am indebted to my parents whose love, support, and inspiration have made my dreams come true. My dad's "new-born king" spirit has taught me how to keep on going

whenever I encounter hardships in life. I could not have reached where I am without their encouragement.

Chapter 2, in part, has been prepared for publication as appeared in a manuscript, "Interactions of p53 and p73 with Human Promoters." Huang, V., Lu, X., Jiang, Y., and Wang, JYJ. The dissertation author was the primary investigator and author of this manuscript.

Chapter 3, in full, has been prepared for publication as appeared in a manuscript, "Interactions of p53 and p73 with Human Promoters." Huang, V., Lu, X., Jiang, Y., and Wang, JYJ. The dissertation author was the primary investigator and author of this manuscript.

This work was mainly supported by the UCSD School of Medicine training grant, NRSA, NIH.

VITAE

EDUCATION :

University of California, San Diego
Ph.D., Biology, 2007

University of California, Berkeley
B.A. with Honors, Molecular and Cell Biology (MCB), 2000

HONORS AND AWARDS:

2005	EMS Student and New Investigator Travel Award, 9th ICEM conference, San Francisco
2004-2007	UCSD School of Medicine Training Grant
2000	MCB Honors Program, UC Berkeley
1999-2000	Biology Fellows Program, UC Berkeley and Howard Hughes Medical Institute
1998	General scholarship, UC Berkeley

PROFESSIONAL EXPERIENCE:

04/2002 - Present	Graduate Student Division of Biological Sciences University of California, San Diego Principal Investigator: Jean Y.J. Wang, Ph.D.
1/2001-6/2001:	Staff Research Associate Department of Molecular and Cell Biology University of California, Berkeley Principal Investigator: Terry Machen, Ph.D.
12/1999 – 12/2000:	Honors Undergraduate research Department of Molecular and Cell Biology University of California, Berkeley Principal Investigator: Terry Machen, Ph.D.
7/1999-12/1999:	Undergraduate research Department of Molecular and Cell Biology University of California, Berkeley Principal Investigator: Astar Winoto, Ph.D.

TEACHING EXPERIENCE:

Spring 03:	Graduate Student Instructor Division of Biological Sciences University of California, San Diego BIBC 103: Biochemical Techniques
Winter 04	Graduate Student Instructor Division of Biological Sciences University of California, San Diego BIBC 102: Metabolic Biochemistry
Winter 05:	Graduate Student Instructor Division of Biological Sciences University of California, San Diego BIMM 100: Molecular Biology
2004-2005	Undergraduate Research Mentor Division of Biological Sciences University of California, San Diego BISP 199: Undergraduate Research

PUBLICATIONS

Hybiske, K., Ichikawa, J., **Huang, V**., Lory, S., and Machen T. (2004). Cystic Fibrosis airway epithelial cell polarity and bacterial flagellin determine host response to *Pseudomonas aeruginosa.* **Cell Microbiol.** 6(1): 49-63.

Huang, V., Jiang, Y., Lu, X., and Wang, J.Y.J. (2007). Interactions of p53 and p73 with Human Promoters (manuscript in preparation).

CONFERENCE PROCEEDINGS/PRESENTATIONS

Huang, V., Jiang, Y., Lu, X., and Wang, J.Y.J. (2007). Interactions of p53 and p73 with human promoters, Models and Mechanisms of Cancer Meeting, Salk Institute, La Jolla, selected speaker.

Huang, V., Kwon, Y-S., Jiang, Y., Fu, X-D., and Wang, J.Y.J. (2006) "Comparative Analysis of in situ DNA binding sites of p53 and p73 in response to Hydroxyurea " Poster presentation at 46th Annual ASCB meeting, San Diego

Huang, V., Kwon, Y-S., Fu, X-D, and Wang, J.Y.J. (2005) "Analysis of in situ DNA binding sites of p53 and p73 in response to HU" Poster presentation at 9th ICEM conference, San Francisco.

Huang, V., Kwon, Y-S., Fu, X-D, and Wang, J.Y.J. (2005) "Analysis of in situ DNA binding sites of p53 and p73 in response to HU" 4Th Salk Institute Cell Cycle Meeting, La Jolla, selected speaker

Hybiske, K., **Huang, V**., Ichikawa J., Lory, S., and Machen. T. (2001) "Role of Airway Epithelial Cell Polarity in Mediating NFκB-Dependent and –Independent Inflammatory Responses to *P. aeruginosa"* 15th North American Cystic Fibrosis Annual Conference, **Pediatric Pulmonology** 32: S22, 2001

Huang, V., and Machen, T. "*P. aeruginosa*-epithelial host interaction in Cystic Fibrosis" 2000 Fall MCB Honors Poster Session, UC Berkeley

Huang, V., and Winoto, A. "Receptor-mediated apoptosis" 1999 Fall Biology Fellows Program Symposium, UC Berkeley, Howard Hughes Medical Institute.

Huang W., **Huang V**. "Operations Simulation of Human Genetic and Environmental Causes of Aging and Prevention." 1999 Keystone Symposia (Aging: Genetic & Environmental Influences on Life Span)

ABSTRACT OF THE DISSERTATION

Interactions of p53 and p73 with Human Promoters

by

Vera Huang

Doctor of Philosophy in Biology

University of California, San Diego 2007

Professor Jean Y.J. Wang, Chair

Professor Michael David, Co-Chair

The p53 family of transcription factors, p53, p63, and p73, mediates both common and differential biological functions. While p53 has its crucial role in tumor suppression, p63 and p73 have essential functions in embryonic development and differentiation control. This dissertation describes the use of chromatin immunoprecipitation coupled with microarray analysis (ChIP-chip) to study the promoter specificity of p53 and p73. A direct comparison of the promoter occupancy profiles of p53 and p73 was performed in the same cellular context, both at steady state and following hydroxyurea (HU) treatment. As expected, we found that p53 and p73 have overlapping and distinct promoter occupancy and target gene expression profiles under

both conditions. Interestingly, HU appears to alter the promoter occupancy profile of p73 more than that of p53. Moreover, our results demonstrated that p53 and p73 are likely to associate with the same 250 bp genomic region in their overlapping promoters. Expression profiling in cells depleted for both p53 and p73 suggests that ~10% of the p53 and p73 binding sites show p53 and p73- dependent transcriptional effects. Together with our motif analysis, our results suggest that p53 and p73 can also interact indirectly with the promoter-proximal region possibly via protein-protein interactions with other transcription factors.

Chapter 1 introduces the common and differential functions of the p53 family members and summarizes the current high-throughput technologies employed to identify protein-DNA interactions.

Chapter 2 describes a small-scale comparison of p53 and p73 promoter occupancy profiles using the ChIP-DSL technology.

Chapter 3 describes a detailed comparison of p53 and p73 interactions with the promoter-proximal region using ChIP-coupled with the NimbleGen 1.5 kb human promoter arrays. It also introduces a model-based algorithm and other bioinformatics tools for the identification and characterization of the *in vivo* binding sites of p53 and p73. Finally, integration of ChIP-chip data with target gene expression analysis led to the identification of potential direct transcriptional targets of p53 and p73.

Chapter 4 discusses the possible mechanisms by which the p53 family members mediate differential target gene specificity and presents some of the future challenges for ChIP-chip studies.

Chapter 1:
General Introduction

1.1 The p53 Family

The p53 family comprises three highly homologous sequence-specific transcription factors-p53, p63, and p73. p53, known as the "guardian of the genome", is mutated in 50% of human cancers and has been a main focus in cancer research for many decades since its discovery in 1979. p53 was initially discovered as a cellular 55-kd protein capable of interacting with the large-T antigen in SV-40 transformed cells (1, 2). Many lines of evidence have demonstrated that p53 plays a crucial role in response to various forms of cellular stress (i.e. DNA damage and oncogenic stress) to maintain genomic stability by transactivating target genes involved in DNA repair, cell cycle arrest, and apoptosis (3). Surprisingly, these target genes also include noncoding RNAs, as recent findings have identified the miR-34 family (miR-34a and miR34-b/c) to be direct transcriptional targets of p53 (4). However, how p53 affects the decision of these three cellular outcomes is not yet fully understood.

p63 and p73 were discovered as homologues of p53 in the late 1990s. In 1997, the p73 gene was identified through a cDNA library screening and was subsequently mapped to chromosome 1p36, a region frequently deleted in neuroblastoma and other tumor cell lines (5). The p63 gene was independently cloned by several laboratories in 1998 (5, 6). Further characterization showed that p63 is primarily expressed within the ectoderm during early development. Recently, it has been shown that p63 is involved in maintaining stem cell property in stratified epithelia (7).

The overall protein structure of p53 is highly conserved from *Drosophila melanogaster* to man (8). In addition, members of the p53 family share a high sequence identity in their functional domains, including an N-terminal transactivation domain

(TA), a central DNA binding domain (DBD), and a C-terminal oligomerization domain (OD). In particular, the DNA binding domain has the highest conservation among the p53 family members (~65% sequence identity between p53 and p63/p73, and ~85% sequence identity between p63 and p73) (Figure1-1). In addition to these functional domains, p63 and p73 also contain a sterile alpha motif (SAM) domain implicated in protein-protein interactions important for developmental regulation (9, 10). Similar to p53, p63 and p73 can bind to the p53 consensus binding site and transactivate a common set of genes involved in cell-cycle arrest and apoptosis when overexpressed (11, 12).

Another common feature shared between p63 and p73 is the ability to give rise to multiple mRNA isoforms resulting from alternative usage of promoters and alternative splicing, which include transactivating (TA) isoforms and deltaN (ΔN) isoforms lacking the transactivating sequences, and different c-terminal splicing variants. ΔN isoforms (N-terminal truncated isoforms) are generated via alternative usage of an intronic promoter and C-terminal splicing variants are generated by alternative splicing of C-terminal exons and the use of cryptic splice sites. The p73 gene expresses at least seven alternatively spliced C-terminal mRNA isoforms (α,β,γ,δ,ε,ζ,η) and at least four alternatively spliced N-terminal mRNA isoforms. The p63 gene expresses at least three different C-terminal mRNA isoforms (13). ΔN isoforms have dominant-negative roles by antagonizing p53 functions under physiological conditions, for instance, ΔN p73 is an essential anti-apoptotic protein that counteracts the pro-apoptotic function of p53 in sympathetic neurons (14). However, the biological functions of other variants are under investigation.

Alternative splicing of the human p53 gene has been first described by Matlashewski et al. in 1987 (15) and later by Flaman et al. (16) in 1996. These

observations were not fully appreciated until 2005 when Bourdon et al. (13) reported that similar to the p63 and p73 genes, the p53 gene also encodes different p53 mRNA variants, through both the use of alternative splicing and the existence of an internal promoter in intron 4. To date, the p53 gene encodes 12 mRNA variants which can in turn give rise to 9 p53 protein isoforms. (Figure 1-1). p53 isoforms appear to have different subcellular localization and are less abundant than full-length p53 protein. Interestingly, these p53 mRNA isoforms are differentially expressed in breast tumors compared with normal tissues. The interplay between the p53 isoforms and p63/p73 and how it may contribute to tumorigenesis remains to be elucidated.

1.2 Overlapping and differential functions of the p53 family members

Despite a high degree of similarity among the p53 family members, studies have shown that they are involved in different biological processes and that they are not functionally redundant. Clearly, mouse knockout studies suggest that p63 and p73 play differential roles in tissue-specific development. As expected, p53-deficient mice develop normally but are highly prone to spontaneous tumor development in many tissues (primarily lymphomas and sarcomas) by six months of age (17, 18). In contrast to p53 deficient mice, p73 deficient mice do not show increased propensity toward tumor development but exhibit neurological defects, chronic inflammation, and abnormalities in pheromone sensory pathway(19). Moreover, the majority of p73 deficient mice live up to 4 to 6 weeks and die of chronic infection. Strikingly, p63 deficient mice are born alive but exhibit developmental malformations mainly in limb and epithelial structures, suggesting its critical role in ectodermal differentiation during embryogenesis(3). These mice die within a day of birth due to maternal neglect. Similar to p63-null mice,

germline mutations in p63 DNA binding domain in humans are associated with abnormal limb development and implicated in ectodermal dysplasia, ectrodactaly, and cleft palate (EEC) syndrome (20).

No homozygous double or triple compound knockout of the p53 family members have been reported. Nevertheless, overexpression of ΔNp73 has been used as an alternate way to create functional compound knockout mice of the p53 gene family (21, 22). Erster et al. (22) have shown that simultaneous inhibition of all p53 family members by deregulated expression of ΔNp73 causes early embryonic lethality. These results suggest that the p53 family members have distinct but complementary functions in early development.

Although the functions of p63 and p73 in tumor development remain controversial as most human tumors lack mutations or deletions in the p73 locus (11), recent studies have suggested they may cooperate with p53 in tumor suppression. Compound heterozygous $p63^{+/-}p53^{+/-}$ or $p73^{+/-}p53^{+/-}$ mice were found to have higher incidence of tumorigenesis and increased metastatic ability than $p53^{+/-}$ single heterozygous mice. Very recently, it has been shown that combined loss of p73 in a p53-deficient background results in exacerbated polyploidy and aneuploidy than the loss of p53 alone, suggesting that p73 maintains genomic integrity when p53 function is lost (23). The collaborative tumor suppression functions of the p53 family in the context of rhabdomyosarcoma development have been demonstrated. Cam et al. have shown that ablation of the p53 family inhibits Rb-dependent myogenic differentiation program, which in turn leads to malignant transformation in muscle cells (24). Therefore, induction of differentiation program contributes to the tumor suppressor activity of the p53 family.

The collaborative role of the p53 family in p53-dependent apopotosis has been established by Flores et al in which they showed that p63/p73 are required for p53-dependent neuronal apoptosis in irradiated embryos (25). Same requirements also hold true in p53-dependent apoptosis in E1A-expressing mouse embryo fibroblasts (MEFs) treated with doxorubicin. Interestingly, chromatin immunoprecipitation (ChIP) experiments showed that p53 is unable to bind to apoptotic promoters and to upregulate their transcription in the absence of p63 and p73. Theses experiments suggest that the p53 family members may cooperate in p53-dependent apoptosis at the promoter level for a subset of genes. However, the generality of the requirement for p63 and p73 in p53-dependent apoptosis was challenged by Senoo et al. (26) in which they showed that p63 and p73 are dispensable for T-cell development in thymocytes. They also concluded that p63 and p73 are not required for radiation-induced death in immature T cells, which is also a p53-dependent process. These disparate findings together reflect the complexity of cell type specificity and their differential responses to stress. Furthermore, the requirement for p63 and p73 in E1A-transformed MEFs to facilitate p53 function may be a requirement imposed by E1A expression. Thymocytes, however, can undergo p53-dependent apoptosis and do not require p63/p73 in response to irradiation in the absence of E1A.

Although several lines of genetic evidence have suggested the genetic interplay between the p53 family members, the mechanism by which the p53 family members collaborate remains to be elucidated. Early work has shown that p73β, but not p73α, interacted, albeit modestly, with p53 in a yeast two-hybrid screen. (5). Later, biochemical studies have suggested that p63 and p73 can form tetramers with each other but neither

can form hetero-tetramers with p53 (27). More than 90% of the mutations found in p53 are located within the DNA-binding domain, between amino acids 102 and 292. These tumor-derived mutant forms of p53 have been shown to physically interact with p63 or p73 in co-immunoprecipitation experiments (28, 29), but no evidence has demonstrated homotypic interactions between the wild-type proteins. *In vitro* studies have shown that p53 binding affinity has a high on and off rates, thus it is conceivable that p63 and/or p73 may have an indirect interaction with p53 in stabilizing p53/DNA complex. Two models for the cooperation of the p53 family members at the promoter level have been proposed by Urist et al. (30). In the "dynamic exchange model", one of the p53 family members binds to the same response element in a promoter at a given time. Alternatively, the "dual site stabilization model" proposes that the presence of discrete binding sequences in the promoter allows simultaneous binding of the p53 family members to the same promoter, which may be required for the complete recruitment of other transcription co-activators (Figure 1-2). Gel shift experiments have shown that p73α can compete with p53 for the same DNA sequence in an ovarian cancer cell line overexpressing p73 (31). If this were true in other cancer types, p73 might function as an oncogene by attenuating p53 functions in tumors with overexpression of p73. Chapter 3 of this dissertation addresses these two models for the interactions between p53 and p73 at the promoter level.

1.3 High throughput detection of DNA-protein interactions by ChIP-chip

Protein–DNA interactions play a crucial role in many biological processes, such as transcription, replication, and recombination. In the past, biochemical and genetic approaches have been used to study protein–DNA interactions. However, these approaches have a few drawbacks as they are indirect and do not study these interactions

under physiological conditions. Recently, chromatin immunoprecipitation (ChIP) has been widely used to examine DNA-protein interaction under physiological conditions. It can also be used to detect indirect protein-DNA interactions via protein-protein interactions. This method begins by crosslinking protein to DNA with formaldehyde in living cells. Chromatin is then isolated and DNA is fragmented by physical shearing or enzymatic digestion to ~500 bp on average. Immunoprecipitation with an antibody against the protein of interest is used to pull down protein-DNA complex. DNA can be purified after the de-crosslinking step and used for subsequent analysis. If the consensus sequence of a protein-binding site is known, PCR can be used to determine the enrichment of a protein to its associated DNA sequence using primers flanking the specific binding site.

ChIP-based approaches coupled with high-throughput methods have been developed to examine quantitative measurement of protein-DNA interactions at the genome-wide level in an unbiased manner (32, 33) (Figure 1-3). Although highly labor some, ChIP combined with large-scale standard cloning followed by sequencing analysis has been used to isolate E2F binding sites (34). Recent developments of sequencing technologies, such as ChIP pair-end tag sequencing (ChIP-PET), have facilitated the robust and high resolution identification of binding sites for p53 (35), c-myc(36), and stem-cell transcription factors NANOG and OCT4 (35, 37). In recent years, advances in DNA microarray technologies have made possible for high-throughput mapping of transcription factor binding sites to circumvent the time and high cost of sequencing-based approaches.

1.4 Overview of ChIP-chip

ChIP combined with microarray analysis (known as ChIP-chip) was initially developed by Richard Young and colleagues to map transcription regulatory circuitry for almost all sequence-specific transcription factors in yeast (38-40). In recent years, several different microarray platforms containing sequences derived from CpG islands (41, 42)or promoter regions (43, 44), as well as consecutive sequences covering nonrepetitive regions of human chromosomes 21 and 22 (45-48) or the entire human genome sequence (49-51) have been successfully employed to map binding sites for many mammalian transcription factors. To carry out ChIP-chip analysis, ChIP-DNA and input DNA (total genomic DNA control) are amplified, fluorescently labeled with different dyes, and co-hybridized to DNA microarrays. Typically, enrichment is measured by comparing the signals between ChIP-enriched DNA and input DNA. After data normalization, a ratio of the two fluorescence dyes (i.e. cy3/cy5 ratio) is calculated for each DNA spot. An enriched genomic-binding site is identified as having a significantly higher fluorescent intensity in the ChIP-DNA channel than in the input channel (32, 52) (Figure 1-4). Due to the large amount of dataset generated by ChIP-chip experiments, much effort has been devoted to develop mathematical models for the identification of ChIP-enriched regions (53-56).

1.5 Identification of the *in vivo* DNA binding sites of the p53 family of transcription factors

Over the last few years, ChIP-based approaches have been applied to identify *in vivo* DNA binding sites for the p53 family members. The first p53 ChIP-chip performed by Cawley et al. (45) uses ChIP coupled with high-density tiling arrays containing human

chromosomes 21 and 22. Interestingly, 48 high-confidence binding sites were identified and many of which are associated with noncoding RNAs. Extrapolation of their findings predicts a total of 1600 p53 binding sites in the human genome. In 2006, Wei et al.(35) combined ChIP with a paired-end di-tag (PET) SAGE-based strategy to map p53 binding sites at the genome-wide level. In this study, at least 542 binding loci were identified that include a large number of remote sites, suggesting a higher level of p53 transcriptional regulation. Through cross-validation in clinical breast tumor samples, 20 novel targets involved in tumor invasion and metastasis were also identified. The number of binding sites identified by Wei et al. (35) is different from what was extrapolated by Cawley et al. (45), which may well be due to differences in the experimental conditions and methodologies between the two studies, such as the presence of repetitive sequences in the binding sites may attribute to the inherent limitation in the discovery capacity of ChIP-chip technology. Similar technical differences may also attribute to the minimal overlap between these two studies: 3/48 p53 binding sites on chromosomes 21 and 22 identified by Cawley et al.(45) are within the region mapped by CHIP-PET.

Recently, identification of p63 target sites by ChIP-chip analysis using high-density oligonucleotide arrays covering the entire human genome provided additional implications for regulatory mechanisms among the p53 family members (50). In this study, 5807 binding sites at an FDR (false discovery rate) of ~9% were identified for p63 in a human cervical carcinoma cell line. Intriguingly, only ~10% of p63 binding sites are located within 1 kb upstream to 1kb downstream of transcription start site. In other words, p63 may also bind to distal sites far away from annotated genes in a similar manner to p53. Sixty-two of p63-bound sequences overlap with p53 binding sites

identified by Wei et al (35). Again, this small overlap may reflect differences between p53 and p63 and/or differences in the methodologies used in the two studies. Consistent with the phenotypes of the $p63^{-/-}$ mice, p63 targets identified in this study include genes involved in epithelial morphogenesis, stem-cell biology, as well as cell adhesion and communication pathways. Another p63 ChIP-chip study carried out by Viagno et al. (57) has identified novel targets of p63 in ectodermal differentiation.

Identification of the *in vivo* targets of p73 has been carried out primarily by conventional strategies (i.e. expression profiling in cells ectopically expressing p73). These study showed that ectopic p73 can activate expression of genes containing p53-binding sites in their promoters (58)). A study by Fontemaggi et al (59) using expression profiling followed by chromatin immunoprecipitation (ChIP) analyses showed that ectopically expressed p53 and p73 in the same cellular context exhibited partially overlapping transcriptional profile. One caveat is that the targets identified by such approaches can be indirect and/or non-physiologically relevant. To circumvent these issues, this dissertation describes a direct comparison between p53 and p73 binding sites using ChIP-chip.

1.6 p53 family and DNA binding

Typically, p53 transactivates its target genes through binding to two or more tandem repeats of the 10-bp half site PuPuPu CA/TA/TG PyPyPy, separated by 0-13 bases (60). Wei et al has further refined the consensus sequence and has shown that the lengths of the spacers between the two half-sites in the high-probability p53 binding sites identified by ChIP-PET are predominantly zero (35). Several features have shown to be present in strong p53 REs: (1)The presence of highly C and G residues in the cores

sequence; (2)Two half sites are separated by 0-1 bp spacer; (3)No more than 3 mismatches within RE (61). Although it remains unknown whether p73 has a DNA sequence selectivity in binding, *in vitro* studies have shown that p53 and p73 exhibit similar sequence-specific affinity for the p53 response element (62, 63). Interestingly, it has been shown that p63 has a differential recognition element of the p53 response element that may attribute to the target specificity and functional differences between p53 and p63 (64). Several ChIP-chip studies have revealed that the p53 family members can bind to genomic region that are located within a few thousand nucleotides upstream or downstream from the transcription start site. Yang et al. reported that 8% of 5800 p63 binding sites are located within 5kb up stream to 1kb downstream relative to well-characterized genes (50). If these binding sites are functional, it is likely that the p53 family members can modulate expression by functioning as enhancers. In line with this concept, Heintzman et al. (unpublished result) have shown that 24.2% of promoter-distal p53 binding sites in HCT116 cells overlap with enhancer prediction in HeLa cells.

It has been shown that p53 can regulate some transcriptional targets through non-consensus sites, such as PAC1 phosphatase (65). p53 may also bind to non-consensus sites through indirect interactions with other DNA-binding proteins that have previously shown to bind p53, such as EGR1(66), TBP(67) and CREB1(68). Chapter 3 of this dissertation discusses this possibility. Motif search for other transcription factor binding sites combined with computational approaches can be applied to dissect the cis-regulatory modules mediated by p53 and its family members. Understanding the transcriptional regulation mediated by the p53 family may be instrumental to the improvement of the efficacy of p53-based cancer therapeutics.

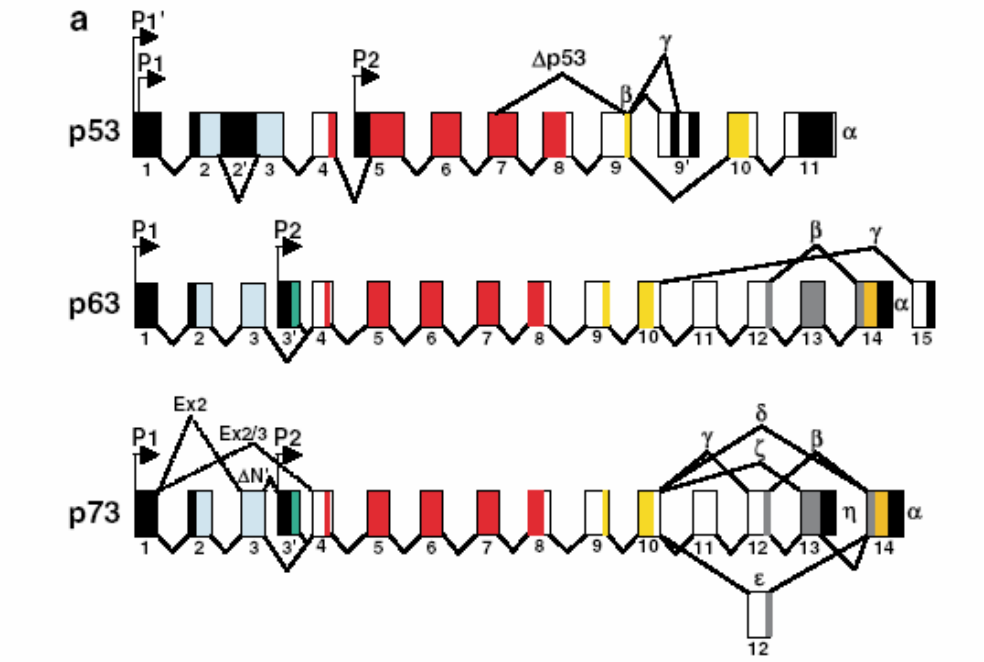

Figure 1-1. Gene structure of the p53 family members
The p53 family members share a high sequence identity in their N-terminal transactivation domain (light blue), DNA binding domain (red), and C-terminal oligomerization domain (yellow). Alternative splicing variants are represented by solid lines. Each numbered box represents an exon.

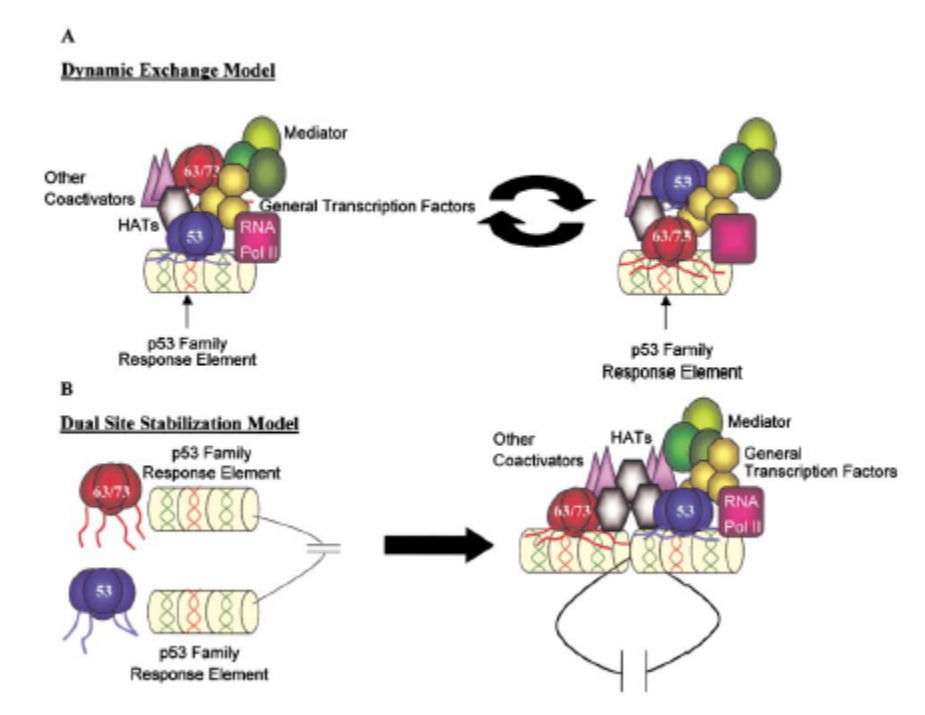

Figure 1-2. Two models for the interactions of the p53 family members at the promoter level (30)
(A)In the "Dynamic Exchange Model", p63 and/or p73 indirectly interact with p53 in a large transcriptional complex in which either p53 or a sibling may bind to the promoter element at a given time. (B) In the "Dual Site Stabilization Model", p53 and one of its family members bind to discrete regions within a single promoter, which is required for the complete recruitment of transcriptional machinery.

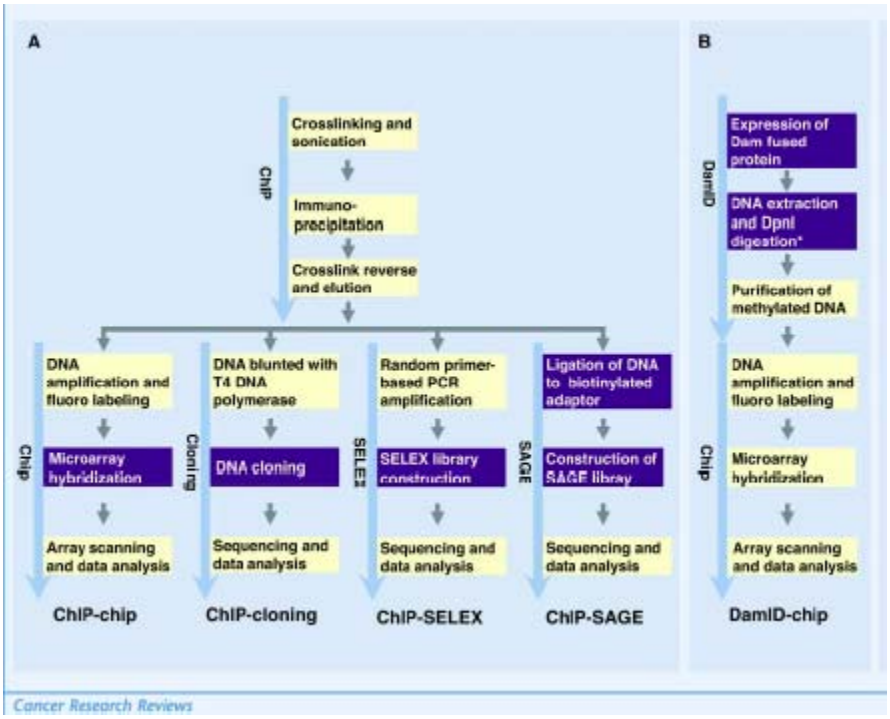

Figure 1-3. ChIP-based technologies for studying DNA-protein interactions (33)
(A,B) Comparison of ChIP-chip with other currently available high-throughput approaches for the identification of DNA-protein interactions.

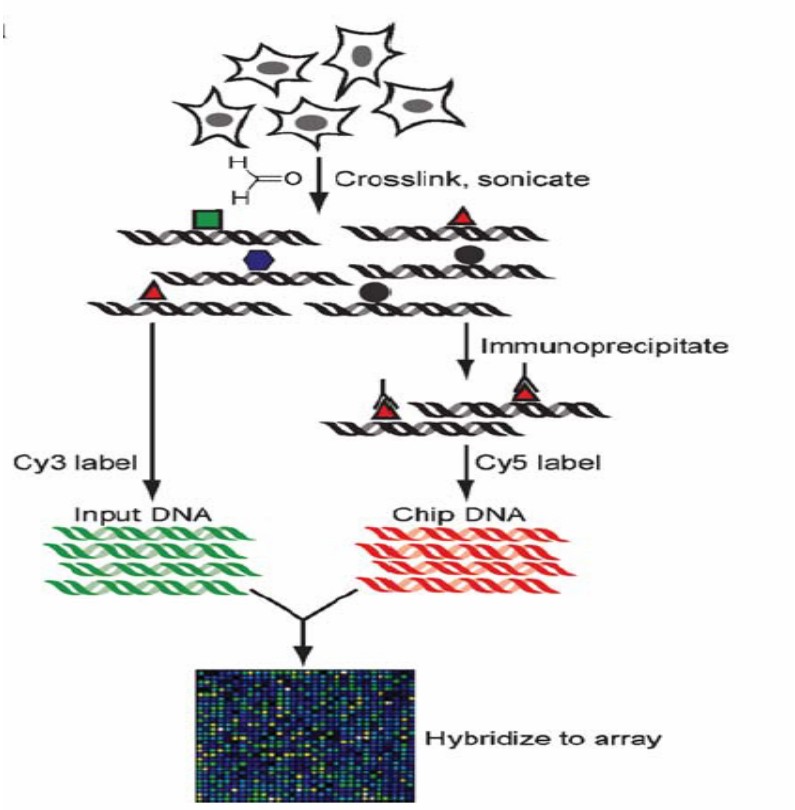

Figure 1-4. Overview of ChIP-chip technology (69)
ChIP-chip begins with the standard ChIP procedure in which protein-DNA and/or protein-protein are crosslinked with formaldehyde in living cells. Chromatin is then isolated and DNA is sonicated. Specific DNA sequences associated with a protein are isolated by immunoprecipitation using an antibody against the protein of interest. DNA can be purified after the de-crosslinking step and is subsequently amplified, labeled with a fluorescent dye, and hybridized to DNA microarrays containing genomic sequences.

1.7 References

1. Lane, D. P., and Crawford, L. V. (1979) T antigen is bound to a host protein in SV40-transformed cells. *Nature* 278, 261-263

2. Linzer, D. I., and Levine, A. J. (1979) Characterization of a 54K dalton cellular SV40 tumor antigen present in SV40-transformed cells and uninfected embryonal carcinoma cells. *Cell* 17, 43-52

3. Harms, K., Nozell, S., and Chen, X. (2004) The common and distinct target genes of the p53 family transcription factors. *Cell Mol Life Sci* 61, 822-842

4. He, L., He, X., Lowe, S. W., and Hannon, G. J. (2007) microRNAs join the p53 network--another piece in the tumour-suppression puzzle. *Nat Rev Cancer* 7, 819-822

5. Kaghad, M., Bonnet, H., Yang, A., Creancier, L., Biscan, J. C., Valent, A., Minty, A., Chalon, P., Lelias, J. M., Dumont, X., Ferrara, P., McKeon, F., and Caput, D. (1997) Monoallelically expressed gene related to p53 at 1p36, a region frequently deleted in neuroblastoma and other human cancers. *Cell* 90, 809-819

6. Yang, A., Kaghad, M., Wang, Y., Gillett, E., Fleming, M. D., Dotsch, V., Andrews, N. C., Caput, D., and McKeon, F. (1998) p63, a p53 homolog at 3q27-29, encodes multiple products with transactivating, death-inducing, and dominant-negative activities. *Mol Cell* 2, 305-316

7. Senoo, M., Pinto, F., Crum, C. P., and McKeon, F. (2007) p63 Is Essential for the Proliferative Potential of Stem Cells in Stratified Epithelia. *Cell* 129, 523-536

8. Jin, S., Martinek, S., Joo, W. S., Wortman, J. R., Mirkovic, N., Sali, A., Yandell, M. D., Pavletich, N. P., Young, M. W., and Levine, A. J. (2000) Identification and characterization of a p53 homologue in Drosophila melanogaster. *Proc Natl Acad Sci U S A* 97, 7301-7306

9. Chi, S. W., Ayed, A., and Arrowsmith, C. H. (1999) Solution structure of a conserved C-terminal domain of p73 with structural homology to the SAM domain. *Embo J* 18, 4438-4445

10. Thanos, C. D., and Bowie, J. U. (1999) p53 Family members p63 and p73 are SAM domain-containing proteins. *Protein Sci* 8, 1708-1710

11. Melino, G., De Laurenzi, V., and Vousden, K. H. (2002) p73: Friend or foe in tumorigenesis. *Nat Rev Cancer* 2, 605-615

12. Jost, C. A., Marin, M. C., and Kaelin, W. G., Jr. (1997) p73 is a simian [correction of human] p53-related protein that can induce apoptosis. *Nature* 389, 191-194

13. Bourdon, J. C., Fernandes, K., Murray-Zmijewski, F., Liu, G., Diot, A., Xirodimas, D. P., Saville, M. K., and Lane, D. P. (2005) p53 isoforms can regulate p53 transcriptional activity. *Genes Dev* 19, 2122-2137

14. Pozniak, C. D., Radinovic, S., Yang, A., McKeon, F., Kaplan, D. R., and Miller, F. D. (2000) An anti-apoptotic role for the p53 family member, p73, during developmental neuron death. *Science* 289, 304-306

15. Matlashewski, G., Pim, D., Banks, L., and Crawford, L. (1987) Alternative splicing of human p53 transcripts. *Oncogene Res* 1, 77-85

16. Flaman, J. M., Waridel, F., Estreicher, A., Vannier, A., Limacher, J. M., Gilbert, D., Iggo, R., and Frebourg, T. (1996) The human tumour suppressor gene p53 is alternatively spliced in normal cells. *Oncogene* 12, 813-818

17. Donehower, L. A., Harvey, M., Slagle, B. L., McArthur, M. J., Montgomery, C. A., Jr., Butel, J. S., and Bradley, A. (1992) Mice deficient for p53 are developmentally normal but susceptible to spontaneous tumours. *Nature* 356, 215-221

18. Jacks, T., Remington, L., Williams, B. O., Schmitt, E. M., Halachmi, S., Bronson, R. T., and Weinberg, R. A. (1994) Tumor spectrum analysis in p53-mutant mice. *Curr Biol* 4, 1-7

19. Yang, A., Walker, N., Bronson, R., Kaghad, M., Oosterwegel, M., Bonnin, J., Vagner, C., Bonnet, H., Dikkes, P., Sharpe, A., McKeon, F., and Caput, D. (2000) p73-deficient mice have neurological, pheromonal and inflammatory defects but lack spontaneous tumours. *Nature* 404, 99-103

20. van Bokhoven, H., and McKeon, F. (2002) Mutations in the p53 homolog p63: allele-specific developmental syndromes in humans. *Trends Mol Med* 8, 133-139

21. Huttinger-Kirchhof, N., Cam, H., Griesmann, H., Hofmann, L., Beitzinger, M., and Stiewe, T. (2006) The p53 family inhibitor DeltaNp73 interferes with multiple developmental programs. *Cell Death Differ* 13, 174-177

22. Erster, S., Palacios, G., Rosenquist, T., Chang, C., and Moll, U. M. (2006) Deregulated expression of DeltaNp73alpha causes early embryonic lethality. *Cell Death Differ* 13, 170-173

23. Talos, F., Nemajerova, A., Flores, E. R., Petrenko, O., and Moll, U. M. (2007) p73 suppresses polyploidy and aneuploidy in the absence of functional p53. *Mol Cell* 27, 647-659

24. Cam, H., Griesmann, H., Beitzinger, M., Hofmann, L., Beinoraviciute-Kellner, R., Sauer, M., Huttinger-Kirchhof, N., Oswald, C., Friedl, P., Gattenlohner, S., Burek, C., Rosenwald, A., and Stiewe, T. (2006) p53 family members in myogenic differentiation and rhabdomyosarcoma development. *Cancer Cell* 10, 281-293

25. Flores, E. R., Tsai, K. Y., Crowley, D., Sengupta, S., Yang, A., McKeon, F., and Jacks, T. (2002) p63 and p73 are required for p53-dependent apoptosis in response to DNA damage. *Nature* 416, 560-564

26. Senoo, M., Manis, J. P., Alt, F. W., and McKeon, F. (2004) p63 and p73 are not required for the development and p53-dependent apoptosis of T cells. *Cancer Cell* 6, 85-89

27. Davison, T. S., Vagner, C., Kaghad, M., Ayed, A., Caput, D., and Arrowsmith, C. H. (1999) p73 and p63 are homotetramers capable of weak heterotypic interactions with each other but not with p53. *J Biol Chem* 274, 18709-18714

28. Di Como, C. J., Gaiddon, C., and Prives, C. (1999) p73 function is inhibited by tumor-derived p53 mutants in mammalian cells. *Mol Cell Biol* 19, 1438-1449

29. Strano, S., Fontemaggi, G., Costanzo, A., Rizzo, M. G., Monti, O., Baccarini, A., Del Sal, G., Levrero, M., Sacchi, A., Oren, M., and Blandino, G. (2002) Physical interaction with human tumor-derived p53 mutants inhibits p63 activities. *J Biol Chem* 277, 18817-18826

30. Urist, M., and Prives, C. (2002) p53 leans on its siblings. *Cancer Cell* 1, 311-313

31. Vikhanskaya, F., D'Incalci, M., and Broggini, M. (2000) p73 competes with p53 and attenuates its response in a human ovarian cancer cell line. *Nucleic Acids Res* 28, 513-519

32. Elnitski, L., Jin, V. X., Farnham, P. J., and Jones, S. J. (2006) Locating mammalian transcription factor binding sites: a survey of computational and experimental techniques. *Genome Res* 16, 1455-1464

33. Wu, J., Smith, L. T., Plass, C., and Huang, T. H. (2006) ChIP-chip comes of age for genome-wide functional analysis. *Cancer Res* 66, 6899-6902

34. Weinmann, A. S., Bartley, S. M., Zhang, T., Zhang, M. Q., and Farnham, P. J. (2001) Use of chromatin immunoprecipitation to clone novel E2F target promoters. *Mol Cell Biol* 21, 6820-6832

35. Wei, C. L., Wu, Q., Vega, V. B., Chiu, K. P., Ng, P., Zhang, T., Shahab, A., Yong, H. C., Fu, Y., Weng, Z., Liu, J., Zhao, X. D., Chew, J. L., Lee, Y. L., Kuznetsov, V. A., Sung, W. K., Miller, L. D., Lim, B., Liu, E. T., Yu, Q., Ng, H. H., and Ruan, Y. (2006) A global map of p53 transcription-factor binding sites in the human genome. *Cell* 124, 207-219

36. Zeller, K. I., Zhao, X., Lee, C. W., Chiu, K. P., Yao, F., Yustein, J. T., Ooi, H. S., Orlov, Y. L., Shahab, A., Yong, H. C., Fu, Y., Weng, Z., Kuznetsov, V. A., Sung, W. K., Ruan, Y., Dang, C. V., and Wei, C. L. (2006) Global mapping of c-Myc binding sites and target gene networks in human B cells. *Proc Natl Acad Sci U S A* 103, 17834-17839

37. Loh, Y. H., Wu, Q., Chew, J. L., Vega, V. B., Zhang, W., Chen, X., Bourque, G., George, J., Leong, B., Liu, J., Wong, K. Y., Sung, K. W., Lee, C. W., Zhao, X.

D., Chiu, K. P., Lipovich, L., Kuznetsov, V. A., Robson, P., Stanton, L. W., Wei, C. L., Ruan, Y., Lim, B., and Ng, H. H. (2006) The Oct4 and Nanog transcription network regulates pluripotency in mouse embryonic stem cells. *Nat Genet* 38, 431-440

38. Lee, T. I., Rinaldi, N. J., Robert, F., Odom, D. T., Bar-Joseph, Z., Gerber, G. K., Hannett, N. M., Harbison, C. T., Thompson, C. M., Simon, I., Zeitlinger, J., Jennings, E. G., Murray, H. L., Gordon, D. B., Ren, B., Wyrick, J. J., Tagne, J. B., Volkert, T. L., Fraenkel, E., Gifford, D. K., and Young, R. A. (2002) Transcriptional regulatory networks in Saccharomyces cerevisiae. *Science* 298, 799-804

39. Harbison, C. T., Gordon, D. B., Lee, T. I., Rinaldi, N. J., Macisaac, K. D., Danford, T. W., Hannett, N. M., Tagne, J. B., Reynolds, D. B., Yoo, J., Jennings, E. G., Zeitlinger, J., Pokholok, D. K., Kellis, M., Rolfe, P. A., Takusagawa, K. T., Lander, E. S., Gifford, D. K., Fraenkel, E., and Young, R. A. (2004) Transcriptional regulatory code of a eukaryotic genome. *Nature* 431, 99-104

40. Borneman, A. R., Leigh-Bell, J. A., Yu, H., Bertone, P., Gerstein, M., and Snyder, M. (2006) Target hub proteins serve as master regulators of development in yeast. *Genes Dev* 20, 435-448

41. Cheng, A. S., Jin, V. X., Fan, M., Smith, L. T., Liyanarachchi, S., Yan, P. S., Leu, Y. W., Chan, M. W., Plass, C., Nephew, K. P., Davuluri, R. V., and Huang, T. H. (2006) Combinatorial analysis of transcription factor partners reveals recruitment of c-MYC to estrogen receptor-alpha responsive promoters. *Mol Cell* 21, 393-404

42. Weinmann, A. S., Yan, P. S., Oberley, M. J., Huang, T. H., and Farnham, P. J. (2002) Isolating human transcription factor targets by coupling chromatin immunoprecipitation and CpG island microarray analysis. *Genes Dev* 16, 235-244

43. Li, Z., Van Calcar, S., Qu, C., Cavenee, W. K., Zhang, M. Q., and Ren, B. (2003) A global transcriptional regulatory role for c-Myc in Burkitt's lymphoma cells. *Proc Natl Acad Sci U S A* 100, 8164-8169

44. Ren, B., Cam, H., Takahashi, Y., Volkert, T., Terragni, J., Young, R. A., and Dynlacht, B. D. (2002) E2F integrates cell cycle progression with DNA repair, replication, and G(2)/M checkpoints. *Genes Dev* 16, 245-256

45. Cawley, S., Bekiranov, S., Ng, H. H., Kapranov, P., Sekinger, E. A., Kampa, D., Piccolboni, A., Sementchenko, V., Cheng, J., Williams, A. J., Wheeler, R., Wong, B., Drenkow, J., Yamanaka, M., Patel, S., Brubaker, S., Tammana, H., Helt, G., Struhl, K., and Gingeras, T. R. (2004) Unbiased mapping of transcription factor binding sites along human chromosomes 21 and 22 points to widespread regulation of noncoding RNAs. *Cell* 116, 499-509

46. Euskirchen, G., Royce, T. E., Bertone, P., Martone, R., Rinn, J. L., Nelson, F. K., Sayward, F., Luscombe, N. M., Miller, P., Gerstein, M., Weissman, S., and Snyder, M. (2004) CREB binds to multiple loci on human chromosome 22. *Mol Cell Biol* 24, 3804-3814

47. Martone, R., Euskirchen, G., Bertone, P., Hartman, S., Royce, T. E., Luscombe, N. M., Rinn, J. L., Nelson, F. K., Miller, P., Gerstein, M., Weissman, S., and Snyder, M. (2003) Distribution of NF-kappaB-binding sites across human chromosome 22. *Proc Natl Acad Sci U S A* 100, 12247-12252

48. Carroll, J. S., Liu, X. S., Brodsky, A. S., Li, W., Meyer, C. A., Szary, A. J., Eeckhoute, J., Shao, W., Hestermann, E. V., Geistlinger, T. R., Fox, E. A., Silver, P. A., and Brown, M. (2005) Chromosome-wide mapping of estrogen receptor binding reveals long-range regulation requiring the forkhead protein FoxA1. *Cell* 122, 33-43

49. Carroll, J. S., Meyer, C. A., Song, J., Li, W., Geistlinger, T. R., Eeckhoute, J., Brodsky, A. S., Keeton, E. K., Fertuck, K. C., Hall, G. F., Wang, Q., Bekiranov, S., Sementchenko, V., Fox, E. A., Silver, P. A., Gingeras, T. R., Liu, X. S., and Brown, M. (2006) Genome-wide analysis of estrogen receptor binding sites. *Nat Genet* 38, 1289-1297

50. Yang, A., Zhu, Z., Kapranov, P., McKeon, F., Church, G. M., Gingeras, T. R., and Struhl, K. (2006) Relationships between p63 binding, DNA sequence, transcription activity, and biological function in human cells. *Mol Cell* 24, 593-602

51. Kim, T. H., Abdullaev, Z. K., Smith, A. D., Ching, K. A., Loukinov, D. I., Green, R. D., Zhang, M. Q., Lobanenkov, V. V., and Ren, B. (2007) Analysis of the Vertebrate Insulator Protein CTCF-Binding Sites in the Human Genome. *Cell* 128, 1231-1245

52. Kim, T. H., and Ren, B. (2006) Genome-Wide Analysis of Protein-DNA Interactions. *Annu Rev Genomics Hum Genet* 7, 81-102

53. Buck, M. J., and Lieb, J. D. (2004) ChIP-chip: considerations for the design, analysis, and application of genome-wide chromatin immunoprecipitation experiments. *Genomics* 83, 349-360

54. Buck, M. J., Nobel, A. B., and Lieb, J. D. (2005) ChIPOTle: a user-friendly tool for the analysis of ChIP-chip data. *Genome Biol* 6, R97

55. Johnson, W. E., Li, W., Meyer, C. A., Gottardo, R., Carroll, J. S., Brown, M., and Liu, X. S. (2006) Model-based analysis of tiling-arrays for ChIP-chip. *Proc Natl Acad Sci U S A* 103, 12457-12462

56. Kim, T. H., Barrera, L. O., Zheng, M., Qu, C., Singer, M. A., Richmond, T. A., Wu, Y., Green, R. D., and Ren, B. (2005) A high-resolution map of active promoters in the human genome. *Nature* 436, 876-880

57. Vigano, M. A., Lamartine, J., Testoni, B., Merico, D., Alotto, D., Castagnoli, C., Robert, A., Candi, E., Melino, G., Gidrol, X., and Mantovani, R. (2006) New p63 targets in keratinocytes identified by a genome-wide approach. *Embo J* 25, 5105-5116

58. Zhu, J., Jiang, J., Zhou, W., and Chen, X. (1998) The potential tumor suppressor p73 differentially regulates cellular p53 target genes. *Cancer Res* 58, 5061-5065

59. Fontemaggi, G., Kela, I., Amariglio, N., Rechavi, G., Krishnamurthy, J., Strano, S., Sacchi, A., Givol, D., and Blandino, G. (2002) Identification of direct p73 target genes combining DNA microarray and chromatin immunoprecipitation analyses. *J Biol Chem* 277, 43359-43368

60. el-Deiry, W. S., Kern, S. E., Pietenpol, J. A., Kinzler, K. W., and Vogelstein, B. (1992) Definition of a consensus binding site for p53. *Nat Genet* 1, 45-49

61. Tomso, D. J., Inga, A., Menendez, D., Pittman, G. S., Campbell, M. R., Storici, F., Bell, D. A., and Resnick, M. A. (2005) Functionally distinct polymorphic sequences in the human genome that are targets for p53 transactivation. *Proc Natl Acad Sci U S A* 102, 6431-6436

62. Lokshin, M., Li, Y., Gaiddon, C., and Prives, C. (2007) p53 and p73 display common and distinct requirements for sequence specific binding to DNA. *Nucleic Acids Res* 35, 340-352

63. Mondal, N., and Parvin, J. D. (2005) The tumor suppressor protein p53 functions similarly to p63 and p73 in activating transcription in vitro. *Cancer Biol Ther* 4, 414-418

64. Osada, M., Park, H. L., Nagakawa, Y., Yamashita, K., Fomenkov, A., Kim, M. S., Wu, G., Nomoto, S., Trink, B., and Sidransky, D. (2005) Differential recognition of response elements determines target gene specificity for p53 and p63. *Mol Cell Biol* 25, 6077-6089

65. Yin, Y., Liu, Y. X., Jin, Y. J., Hall, E. J., and Barrett, J. C. (2003) PAC1 phosphatase is a transcription target of p53 in signalling apoptosis and growth suppression. *Nature* 422, 527-531

66. Liu, J., Grogan, L., Nau, M. M., Allegra, C. J., Chu, E., and Wright, J. J. (2001) Physical interaction between p53 and primary response gene Egr-1. *Int J Oncol* 18, 863-870

67. Martin, D. W., Munoz, R. M., Subler, M. A., and Deb, S. (1993) p53 binds to the TATA-binding protein-TATA complex. *J Biol Chem* 268, 13062-13067

68. Van Orden, K., Giebler, H. A., Lemasson, I., Gonzales, M., and Nyborg, J. K. (1999) Binding of p53 to the KIX domain of CREB binding protein. A potential link to human T-cell leukemia virus, type I-associated leukemogenesis. *J Biol Chem* 274, 26321-26328

69. Ren, B., Robert, F., Wyrick, J. J., Aparicio, O., Jennings, E. G., Simon, I., Zeitlinger, J., Schreiber, J., Hannett, N., Kanin, E., Volkert, T. L., Wilson, C. J., Bell, S. P., and Young, R. A. (2000) Genome-wide location and function of DNA binding proteins. *Science* 290, 2306-2309

Chapter 2:
Analysis of *in vivo* DNA binding sites of p53 and p73 by ChIP-DSL

2.1 Abstract

Genotoxic agents activate the p53-family of transcription factors to regulate DNA damage repair, cell cycle checkpoints and cell death. The three members of the p53-family p53, p63 and p73 share a significant identity in the DNA binding domain and can regulate common genes. However, mouse knock-out studies suggest that p63 and p73 play different roles than p53 during development. In this study, we compared the promoter occupancy profiles of p53 and p73 in a human colorectal cancer cell line. We examined the *in vivo* DNA binding sites of p53 and p73 using chromatin immunoprecipitation (ChIP) and oligonucleotide-based microarray analysis, or ChIP-DSL technology. Analysis was performed under steady state conditions and after exposure to HU, which caused a three-fold increase in the levels of p53 and p73 protein. Of the ~2000 human promoters surveyed, we found 166 and 253 binding sites that are constitutively occupied by p53 and p73, respectively. Among them, 112 are occupied by both p53 and p73. Interestingly, p53 and p73 show differential occupancy profiles following HU treatment, in which only 17 binding sites are common between p53 and p73. Our results suggest that p53 and p73 constitutively co-occupy a large number of binding sites in the absence of DNA damage. p53 and p73 share a smaller set of binding sites following HU treatment. Taken together, these findings support the mouse genetic studies that p53 and p73 have overlapping as well as non-redundant functions. Furthermore, the non-overlapping promoter occupancy profiles of p53 and p73 in HU-treated cells imply that these related transcription factors might regulate distinct biological responses to genotoxic stress.

2.2 Introduction

The three members of the p53-family p53, p63 and p73, encode sequence-specific transcription factors that regulate genes involved in DNA repair, cell cycle checkpoints, and apoptosis in response to cellular stress (1). Despite a high degree of similarity in their functional domains, phenotypic defects of the p53, p63 and p73 knockout mice suggest that they regulate distinct sets of genes. In contrast to p53 deficient mice, which are predisposed to early cancer development(2), mice with loss of p63 and p73 have profound defects in their epithelial and neuronal development, respectively (3, 4). A more recent genetic study has shown that $p53^{+/-}p63^{+/-}$ or $p53^{+/-}p73^{+/-}$ double heterozygous mice have a higher tumor burden than $p53^{+/-}$ single heterozygous mice, suggesting a collaborative role for the p53 family in tumor suppression (5). Taken together, these genetic data suggest that p53, p63, and p73 do not simply function as redundant transcription factors, but may regulate distinct sets of genes depending upon cellular context.

To further understand the biological functions of p53 and p73, we used an optimized ChIP-chip technology, ChIP-DSL (6, 7), to compare the promoter occupancy profiles of endogenous p53 and p73 at steady state an following hydroxyurea (HU) treatment. Our findings suggest that p53 and p73 co-occupy a large set of binding sites under steady state, and that p53 and p73 exhibit differential occupancy profiles following HU treatment. Based on our ChIP-DSL study, our findings support the genetic data that p53 and p73 can mediate both common and unique functions. Identification of novel targets by this approach may help to decipher the molecular mechanisms underlying the phenotypes caused by p53 or p73 deficiency.

2.3 Materials and Methods

Cell culture and drug treatment

HCT116-3(6) human colorectal cancer cells (ATCC) were grown in high-glucose (4.5-g/liter) Dulbecco's modified Eagle medium (CellGro) supplemented with penicillin G (100 U/ml), streptomycin (100 μg/ml), 10% fetal bovine serum, and L-glutamine (2 mM). Cells at ~80% confluency were treated with 1mM hydroxyurea (Sigma) for 16 hrs.

Immunoblotting

Cells were washed with PBS and lysed in RIPA buffer for 15 min at 4°C. Lysates were clarified by centrifugation for 15 min at 14,000 rpm and supernatants were collected. Protein concentration in the soluble fraction was determined by BioRad DC protein assay. The following antibodies were used at the indicated dilution to detect endogenous proteins: Mouse monoclonal anti-p53 (DO1; CalBiochem) at 1:1000, mouse monoclonal anti-p73 (429; Imgenex) at 1:200, and mouse monoclonal anti-p63 (4A4; Pharmingen) at 1:300, and mouse monoclonal anti-α-tubulin (Clone B-5-1-2; Sigma) at 1:1000. Tubulin was used as a loading control.

Chromatin immunoprecipitation (ChIP)

HCT116-3(6) cells were cultured in 10 cm plates to 70-80% confluence prior to drug treatment. Cells were fixed with 1% formaldehyde in serum-free media for 10 minutes at room temperature. Formaldehyde crosslinking was quenched with 125 μM glycine (final concentration). Cells were washed in PBS and nuclei were prepared as previously described (8). Cell suspension was sonicated 20 seconds for 8 times to yield DNA fragments with average length ~500 bp using Branson 450 sonifier, setting 4 (25% power output). Lysates were pre-cleared with Protein A/G sepharose for 2 hrs at 4°C.

Approximately $3x10^7$ cells were prepared per immunoprecipitation incubated with 5ug of total monoclonal anti-p53 (1:1 mixtures of Ab-1 and Ab-12, CalBiochem) or affinity-purified polyclonal anit-p73 (827) at 4°C overnight. Equivalent amounts of normal IgG were used as negative controls. Protein A/G beads were then added to the immunoprecipitate and incubated for 2 hrs. Beads were then washed sequentially once in low salt buffer, once in high salt buffer, and three times in TE. DNA/protein complexes were eluted and decrosslinked by heating at 65°C overnight. Eluates were treated with Proteinase K and DNA fragments were extracted with phenol/chloroform 2X and treated with RNAse A. DNA fragments were then purified and eluted in TE using Qiaquick PCR purification columns (Qiagen).

DNA microarray design and DNA Selection and Ligation (DSL)

The oligonucleotide-based array contains ~2000 unique signature 40mer oliogonucleotide probes corresponding to a proximal region from –800 bp to +200 bp relative to the transcription initiation site. Consecutive 40mers were also included to cover regions of selected chromosomes at 500 bp increments. As positive controls, we included the genomic sequences containing p53 consensus binding sites of two known p53 regulated promoters (i.e. p21CIP1, p53R2) to the current 2000 promoter oligonucleotide array. Probes were prepared by the DSL technology as previously described (6). To examine the steady state promoter occupancy by p53 and p73, we labeled ChIP DNA with Cy3 and input DNA with Alexa 647. To compare the promoter occupancy profiles of untreated and HU-treated samples, we labeled HU-treated ChIP DNA with Cy3, and untreated ChIP DNA with Alexa 647. By a two-color comparison, the enrichment ratio was determined for each binding site. Data were normalized by

SNOMAD (**S**tandardization and **NO**rmalization of **M**icro**A**rray **D**ataset). See website: http://pevsnerlab.kennedykrieger.org/snomadinput.html. Three independent biological replicates were prepared for statistical analysis by SAM (**S**tatistical **A**nalysis of **M**icroarray), http://wwwstat.stanford.edu/~tibs/SAM/.

Quantitative PCR analysis

Selected DNA binding sites were verified by SYBR Green quantitative PCR analysis. Primers were designed to in proximity to the 40mer probe using Primer Express (Applied Biosystems). For validation of ChIP-DSL results, each PCR reaction was performed in duplicate in a 25 µl relation with 5 µL of total or ChIP DNA and 1X SYBR Green master mix (Applied Biosystems). Fluorescence values were determined by ABI Prism 7900 sequence detection system. Fold enrichment for an enriched region relative to TK1 was calculated as described in Yang et al: fold enrichment (occupancy units OU)= $1.9^{-(\text{delta CT}_{\text{expt}}-\text{delta CT}_{\text{Tk1}})}$ where delta $CT=CT_{IP}-CT_{Input.}$ Specificity of the PCR reaction was confirmed by the presence of a single peak in dissociation analysis. Primer sequences are shown in Table 2-4.

RNA extraction and reverse transcription and real-time PCR (RT-qPCR)

Total RNA from untreated or HU-treated HCT116-3(6) cells was isolated using RNeasy Mini Kit (Qiagen). 1-5 ug of total RNA was reverse transcribed using High Archive cDNA synthesis kit (Applied Biosystems). SYBR Green quantitative PCR analyses were performed using gene-specific primers designed by Primer Express. p73 mRNA expression was measured by Taqman assay using Taqman assays-on-demand gene expression products (Applied Biosystems; ID# Hs00232088_m1). All samples were normalized to β-actin values. Primer sequences are shown in Table 2-1.

Table 2-1. Primer sequences used for real-time RT-PCR analysis

p53	TGCAATAGGTGTGCGTCAGAA	(forward)
	CCCCGGGACAAAGCAAA	(reverse)
p63	TCTCTTTCCCACCCCGAGAT	(forward)
	CGGCGAGCATCCATGTC	(reverse)
β-actin	CGAGAAGATGACCCAGATCATGTT	(forward)
	CCTCGTAGATGGGCACAGTGT	(reverse)

siRNA transfection

Small interfering RNA (siRNA) duplexes against p53, p73 and lacZ were obtained from Dharmacon. HCT116-3(6) cells were seed at 30% confluence prior to transfection. Cells were transfected with RNA duplexes using Oligofectamine (Invitrogen) as previously described (9).

p53 Motif search

We performed the p53 motif search using the perfect consensus sequence with the following criteria:

(I) No more than two mismatches are allowed per quarter site.

(II)The core sequence must contain C A/T A/T G.

(III)Two half sites must be tandemly located within 0-13 bp gap.

2.4 Results

2.4.1 Defining the experimental system.

To examine the *in vivo* DNA binding sites of p53 and p73 in the absence of p63, we determined the levels of p63 and p73 in several human cancer cell lines expressing wild type p53 (data not shown). We found that colon cancer cell line HCT116-3(6) expresses p53 and p73, both of which can be induced to three fold above the basal level

by hydroxyurea (HU) treatment (Figure 2-1A; left panel). The basal level of p63 is negligible compared to p53 or p73, and HU does not appear to cause p63 induction in HCT116-3(6) cells (Figure 2-1A; right panel and Table 1) or MCF7 cells (Figure 2-1A; right panel). Consistent with previous findings that p73 mRNA expression is cell-cycle dependent (10), we found that HU treatment causes a two- to threefold increase in p73 mRNA levels as a result of S-phase arrest (Table1 and data not shown).

p53 and p73 are known to induce apoptosis by many chemotherapeutic agents (11, 12). We previously found that HU at 1mM does not induce apoptosis in HCT116-3(6) cells (Ki S., unpublished data). Time-course experiments were performed to determine the levels of p53 and p73 induced by HU. Whereas p53 levels increased steadily between 12-48 hours, p73 reached a peak of induction between 12-24 hours (Figure 2-1B). Therefore, we chose to perform subsequent experiments at 16 hour, a time at which both p53 and p73 levels are reasonably high.

In order to determine the feasibility of the ChIP-based approach for this study, we first confirmed the specificity of our anti-p73 polyclonal antibody (827) by performing a western blot analysis in HEK293 cells transfected with HA-tagged p73 isoforms. As expected, anti-p73 (827) antibody reacted with all four isoforms of p73 but not p53 (Figure 2-2A). Next, we performed ChIPs with anti-p53 and anti-p73 (827) antibodies followed by western blotting with anti-p53 and anti-p73 in HCT116-3(6) cells to confirm that the antibodies can recognize the epitope in the context of crosslinked-chromatin (Figure 2-2B).

We next tested whether ChIP can be carried out with anti-p53 and anti-p73 antibodies in HCT116-3(6) cells using p21CIP1 promoter as a positive control. The

human p21CIP1 promoter contains two p53 binding sites, a distal response element located 2.3 kb and a proximal response element located 1.5 kb upstream of the transcription start site (Figure 2-3A; top panel). It has been shown that p53 can bind to the distal binding site with high affinity (13). To this end, crosslinked chromatin from untreated or HU-treated HCT116-3(6) cells was immunoprecipitated with antibodies against p53 or p73 and checked for the enrichment of the p21CIP1 promoter by PCR with primers encompassing the p53 distal binding site. We found that both p53 and p73 constitutively occupy the p53 distal binding site (Figure 2-3A; bottom panel) but not the promoter-proximal region (data not shown). Moreover, p21cip1 promoter occupancy by p53 and p73 is moderately increased following HU treatment as determined by quantitative real-time PCR (Figure 2-3B). Negative controls using non-specific IgGs failed to generate specific signal. To further demonstrate the specificity of our anti-p73 antibody in ChIP experiments, we also performed the same control experiments in $p73^{-/-}$ 3T3 cells reconstituted with MSCV or human p73-α. We found that our anti-p73 antibody can specifically bring down the p21cip1 distal promoter in $p73^{-/-}$ 3T3 cells reconstituted with p73-α but not with vector control (Figure 2-3C; top panel). Similarly, we performed ChIP with anti-p53 in Saos2 cells ($p53^{-/-}$) and detected no enrichment of the p21cip1 distal promoter (Figure 2-3C; bottom panel). Taken together, we conclude that these antibodies can specifically immunoprecipitate p53 and p73-chromatin.

2.4.2 p53 and p73 co-occupy a large set of binding sites at steady state

Given the fact that p53 and p73 share 60% sequence identity within the DNA binding domain, we asked whether p53 and p73 regulate overlapping set of promoters both before and after HU treatment. To compare the promoter occupancy profiles of p53

and p73 in a high-throughput manner, we used a modified ChIP-chip developed by Dr. Xiang-Dong Fu (UCSD). The ChIP-DSL (DNA Selected Ligation) technology has significantly improved the conventional ChIP-chip in terms of sensitivity and specificity (6, 7). This is achieved by enhancing DNA hybridization in two rounds of target section without the use of immunoprecipaited DNA as the direct template. Specificity and efficiency are further improved by using a unique 80 base pair target amplification in the probe labeling process (Figure 2-4).

To compare the DNA binding sites of p53 and p73 among the 2000 selected promoters, a total of three independent chromatin immunoprecipitations were carried out in untreated HCT116-3(6) cells. All three ChIP DNA were independently labeled with Cy3 (anti-p53 or anti-p73) and the corresponding input DNA were labeled with Alexa647 using the ChIP-DSL technology. Each set of these probes were co-hybridized to the oligonucleotide array containing 2000 promoters. Data from three independent experiments were combined, normalized, and analyzed by the statistical analysis program SAM (14) (Figure 2-5A). Threshold for calling significance was determined by the delta value. For the IP vs. input analysis, we set the delta value at which no binding sites were enriched in the input samples. As expected, we found that both p21cip1 and p53R2 were among the significantly enriched binding sites. A similar delta value was chosen for a direct comparison of promoter occupancy profiles between p53 and p73. Using the equivalent delta value we identified 166 and 148 binding sites for p53 and p73, respectively (Figure 2-5B). As shown by the Venn diagram, we found that 47% of the binding sites occupied by p73 overlap with those occupied by p53. The significance of this overlap was calculated based on the hypergeometric distribution (Figure 2-5C, left

diagram). As a control, we randomly chose 200 promoters that fell below the defined delta value from the p53 and p73 IP/input experiments and performed the same comparison. We found nearly no overlap between the two randomly selected sets and the overlapping p-value calculated by the hypergeometric test is highly insignificant (Figure 2-5C, right diagram).

2.4.3 The effect of HU on the promoter occupancy profiles of p53 and p73

To compare the promoter occupancy profiles of p53 and p73 following HU treatment, a total of three independent chromatin immunoprecipitations were carried out in either untreated or HU treated HCT116-3(6) cells. All three ChIP DNA (anti-p53 or anti-p73) from untreated cells were independently labeled with Alexa647 and ChIP DNA (anti-p53 or anti-p73) from HU-treated cells were labeled with Cy3 using DSL technology. Each set of probes were co-hybridized to the oligonucleotide array. Data from the three independent experiments were combined, normalized, and analyzed by the statistical analysis program SAM (Figure 2-6A). For the IP vs. IP analysis, we chose a delta value to include at least one of the two positive controls. As expected, p53R2 were among the binding sites that showed significant increase in occupancy by both p53 and p73 after HU treatment. Limited by the sensitivity of the ChIP-DSL assay, HU-induced increase in p21cip1 promoter occupancy by p53 or p73 was marginal, since a minimum of five-fold difference is required to be detected by ChIP-DSL. A similar delta value was picked for p53 and p73 to allow direct comparison. Using the equivalent delta value, we identified 33 and 64 binding sites which showed increased occupancy by p53 and p73 following HU treatment, respectively (Figure 2-6B). 13 of these promoters are shared between p53 and p73 as depicted by the Venn diagram. The significance of this overlap

was calculated using the hypergeometric test (Figure 2-6C; left diagram). As a control, we found the overlapping p-value from two randomly selected sets of promoters is highly insignificant (Figure 2-6C; right diagram).

2.4.4 Validation of ChIP-DSL analysis by ChIP-qPCR

We performed ChIP and real-time quantitative PCR assays (ChIP-qPCR) on selected DNA binding sites identified by ChIP-DSL. We first tested the effectiveness of ChIP-qPCR method on the two positive controls used for ChIP-DSL, p21CIP1 and p53R2, by using gene-specific primers spanning the previously characterized p53 response element. Promoter enrichment was calculated in terms of occupancy units as described in Yang et al (15). Consistent with the ChIP-DSL data, both p21CIP1 and p53R2 promoters were constitutively occupied by both p53 and p73. As a negative control, we did not detect enrichment of promoters that fell below the threshold in SAM analysis (i.e. TK1). Based on the delta CT values of the negative controls, we considered occupancy units of two or greater as positive confirmation. Primers used for validation experiment were designed within 1kb from either side of the 40mer sequence (Figure 2-7B). Examples of verified binding sites and their occupancy units are shown in Table 2. In summary, approximately 80-85% of binding sites identified by ChIP-DSL in this study can be confirmed by ChIP-qPCR. According to Kwon, Y-S et al., the false positive and false negative rate of the ChIP-DSL technology was estimated around 3% and 33%, respectively(6).

2.4.5 Transcriptional activity of promoters co-occupied by p53 and p73 is mainly contributed by p53

To determine whether these candidate binding sites are *bona fide* direct transcriptional targets of p53 or p73, we examined the effect of siRNA-mediated downregulation of p53 and p73 on basal transcript level of several candidate genes using quantitative real time RT-PCR. p53 and p73 protein level can be knocked down by at least 75% as compared to that of lacZ transfected (Figure 2-8A). We then examined the transcript level of five p53 and p73 co-occupied promoters identified from ChIP-DSL. As shown in Figure, p53 siRNA-mediated downregulation resulted in at least 50% reduction in basal transcript level with the exception of SOD2. However, p73 siRNA-mediated downregulation resulted in 30-50% reduction in the basal transcript of all five genes. Consistent with previous findings (16), we concluded that p53 and p73 can regulate constitutive expression of some genes in proliferating cells in the absence of genotoxic stress. Furthermore, transcriptional activity of promoters co-occupied by p53 and p73 are regulated mostly by p53 (Figure 2-8B).

We found that SOD2 (superoxide dismutase 2), which was previously identified as an NFκB target gene, is constitutively occupied by both p53 and p73. As previously reported (17), exposure of cells to TNF-α/CHX resulted in a time-dependent increase in SOD2 mRNA levels. Moreover, siRNA-mediated knockdown of p53 or p73 resulted in a reduction of SOD2 mRNA level in response to TNF-α/CHX (Figure 2-8C), suggesting that, in addition to NFκB, p53 and p73 can regulate SOD2 transcription in response to TNF-α.

KAI1 is a surface glycoprotein that regulates cell-cell adhesion and functions as a metastasis suppressor (18). A typical p53 consensus response element has been identified within its promoter-proximal region(19, 20). Using ChIP-DSL, we have

identified multiple binding sites on the tiled region of KAI1 locus. In agreement with a previous report(20), we found that KAI1 gene expression is inducible by several genotoxic agents such as hydroxurea, doxorubicin, and cisplatin. Interestingly, we found that siRNA-mediated knockdown of either p53 or p73 resulted in a reduction of KAI1 mRNA level in response to these agents (Figure 2-8D and not shown).

2.4.6 p53 Motif Analysis

It is known that p53 and p73 activate their target genes by binding to tandem repeats of p53 consensus response element PuPuPu CA/TA/TG PyPyPy, where Pu=purine and Py=pyrimidine (21). Therefore, we conducted p53 motif search within 2kb up- and downstream of the 40mer probe sequence from a total of 391 candidate binding sites. We first categorized the promoters into three groups according to their response to HU (Table 2-3; top). By scanning the binding sites for a p53 consensus element using defined criteria, we found that ~20-40% of p53 and p73 constitutive binding sites (Category I) contain the canonical p53 response element, respectively (Table 2-3; bottom). Interestingly, we found that 8-25% of p53 and p73 HU-inducible binding sites (Category II/III) contain the canonical p53 response element (Table 2-3; bottom). Based on our finding, we speculate that p53 and p73 may have differential binding affinity and/or differential recognition of p53 response element in response to genotoxic stress. Consistent with previous findings that more than 50% of the candidate binding sites do not contain the canonical p53 consensus element, we reasoned that it is likely that p53 and p73 can bind to non-consensus sequence through direct interaction and/or indirect tethering to other transcription factors.

2.5 Discussion

In this study, we compared promoter occupancy profiles of p53 and p73 in parallel using ChIP combined with microarray analysis. Of the 2000 binding sites surveyed in this ChIP-DSL study, we found that: (1) p53 and p73 share at least 50% of their binding sites in the absence of genotoxic stress; (2) Following HU treatment, we found no significant change in the overall promoter occupancy profiles of p53 and p73 where more than 80% of the constitutive binding sites remained bound by either p53 or p73; (3) HU induces change in occupancy profiles of a small fraction of promoters, 20% of which showed increased occupancy by both p53 and p73. The actual degree of overlap of between p53 and p73 may well be underestimated due to an increased number of false negatives when a stringent cutoff was used

Our results suggest that p53 and p73 constitutively co-occupy a large set of promoters at steady state, which implies that p53 binding to a subset of promoters may require the presence of p73/p63. Constitutive binding activity of p53 and p73 at these promoters may attribute to functions other than transcription, such as pre-initiation. For example, a previous study by Espinosa et al. have shown that p53 is crucial for the assembly of the pre-initiation complex on promoters prior to DNA damage as well as transactivating genes following DNA damage (22).

Since more than 50% of loci identified in this study contain p53 consensus response element located at least 2kb from the 40mer probe sequence, our results indicate that p53 and p73 may function as enhancers. Moreover, additional co-factors are recruited to the promoter to activate transcription through combinatorial interactions with p53 or p73. Since binding does not directly correlate with gene regulation, we utilized

siRNA technology to examine the effect of p53 or p73 siRNA knockdown on the basal expression of a subset of p53 and p73 co-occupied promoters. Our results shows that while p53 knockdown caused at least 50-75% reduction in the basal expression of the majority of p53 and p73 co-occupied promoters, p73 knockdown had either no or modest effect on the basal expression of these genes. These results suggest that, although p53 and p73 can occupy the same promoters, the transcript levels of these genes are mainly contributed by p53. The mechanism by which p53 cooperates with p73 or p63 in transactivating the common set of genes remains to be elucidated.

Of the 166 p53 binding sites identified in this study by the ChIP-DSL technology, we found two binding sites (RUNX1 and EP300) mapped to the previously identified p53 binding sites on chromosome 21 and 22 (23). We have also found additional p53 binding sites in TGFA, RRAD, FAT, and ATM, which were also identified by a ChIP-PET study(24). Functional classification of candidate targets identified in this study included genes involved in signal transduction, metabolism, transcriptional regulation, cell contact/motility, inflammation, cell-cycle, and neuronal development (not shown). Consistent with Fontemaggi et al (25), we conclude that the p53 family may have more diverse functions than previously recognized.

In conclusion, our findings suggest that p53 and p73 can occupy both common and non-overlapping promoters in the absence of cellular stress. Furthermore, their differential promoters occupy profiles in response to HU implies that they might regulate distinct biological responses to genotoxic stress.

2.6 Acknowledgements

Chapter 2, in part, is taken from the material as appeared in a manuscript "Interactions of p53 and p73 with Human Promoters." Huang, V., Lu, X., Jiang, Y., and Wang. J. Y.J. The dissertation author was the primary investigator and author of this manuscript.

We thank Dr. Young-Soo Kwon for performing the ChIP-DSL experiments, and Dr. Xiang-Dong Fu for providing the oligonucleotide arrays for the ChIP-DSL study.

2-1A)

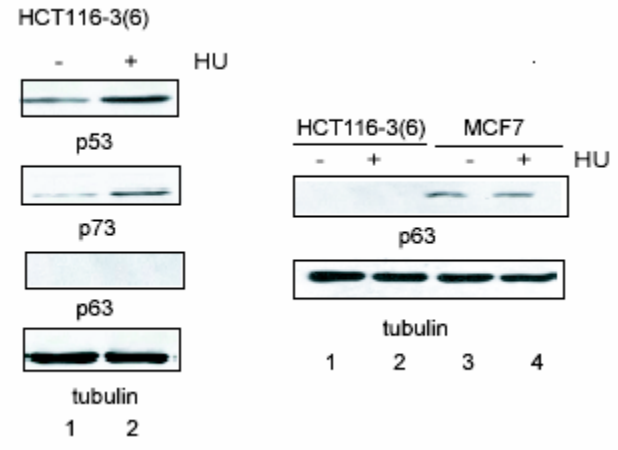

2-1B)

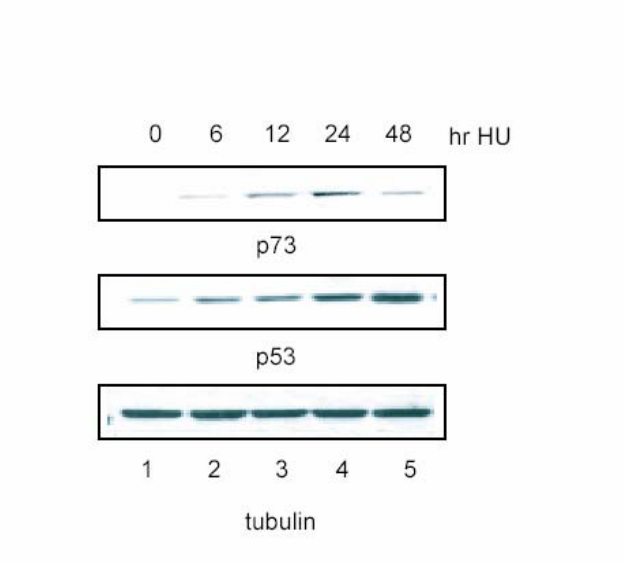

Figure 2-1. HU-induces p53 and p73 expression in HCT116-3(6) cells
(A) Time course of p53 and p73 protein accumulation in response to HU (1 mM). p53 and p73 protein were detected by immunoblotting with a p53 monoclonal antibody (DO1) and with a monoclonal p73 antibody (429), respectively. (B) Expression of p53, p63, and p73 in response to HU (1mM, 16 hrs). The level of p63 was detected by a p63 monoclonal antibody (4A4). Tubulin was used as a loading control.

Table 2-2. p53, p63, and p73 mRNA levels in HCT116-3(6) cells.
Total RNA was extracted and subjected to RT-qPCR analysis using primers specific to p53, p63, and p73. β-actin normalized CT values and HU-fold induction relative to untreated are shown.

	CT value[1]		
	p53	**p63**	**p73**
-HU	**20.23±0.005**	**30.33±0.66**	**28.18±0.11**
+HU	**20.20±0.1**	**31.27±0.144**	**26.75±0.13**
HU inducibility (fold change)[2]	**1.02±0.05**	**0.52±0.02**	**2.69±0.39**

[1] CT value=β-actin normalized CT value
[2] HU inducibility (fold change) = 2^(CT(-HU)-CT(+HU))

2-2A)

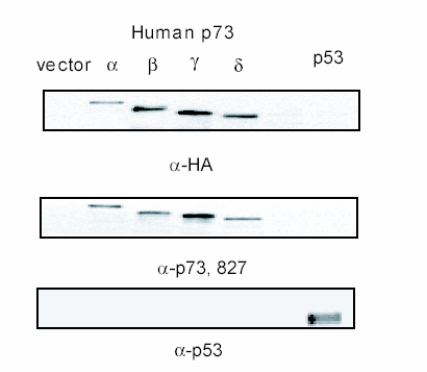

2-2B)

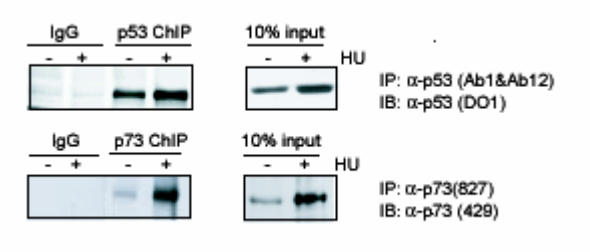

Figure 2-2. Validation of p73 antibody used in this study. (A) Extracts of 293T cells transfected with empty vector, HA-tagged p53, or p73 α/β/χ/δ were subjected to SDS-PAGE and immunobloting with p73 polyclonal (827) and p53 monoclonal (DO1) antibodies. Anti-HA was used as a positive control. (B) Antibody accessibility control. Crosslinked chromatins from untreated and HU-treated cells were immunoprecipitated using a p73 polyclonal antibody (827) and followed by immunoblotting with a monoclonal anti-p73 (429) antibody (bottom panel). Same ChIP experiment was performed using a mixture of p53 monoclonal antibodies (Ab1 and Ab12) and followed by immunoblotting with a monoclonal anti-p53 (DO1) antibody (top panel).

Figure 2-3. HU-induced p53 and p73 accumulation correlates with increased occupancy of the p21cip1 promoter

(A) PCR analysis of the p21cip1 promoter occupancy by p53 and p73. Chromatin from untreated and HU treated cells were immunoprecipitated with anti-p53 and anti-p73 (lanes 2,4,6,8). Immunoprecipitations with IgGs were used as negative controls (lanes 1,3,5,7). Total input DNA was used as a positive control (lanes 9,10). PCR was performed using primers encompassing the p53 binding site in the distal region of the p21cip1 promoter as shown in the top schematic diagram. Constitutive occupancy by p53 and p73 were observed at the p53 distal binding site of the p21CIP1 promoter (lanes 2,6). M: Mouse IgG, R: Rabbit IgG. (B) Quantitative real time-PCR analysis. Enrichment of the p21cip1 promoter is expressed in terms of occupancy units (OU). (C) ChIP specificity controls. p73 ChIP was performed in $p73^{-/-}$ 3T3 cells reconstituted with MSCV (Top panel, lanes 5,6) or human p73α (Top panel, lanes 7,8) and p53 ChIP was performed in Saos2 cells using antibodies to p53 (Bottom panel, lane 4) and a nonspecific IgG control (bottom panel, lane 3). Enrichment of the p21cip1 distal promoter was not observed in cells without p53 or p73.

2-3A)

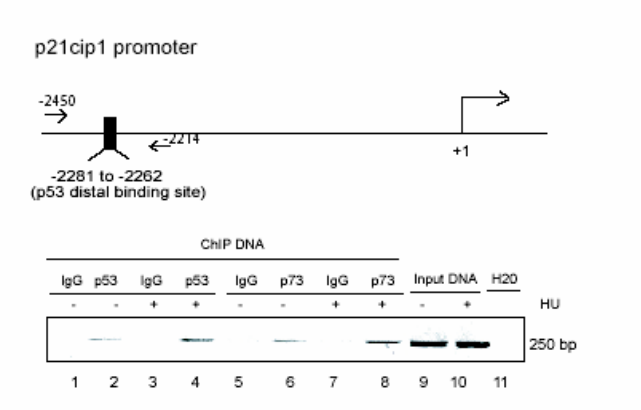
p21cip1 promoter
-2450
-2214
+1
-2281 to -2262
(p53 distal binding site)
ChIP DNA
IgG p53 IgG p53 IgG p73 IgG p73 Input DNA H20
HU
250 bp
1 2 3 4 5 6 7 8 9 10 11

2-3B)

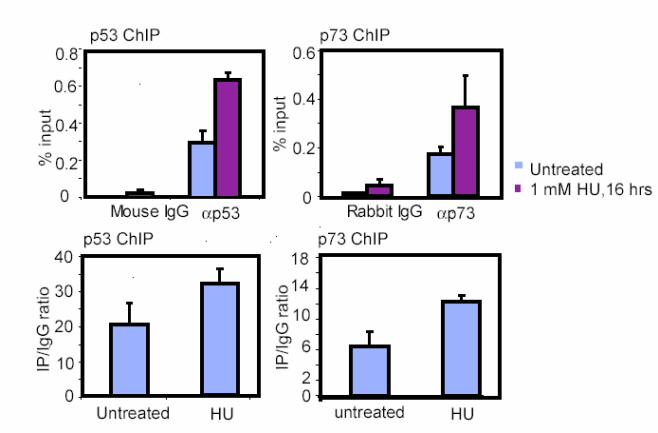
p53 ChIP
p73 ChIP
% input
Mouse IgG αp53
Rabbit IgG αp73
Untreated
1 mM HU,16 hrs
IP/IgG ratio
Untreated
HU
untreated
HU

2-3C)

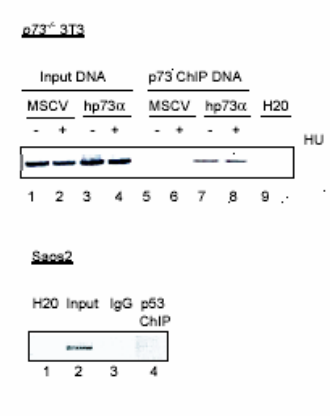
p73-/- 3T3
Input DNA
p73 ChIP DNA
MSCV hp73α MSCV hp73α H20
HU
1 2 3 4 5 6 7 8 9
Saos2
H20 Input IgG p53 ChIP
1 2 3 4

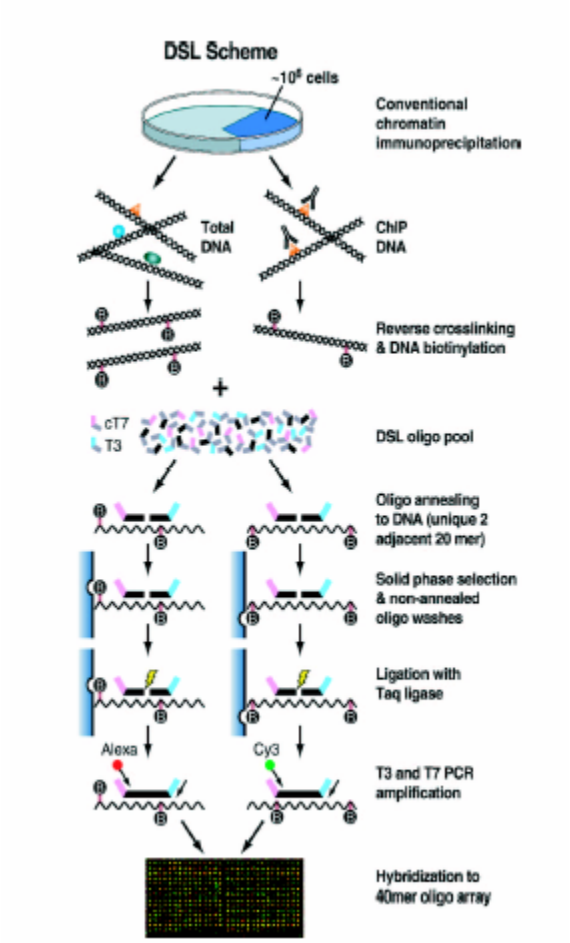

Figure 2-4. The ChIP-DSL scheme (6)
Total input DNA or ChIP-DNA isolated from standard ChIP is first randomly biotinylated and annealed to the oligonucleotide pool consists of 2000 primers sets. Annealed oligonucleotides are selected on streptavidin-coated magnetic beads. Selected oligos that are paired with the target DNA are ligated, which subsequently form PCR amplicons for PCR amplification. PCR products can be directly hybridized to the 40-mer oligonucleotide array using one of the primers end-labeled with a fluorescent dye.

2-5A)

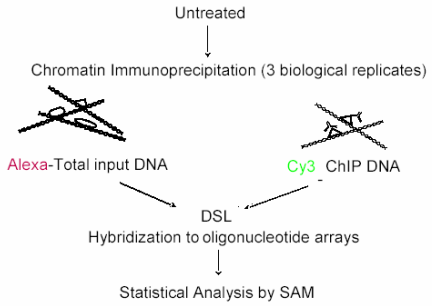

2-5B)

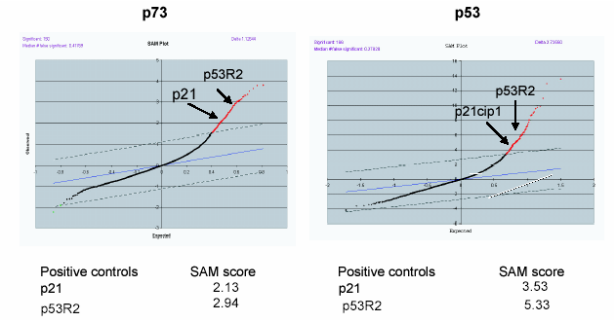

2-5C)

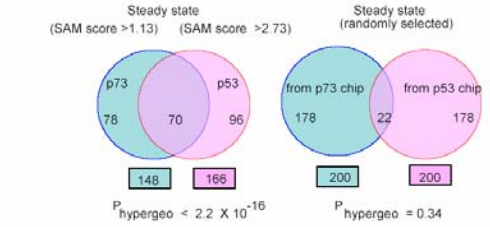

Figure 2-5. ChIP-DSL analysis of p53 and p73 promoter occupancy profiles at steady state

(A) Summary of the experimental procedure for ChIP-DSL analysis of input vs. IP. Three independent experiments were performed and subjected to SAM analysis. (B) SAM plots depicting microarray analysis obtained from input vs. IP for p53 and p73 under steady state. Enriched binding sites at significant levels are shown in red. (C) Venn diagram representing the number of constitutive binding sites occupied by p53 or p73, or both (left). Number inside the box represents the total number of binding sites. Control experiment using 200 randomly selected promoters from each experiment is shown (right).

2-6A)

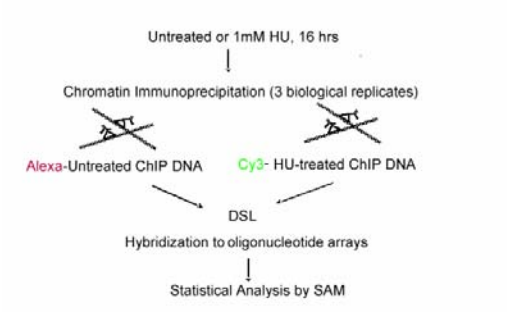

2-6B)

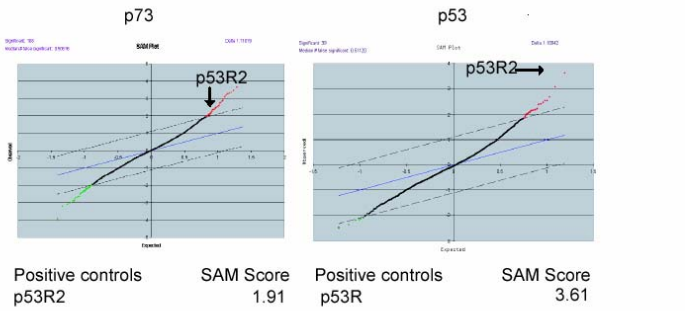

2-6C)

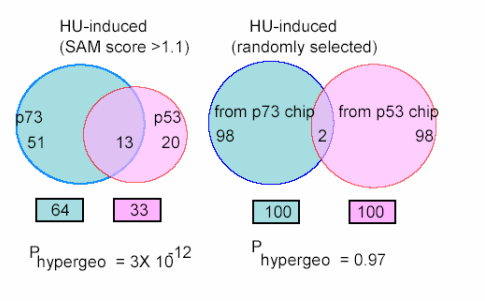

Figure 2-6. ChIP-DSL analysis of p53 and p73 promoter occupancy profiles following HU treatment

(D) Summary of the experimental procedure for ChIP-DSL analysis of HU-treated IP vs. untreated IP. Three independent experiments were performed and subjected to SAM analysis. (E) SAM plots depicting microarray analysis obtained from untreated ChIP vs. HU-treated ChIP for p53 and p73. Binding sites with increased occupancy at significant levels are shown in red. (F) Venn diagram representing the number of binding sites occupied by p53, p73, or both following HU treatment (left). Control experiment using 100 randomly selected promoters from each experiment is shown (right).

2-7A)

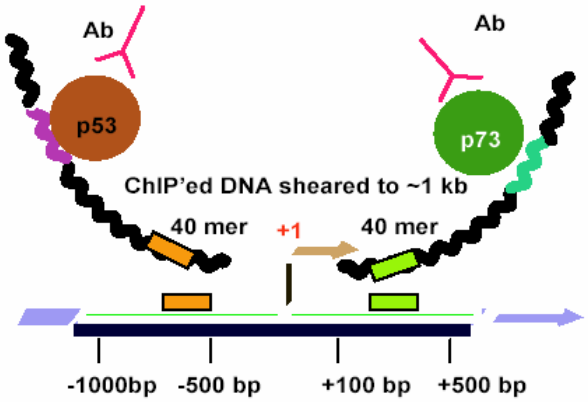

2-7B)

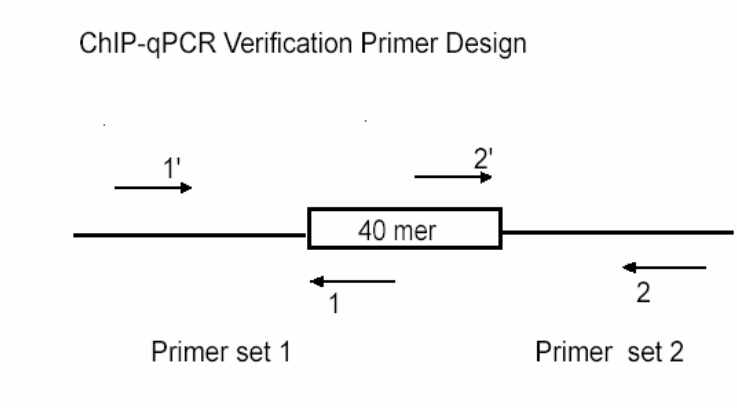

Figure 2-7. Primer design for ChIP-qPCR verification
(A) Resolution of the ChIP-DSL technology. Binding sites located within 500 bp-1kb from the 40mer sequence can be readily detected by microarray. (B) Primers flanking either end of the 40mer sequence are designed for validation.

Table 2-3. Summary of ChIP-qPCR verification of selected candidate binding sites
Two independent ChIPs were performed using indicated antibodies and enriched DNA was detected by qPCR using primers designed as in Figure 2-7.

	-HU						+HU	
binding site[a]	**p53 OU[b]**	**ChIP-DSL[c]**	**SAM Score**	**p73 OU[b]**	**ChIP-DSL[c]**	**SAM Score**	**p53 OU[d]**	**p73 OU[d]**
p21	18.465	**Y**	3.534	10.641	**Y**	2.131	37.535	20.974
p53R2	27.134	**Y**	5.327	15.877	**Y**	2.941	71.521	18.881
TK	1.000	**Y**	0.134	1.000	**Y**	-0.468	1.000	1.000
casp7_147	0.066	**Y**	1.637	3.725	**Y**	1.694	0.194	9.454
casp7_165	0.154	**Y**	2.128	0.123	**Y**	0.853	0.652	1.876
SOD2	15.674	**Y**	4.807	30.950	**Y**	3.305	1.685	15.326
serpinC1	6.893		1.578	39.121	**Y**	3.793	20.856	15.082
ATM	16.875	**Y**	4.125	47.580		0.443	29.495	40.526
EP300	4.905	**Y**	12.943	65.375	**Y**	2.678	22.671	1.621
MCM6	0.363	**Y**	0.753	0.357	**Y**	0.542	1.137	1.108
NrCAM	69.932	**Y**	9.719	26.617	**Y**	2.597	30.851	47.124
TDG	37.170	**Y**	4.144	40.312	**Y**	1.332	56.719	59.169

[a]: Binding site is represented by a unique 40mer sequence that corresponds to the promoter-proximal region (-800 to +200) of 2000 human promoters. p21cip1 and p53 R2 40mer sequence contains the previously identified p53RE.
[b]: Occupancy units (OU) for p53 and p73 (-HU) determined by real-time PCR.
[c]: Consistency with ChIP-DSL microarray result. OU>2 is considered positive confirmation. Y=consistent
[d]: Occupancy units (OU) for p53 and p73 (+HU) determined by real-time PCR.

Figure 2-8. Functional impact of p53 and p73 on transcript level of candidate genes. (A) The efficacy of transient siRNA-mediated knockdown of p53 or p73 in HCT16-3(6) cells. Immunoblot of lysates from HCT116-3(6) cells following transfection with chemically synthesized siRNA oligos against p53, p73, or lacZ. (B) The effect of siRNA mediated knockdown of p53 or p73 on basal transcript level of selected candidate genes. Quantitative real-time RT-PCR was used to examine mRNA levels using the identical samples from (A). Levels were normalized to β-actin expression. (C) The effect of siRNA-mediated knockdown of p53 or p73 in TNF-α induced SOD2 mRNA upregulation. Cells were transfected with lacZ, p53, or p73 siRNA and followed by treatment with recombinant human TNF-α and cyclohexamide at the indicated time. mRNA level was determined by Taqman real-time RT-PCR. (D) The effect of siRNA-mediated knockdown of p53 or p73 on genotoxic stress-induced KAI1 mRNA upregulation. Cells were transfected with lacZ, p53, or p73 siRNA and followed by drug treatment at the indicated time. SYBR Green Quantitative real-time RT-PCR was used to examine mRNA level.

2-8A) **2-8B)**

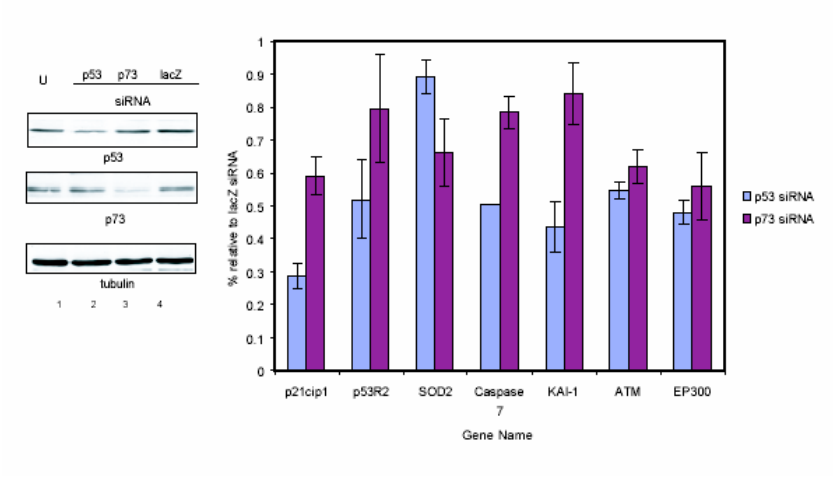
U
p53
p73
lacZ
siRNA
p53
p73
tubulin
1
2
3
4
% relative to lacZ siRNA
p21cip1
p53R2
SOD2
Caspase 7
KAI-1
ATM
EP300
Gene Name
p53 siRNA
p73 siRNA

2-C)

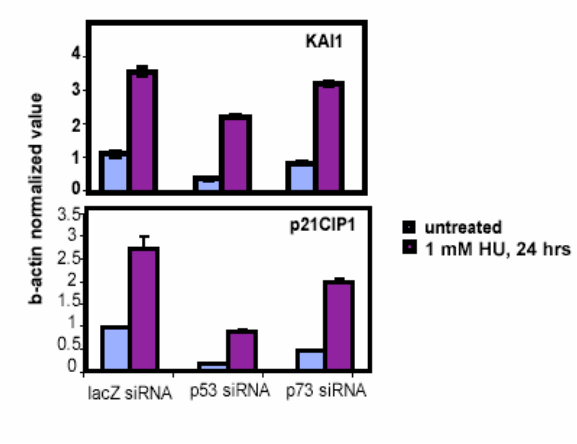
KAI1
p21CIP1
b-actin normalized value
lacZ siRNA
p53 siRNA
p73 siRNA
untreated
1 mM HU, 24 hrs

2-D)

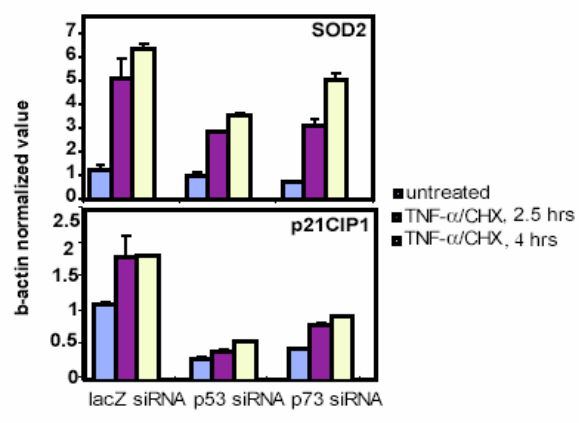
SOD2
p21CIP1
b-actin normalized value
lacZ siRNA
p53 siRNA
p73 siRNA
untreated
TNF-α/CHX, 2.5 hrs
TNF-α/CHX, 4 hrs

Table 2-4. p53 motif search

Category	Untreated[1]	1 mM HU 16 hrs[2]
I	+	+
II	+	++
III	-	+

p53 Category	# Positives[3]	% Positives[4] Total =180	p73 Category	# Positives[3]	% Positives[4] Total =391
I	67	37.2	I	83	21.2
II/III	14	7.78	II/III	98	25

[1] p53 or p73 binding status in untreated condition
[2] p53 or p73 binding status in +HU condition
-: No binding; +: binding; ++: increased binding
[3] # positives: # promoters containing p53 consensus response element
[4] % promoters= # positives/total X 100

Table 2-5. Primer sequences used for ChIP-qPCR validation

Gene Name	Gene Acession ID	Forward	Reverse
ATM	NM_000051	TCCCAACACTGAACCAAGGAA	GCATGACGGACGGATTGC
CASP7_147	NM_001227	CCTGCCTACCTGTCCTGGTTT	CATAGTTCAGTCCATAGCAAGGGATA
CASP7_165	NM_001227	CCTATGATCTCCAGCAGCTTGA	CCCATGCAGTGGAGAGGAA
EP300	NM_001429	GCCCCTCCCCCCTTAAA	GGCCCCAACGCGGTTA
MCM6	NM_005915	CGGGCCACGGCTACACT	GCCCACGGAAAGGGATTT
NrCAM	NM_005010	CGGAGGGCGGGAGTGT	AGTGGCATTCAAAAACTACCCATT
SERPINC1	NM_000488	CAAAGTGTAGAGCCCAGTGTTGTT	GAGGTGGCTCAGGCTTTCC
SOD2	NM_000636	CTTTCTTCTCACCCGCACACT	GCAGCGGTTCAGCAGAT
TDG	NM_003211	CCGAAAATACTGGAGACAAAAGC	AAGGGTGGAGGACCAGAAGAC
p21cip1	NM_000389	AGGCTGAGCCTCCCTCCAT	CTTCTATGCCAGAGCTCAACATGT
p53R2(RRM2B)	NM_015713	GGGCATCGTAAGTGCTTGCT	TGGTCACCCAGTTGGAAGACA

2.7 References

1. Harms, K., Nozell, S., and Chen, X. (2004) The common and distinct target genes of the p53 family transcription factors. *Cell Mol Life Sci* 61, 822-842

2. Donehower, L. A., Harvey, M., Slagle, B. L., McArthur, M. J., Montgomery, C. A., Jr., Butel, J. S., and Bradley, A. (1992) Mice deficient for p53 are developmentally normal but susceptible to spontaneous tumours. *Nature* 356, 215-221

3. Yang, A., Schweitzer, R., Sun, D., Kaghad, M., Walker, N., Bronson, R. T., Tabin, C., Sharpe, A., Caput, D., Crum, C., and McKeon, F. (1999) p63 is essential for regenerative proliferation in limb, craniofacial and epithelial development. *Nature* 398, 714-718

4. Yang, A., Walker, N., Bronson, R., Kaghad, M., Oosterwegel, M., Bonnin, J., Vagner, C., Bonnet, H., Dikkes, P., Sharpe, A., McKeon, F., and Caput, D. (2000) p73-deficient mice have neurological, pheromonal and inflammatory defects but lack spontaneous tumours. *Nature* 404, 99-103

5. Flores, E. R., Sengupta, S., Miller, J. B., Newman, J. J., Bronson, R., Crowley, D., Yang, A., McKeon, F., and Jacks, T. (2005) Tumor predisposition in mice mutant for p63 and p73: evidence for broader tumor suppressor functions for the p53 family. *Cancer Cell* 7, 363-373

6. Kwon, Y. S., Garcia-Bassets, I., Hutt, K. R., Cheng, C. S., Jin, M., Liu, D., Benner, C., Wang, D., Ye, Z., Bibikova, M., Fan, J. B., Duan, L., Glass, C. K., Rosenfeld, M. G., and Fu, X. D. (2007) Sensitive ChIP-DSL technology reveals an extensive estrogen receptor {alpha}-binding program on human gene promoters. *Proc Natl Acad Sci U S A*

7. Garcia-Bassets, I., Kwon, Y. S., Telese, F., Prefontaine, G. G., Hutt, K. R., Cheng, C. S., Ju, B. G., Ohgi, K. A., Wang, J., Escoubet-Lozach, L., Rose, D. W., Glass, C. K., Fu, X. D., and Rosenfeld, M. G. (2007) Histone methylation-dependent mechanisms impose ligand dependency for gene activation by nuclear receptors. *Cell* 128, 505-518

8. Shang, Y., Hu, X., DiRenzo, J., Lazar, M. A., and Brown, M. (2000) Cofactor dynamics and sufficiency in estrogen receptor-regulated transcription. *Cell* 103, 843-852

9. Pediconi, N., Ianari, A., Costanzo, A., Belloni, L., Gallo, R., Cimino, L., Porcellini, A., Screpanti, I., Balsano, C., Alesse, E., Gulino, A., and Levrero, M. (2003) Differential regulation of E2F1 apoptotic target genes in response to DNA damage. *Nat Cell Biol* 5, 552-558

10. Irwin, M., Marin, M. C., Phillips, A. C., Seelan, R. S., Smith, D. I., Liu, W., Flores, E. R., Tsai, K. Y., Jacks, T., Vousden, K. H., and Kaelin, W. G., Jr. (2000) Role for the p53 homologue p73 in E2F-1-induced apoptosis. *Nature* 407, 645-648

11. Irwin, M. S., Kondo, K., Marin, M. C., Cheng, L. S., Hahn, W. C., and Kaelin, W. G., Jr. (2003) Chemosensitivity linked to p73 function. *Cancer Cell* 3, 403-410

12. Johnstone, R. W., Ruefli, A. A., and Lowe, S. W. (2002) Apoptosis: a link between cancer genetics and chemotherapy. *Cell* 108, 153-164

13. Resnick-Silverman, L., St Clair, S., Maurer, M., Zhao, K., and Manfredi, J. J. (1998) Identification of a novel class of genomic DNA-binding sites suggests a mechanism for selectivity in target gene activation by the tumor suppressor protein p53. *Genes Dev* 12, 2102-2107

14. Tusher, V. G., Tibshirani, R., and Chu, G. (2001) Significance analysis of microarrays applied to the ionizing radiation response. *Proc Natl Acad Sci U S A* 98, 5116-5121

15. Yang, A., Zhu, Z., Kapranov, P., McKeon, F., Church, G. M., Gingeras, T. R., and Struhl, K. (2006) Relationships between p63 binding, DNA sequence, transcription activity, and biological function in human cells. *Mol Cell* 24, 593-602

16. Tang, H. Y., Zhao, K., Pizzolato, J. F., Fonarev, M., Langer, J. C., and Manfredi, J. J. (1998) Constitutive expression of the cyclin-dependent kinase inhibitor p21 is transcriptionally regulated by the tumor suppressor protein p53. *J Biol Chem* 273, 29156-29163

17. Wong, G. H., and Goeddel, D. V. (1988) Induction of manganous superoxide dismutase by tumor necrosis factor: possible protective mechanism. *Science* 242, 941-944

18. Dong, J. T., Lamb, P. W., Rinker-Schaeffer, C. W., Vukanovic, J., Ichikawa, T., Isaacs, J. T., and Barrett, J. C. (1995) KAI1, a metastasis suppressor gene for prostate cancer on human chromosome 11p11.2. *Science* 268, 884-886

19. Mashimo, T., Watabe, M., Hirota, S., Hosobe, S., Miura, K., Tegtmeyer, P. J., Rinker-Shaeffer, C. W., and Watabe, K. (1998) The expression of the KAI1 gene, a tumor metastasis suppressor, is directly activated by p53. *Proc Natl Acad Sci U S A* 95, 11307-11311

20. Duriez, C., Falette, N., Cortes, U., Moyret-Lalle, C., and Puisieux, A. (2000) Absence of p53-dependent induction of the metastatic suppressor KAI1 gene after DNA damage. *Oncogene* 19, 2461-2464

21. el-Deiry, W. S., Kern, S. E., Pietenpol, J. A., Kinzler, K. W., and Vogelstein, B. (1992) Definition of a consensus binding site for p53. *Nat Genet* 1, 45-49

22. Espinosa, J. M., Verdun, R. E., and Emerson, B. M. (2003) p53 functions through stress- and promoter-specific recruitment of transcription initiation components before and after DNA damage. *Mol Cell* 12, 1015-1027

23. Cawley, S., Bekiranov, S., Ng, H. H., Kapranov, P., Sekinger, E. A., Kampa, D., Piccolboni, A., Sementchenko, V., Cheng, J., Williams, A. J., Wheeler, R., Wong, B., Drenkow, J., Yamanaka, M., Patel, S., Brubaker, S., Tammana, H., Helt, G., Struhl, K., and Gingeras, T. R. (2004) Unbiased mapping of transcription factor binding sites along human chromosomes 21 and 22 points to widespread regulation of noncoding RNAs. *Cell* 116, 499-509

24. Wei, C. L., Wu, Q., Vega, V. B., Chiu, K. P., Ng, P., Zhang, T., Shahab, A., Yong, H. C., Fu, Y., Weng, Z., Liu, J., Zhao, X. D., Chew, J. L., Lee, Y. L., Kuznetsov, V. A., Sung, W. K., Miller, L. D., Lim, B., Liu, E. T., Yu, Q., Ng, H. H., and Ruan, Y. (2006) A global map of p53 transcription-factor binding sites in the human genome. *Cell* 124, 207-219

25. Fontemaggi, G., Kela, I., Amariglio, N., Rechavi, G., Krishnamurthy, J., Strano, S., Sacchi, A., Givol, D., and Blandino, G. (2002) Identification of direct p73 target genes combining DNA microarray and chromatin immunoprecipitation analyses. *J Biol Chem* 277, 43359-43368

Chapter 3:
Interactions of p53 and p73 with Human Promoter-Proximal Regions

3.1 Abstract

The p53-family of transcription factors, p53, p63 and p73, regulate both common and distinct sets of genes in a cell-context dependent manner. In this study, we performed a ChIP-chip analysis using the NimbleGen 1.5 kb human promoter arrays to compare the promoter occupancy profiles of p53 and p73 in a human colon cancer cell line at steady state and following hydroxyurea (HU) treatment. HU is a commonly used anticancer drug that induces the cellular levels of p53 and p73. We developed a Model-based Analysis for Promoter array (MAP) algorithm to identify p53 and p73 binding sites with high statistical confidence. Using a cutoff of false discover rate (FDR_{MAP}) <0.005, we identified 201 p53-bound promoters and 360 p73-bound promoters at steady state, 97 of which are bound by both p53 and p73. Following HU treatment, we identified 216 p53-bound promoters and 526 p73-bound promoters, 100 of which are bound by both p53 and p73. Interestingly, we found that p53 and p73 have overlapping and distinct promoter occupancy profiles, both at steady state and following HU treatment. Moreover, HU appears to alter p73 promoter occupancy profile more than that of p53. Detailed mapping demonstrated that p53 and p73 are likely to associate with the same 200 bp genomic region in their overlapping promoters. Expression profiling in cells depleted for both p53 and p73 suggests that ~10% of the binding sites show p53- and p73- dependent transcriptional effects, together with our motif analysis, our results suggest that p53 and p73 may interact indirectly with the promoter-proximal region possibly via protein-protein interactions with other transcription factors.

3.2 Introduction

The three members of the p53-family, p53, p63 and p73, encode sequence-specific transcription factors that regulate genes involved in DNA repair, cell cycle checkpoints, and apoptosis in response to cellular stress (1). Despite a high degree of similarity in their functional domains, mouse knockout studies have shown that these transcription factors have unique functions. In contrast to p53 deficient mice, which are predisposed to early cancer development (2), mice with loss of p63 and p73 have profound defects in their epithelial and neuronal development, respectively (3, 4). Compound heterozygous $p63^{+/-}p53^{+/-}$ or $p73^{+/-}p53^{+/-}$ mice were found to have higher incidence of tumorigenesis and increased metastatic ability than $p53^{+/-}$ single heterozygous mice, suggesting a collaborative role for the p53 family in tumor suppression (5). Taken together, these genetic data suggest that p53, p63, and p73 do not simply function as redundant transcription factors, but may regulate distinct sets of genes depending upon cellular context.

Comparisons of the *in vivo* targets of p53 and p73 have been carried out primarily by conventional approaches (i.e. expression profiling in cells over-expressing p53 or p73). A previous study by Fontemaggi et al. (6) using expression profiling and chromatin immunoprecipitation (ChIP) showed that ectopically expressed p53 and p73 in the same cellular context exhibited partially overlapping transcriptional and promoter occupancy profiles. One caveat is that the targets identified by such approaches may be indirect and/or non-physiologically relevant. In order to compare the promoter occupancy profiles of endogenous p53 and p73, both before and following genotoxic stress, we used a more direct ChIP-based approach in this study.

Recent progress in ChIP-based technologies has assisted the comprehensive mapping of protein-DNA interactions in an unbiased manner (7). Over the past few years, ChIP combined with microarray analysis (known as ChIP-chip) has allowed identification of transcription factor binding sites in mammalian cells and has provided biological insights into the mechanistic functions of many transcription factors, including the p53 family members. Cawley et al. (8) have shown that a large number of p53 binding sites are associated with noncoding RNAs. ChIP combined with high-throughput sequencing technologies such as ChIP-paired-end di-tag (ChIP-PET) has identified a large number of remote sites for p53, suggesting a higher level of p53 transcriptional regulation (9). In line with these results, a recent study by Heintzman et al. (unpublished result) has shown that 24.2% of promoter-distal p53 binding sites in HCT116 cells overlap with predicted enhancers in HeLa cells. In addition, identification of p63 target sites by ChIP-chip analysis using high-density oligonucleotide arrays covering the entire human genome showed that 56% of the gene associated p63 binding sites are located >10 kb away from transcription start site (10). These studies together raise a possibility that p53/p63 at distal sites may interact with promoter-proximal elements through protein-protein interactions.

In this study, we used ChIP coupled with human promoter arrays to examine the interactions of endogenous p53 and p73 with 24,135 human promoters in the promoter-proximal region, both at steady state and following hydroxyurea (HU) treatment. We found that p53 and p73 exhibit both similar and distinct promoter occupancy profiles. We also found that p53- and p73-bound promoters contain non-canonical p53 consensus sequences as well as other transcription factor binding motifs, suggesting the possibility

of a cooperative partnership between the p53 family members and other transcription factors in the promoter-proximal region. Finally, integration of ChIP-chip data with target gene expression analysis led to the identification of common and unique direct transcriptional targets of p53 and p73 in the same cellular context. Taken together, our findings support the genetic data that p53 and p73 can mediate both common and unique functions.

3.3 Materials and Methods

Cell culture and drug treatment

HCT116-3(6) human colorectal cancer cells (ATCC) were grown in high-glucose (4.5-g/liter) Dulbecco's modified Eagle medium (CellGro) supplemented with penicillin G (100 U/ml), streptomycin (100 μg/ml), 10% fetal bovine serum, and L-glutamine (2 mM). Cells at ~80% confluency were treated with 1mM hydroxyurea (Sigma) for 16 hrs.

Immunoblotting

Cells were washed with PBS and lysed in RIPA buffer for 15 min at 4°C. Lysates were clarified by centrifugation for 15 min at 14,000 rpm and supernatants were collected. Protein concentration in the soluble fraction was determined by BioRad DC protein assay. The following antibodies were used at the indicated dilution to detect endogenous proteins: Mouse monoclonal anti-p53 (DO1; CalBiochem) at 1:1000, mouse monoclonal anti-p73 (429; Imgenex) at 1:200, and mouse monoclonal anti-p63 (4A4; Pharmingen) at 1:300, and mouse monoclonal anti-α-tubulin (Clone B-5-1-2; Sigma) at 1:1000 was used as a loading control.

Chromatin immunoprecipitation (ChIP)

HCT116-3(6) cells were cultured in 10 cm plates to 70-80% confluence prior to drug treatment. Cells were fixed with 1% formaldehyde in serum-free media for 10 minutes at room temperature. Formaldehyde crosslinking was quenched with 125 μM glycine (final concentration). Cells were washed in PBS and nuclei were prepared as previously described (11). Cell suspension was sonicated 20 seconds for 8 times to yield DNA fragments with average length ~500 bp using Branson 450 sonifier, setting 4 (25% power output). Lysates were pre-cleared with Protein A/G sepharose for 2 hrs at 4°C. Approximately $3x10^7$ cells were prepared per immunoprecipitation incubated with 5ug of total monoclonal anti-p53 (1:1 mixtures of Ab-1 and Ab-12, CalBiochem) or affinity-purified polyclonal anit-p73 (827) at 4°C overnight. Equivalent amounts of normal IgG were used as negative controls. Protein A/G beads were then added to the immunoprecipitate and incubated for 2 hrs. Beads were then washed sequentially once in low salt buffer, once in high salt buffer, and three times in TE. DNA/protein complexes were eluted and decrosslinked by heating at 65°C overnight. Eluates were treated with Proteinase K and DNA fragments were extracted with phenol/chloroform 2X and treated with RNAse A. DNA fragments were then purified and eluted in TE using Qiaquick PCR purification columns (Qiagen).

NimbleGen promoter array analysis

Total input and ChIP DNA prepared from untreated and HU-treated cells were amplified by LM-PCR as previously described (12) and hybridized to 1.5 kb promoter

arrays manufactured by NimbleGen Systems, Inc. (Madison, WI). The 1.5 kb promoter array is a single-array design that covers 24,135 human promoters. For each promoter, 15 50mer probes were designed to tile across the proximal region from -1300 to +200 relative to the transcription start site. Probe labeling and hybridization were performed by NimbleGen (Reykjavik, Iceland).

Quantitative PCR analysis for qChIP validation

Selected promoters were verified by SYBR Green quantitative PCR analysis. Primers were designed to span the peak region using Primer Express v2.0 (Applied Biosystems). Each PCR was performed in duplicate in a 25 μl reaction with 5 ng of LM-PCR amplified total or ChIP DNA and 1X SYBR Green master mix (Applied Biosystems). Fluorescence values were determined by ABI Prism 7900HT sequence detection system (Moores-UCSD Cancer Center Shared Resource). Fold enrichment was calculated in terms of occupancy units as described in Yang et al (10). Fold enrichment (occupancy units OU)= $1.9^{-(\text{delta CT}_{\text{expt}}-\text{delta CT}_{\text{Tk1}})}$ where delta $CT=CT_{IP}-CT_{Input.}$ Specificity of the PCR reaction was confirmed by the presence of a single peak in dissociation curve analysis and a single product on agarose gel electrophoresis. Primer sequences are listed in Table3-12.

Data analysis for NimbleGen promoter arrays

A Model-based Analysis for Promoter array (MAP) algorithm was developed based on the Model-based Analysis for Tiling array (MAT) algorithm (13) to identify p53 and p73 ChIP-enriched sites (see details below). The Pearson correlation coefficient (*r*) is derived from linear regression analysis.

Motif search

We extracted the 2.5 kb query sequence (1.5 kb probe region plus 500 bp surrounding either side of the 1.5kb probe region) for each candidate promoter from the human chromosome build 35 (hg17) assembly. We used the motif search program Clover (Cis-eLement OVERrepresentation) http://zlab.bu.edu/clover/ to search for p53 motif in p53 and p73-bound promoters. A position-specific score matrix (PSSM) for p53 obtained from an open-source transcription factor binding site database, JASPAR (14), was scanned across the target and background sequences. We also searched p53- and p73-bound promoters against the JASPAR database for other overrepresented motifs corresponding to 123 curated transcription factor binding motifs using pval cutoff <0.001.

p53 half site search

70 randomly selected promoters using FDR_{MAP} <0.005 from each of the following four groups were subjected to p53 half site search: p53 (-HU) specific, p53 (+HU) specific, p73 (-HU) specific, and p73 (+HU) specific sequences containing PuPuCA/TA/TGPyPyPy or PyPyPyCA/TA/TGPuPuPu are considered positive hits. One mismatch in either Pu or Py position is allowed.

Go term analysis

Functional classifications of target genes were performed using the web-based program Database for Annotation, Visualization, and Integrated Discovery (DAVID) http://niaid.abcc.ncifcrf.gov/home.jsp

siRNA transfection

Small interfering RNA (siRNA) duplexes against p53, p73 and lacZ were obtained from Dharmacon (15). HCT116-3(6) cells were transfected with RNA duplexes in suspension using Oligofectamine (Invitrogen).

siRNA expression profiling

Total RNA from HCT116-3(6) cells transiently transfected with lacZ or p53/p73 siRNA oligos with/without treatment of HU was isolated using RNeasy Mini Kit (Qiagen), converted to cRNA, labeled with Cy5 or Cy3 dUTP using Agilent Low Input Linear RNA Amplification Kit, and hybridized to the Phalanx Human One array http://www.phalanxbiotech.com/Power/Power.html. After hybridization, the slides were scanned with Axon 4000B, and the raw data were generated by Genepix 6.0. 4 biological repeats were performed for each condition, with 2 technical repeats (dye swap) per biological sample. The data was normalized with quantile normalization of DNAMR (R package DNAMR, http://www.rci.rutgers.edu/~cabrera/DNAMR), fitted with linear model of R package Limma (16). Two comparisons were performed: control vs. double knockdown in –HU and +HU conditions. Pval was calculated using t-statistics. To integrate ChIP-chip data with siRNA gene expression profiling, we first selected promoters bound by p53 or p73 (FDR_{map} <0.005) and are covered by the expression array, and from which we identified differentially expressed genes in p53/p73 knockdown cells (pval <0.1).

Model-based Analysis of Promoter Arrays (MAP)

The probe level hybridization signals were processed by a method that is similar to the Model-based Analysis of Tiling-arrays (MAT) proposed by Johnson et al. (13). The MAP algorithm makes the assumption that in a ChIP-chip experiment only a very small fraction of the probes will hybridize to the protein-bound DNA sequences, while the majority of the probes will measure only background noise, which can be influenced by the sequence configurations of the probes. To distinguish the true biological signals from background noise, we can use a sequence specific model to relate the probes signals to their sequence characteristics and the model fitting residues. In other words, MAP can greatly reduce the background noise caused by probe copy number effect and probe sequence characteristics (i.e. GC content). By this way, we can borrow information from thousands of probes on the chip with similar sequence configurations to eliminate sequence specific noises, and achieve a much better result in locating true binding sites than comparing the signal of individual probes across a very limited number of control experiments.

First, the 50-mer probes were mapped onto build 36.1 finished human genome assembly (hg18, Mar 2006) downloaded from the UCSC Genome Bioinformatics Site (http://genome.ucsc.edu/) using the extreme MApping of OligoNucleotides (xMAN) software developed by Shirley Liu's group (http://chip.dfci.harvard.edu/~wli/xMAN/). Out of the 353,126 probes on NimbleGen array, 1,214 (0.34%) of them cannot be mapped due to the update of human genome sequences, 345,061 (97.72%) of them can be mapped to exactly 1 location, 351,815 (99.63%) of them have 1 to 9 mapped locations

and 97 (0.03%) of them have 10 or more mapped locations. Only probes having 1 to 9 mapped locations were used to in the following model based analysis.

Following probe filtering based on mapped locations, the log of the probe signals for each channel in an experiment were fitted by a linear model (13):

$$\log(y_i) = \alpha n_{iT} + \sum_{j=1}^{50} \sum_{k\in\{A,C,G\}} \beta_{jk} I_{ijk} + \sum_{k\in\{A,C,G,T\}} \gamma_k n_{ik}^2 + \delta \log(c_i) + \varepsilon_i$$

where

- y_i is the signal level of the *ith* probe, $i = 1, \ldots, 351{,}815$;
- n_{ik} is the count of nucleotide k in the *ith* probe, $k \in$ (17 G);
- α is the baseline value (intercept or constant) based on the number of nucleotide T in the probe, e.g., 50α is the baseline when the probe sequence is a run of 50 Ts;
- I_{ijk} is an indicator function, $I_{ijk} = 1$ if the nucleotide at position j is k in the *ith* probe, and $I_{ijk} = 0$ otherwise;
- β_{jk} is the effect of each nucleotide k (except T, which is already modeled in α) at position j;
- γ_k is the effect of nucleotide count squared;
- δ is the effect of the log of the probe copy number;
- c_i is the number of times that the sequence of the *ith* probe appears in the genome by mapping the 50-mer probe sequence against whole human genome sequence;
- ε_i is the probe-specific error term, assumed to follow a Gaussian distribution.

There are 156 parameters in this linear model (1 for α, 3*50 for β_{jk}, 4 for γ_k, and 1 for δ). For each channel in each experiment, the probe signals were fitted by the above model and the 156 parameters were estimated using a robust linear regression

(Venables, W. N. and Ripley, B. D. (2002)) Modern Applied Statistics with S, 4th edition. Springer). We used a robust linear regression instead of the simple least square regression proposed by Johnson et al. (13). With robust linear regression, outliers will be down-weighted so the model can better approximate the background signals. After estimating the sequence specific parameters, we calculated the model fitting residues for each probe on the chip and used the model fitting residues as the standardized probe scores.

According to NimbleGen's chip design files, the probes were grouped into 24,092 promoter regions with most of the regions having 15 probes. In each promoter region, we used a sliding window of 250 bp to calculate window scores as the median of the probe scores in a window when there are at least 5 probes within a window. For a promoter region, we assigned the maximum window score as the score for the promoter. When there is no specific protein binding DNA hybridized on the chip, the model fitting residues as well as the window scores will follow a Gaussian distribution which is symmetric to 0. That is why we can use the negative tail of the pooled window scores to approximate the NULL distribution and to control for false discovery within each channel. For each promoter score x, we first calculated

$$F(x) = \frac{\sum_i I_{w_i > x} / nW}{\sum_j I_{p_j > x} / nP}$$

Where i goes through all windows, wi is the ith window score, nW is the total number of windows we calculated, j goes through all promoters, pj is jth promoter score, nP is the total number of promoters, $I_{w_i > x}$ and $I_{p_j > x}$ are indicator functions. Then the false

discovery rate of x is calculated in a way similar to that of q-value proposed by Storey et al 2003 (18) to guarantee a monotonic relationship between the promoter score and their FDR.

$$FDR(x) = \min(F(t) : t <= x)$$

We noticed that although the variations of the standardized probe scores are very close in all 4 IP and input channels, the promoter scores calculated in the input channels have much higher variation than the IP channels. This may due to the fact that the whole genome DNA were randomly amplified in the input channels, and the amplification bias introduced additional variation to the calculation of the promoter scores. Therefore we were unable to take the promoter scores from input channels to control the FDR for IP channels, even after standardized the standard deviations. We also tried to subtract window scores of the input channel from the corresponding IP channel, but the result was not better than controlling FDR within each individual channel.

3.4 Results

3.4.1 Identification of p53 and p73 binding sites

In light of the high structural similarity between p53 and p73 within the DNA binding domain, we performed ChIP-chip to compare the promoter occupancy profiles between p53 and p73, both before and after HU treatment. To this end, crosslinked chromatin from untreated and HU-treated HCT116-3(6) cells were immunoprecipitated with anti-p53 or anti-p73 (see Chapter 2 for details). ChIPs with non-specific IgGs were performed in parallel as negative controls. Samples for microarray analysis were

amplified by LM-PCR (Figure 3-1A). Prior to hybridization, we tested the specificity of the amplified DNA by PCR using primers specific for the p21cip1 promoter-distal region (Figure 3-1B). As expected, the p21cip1 promoter was enriched in the p53 and p73 amplicons but not in IgG amplicons, suggesting that LM-PCR step had retained the specificity of the original ChIP sample. Having confirmed the specificity of the amplicons, we labeled the experimental p53 IP or p73 IP amplicons and the total input amplicons with Cy3 and Cy5 dye, respectively. Each set of these samples from -HU or +HU condition were co-hybridized to the NimbleGen 1.5kb promoter arrays.

In order to identify binding sites with high statistical confidence, we developed the MAP (Model-based Analysis for Promoter arrays) algorithm to identify p53 and p73 ChIP-enriched sites (Figure 3-2A and details are described in the Materials and Methods section). For each promoter, the algorithm calculates a window score for each 200 bp sliding window over the 1.5 kb probe region and computes the false discovery rate (FDR_{MAP}). In the end, we took the maximum window score as the promoter score. To evaluate the overall correlation between experiments, we plotted pair-wise scatter plots of the promoter scores of all 24,135 promoters between all six possible pairs of conditions for both the IP and input channels. The promoter scores between technical repeats are highly correlated, with R^2 value of 0.6 and 0.9 (Figure 3-2B; left panel). The promoter scores among the IP channels are also correlated, with R^2 values above 0.5 between any pair of conditions (Figure 3-2B; right panel). We next applied MAP to each of the four experiments and identified ChIP-enriched region with defined FDR cutoffs. In summary, using FDR cutoff ranging from 0-0.05, we identified ~500-~3000 ChIP-enriched regions

in each of the four IP channels, and a relatively smaller number of false positives from the corresponding input channels (Table 3-1).

Table 3-1. Summary of MAP analysis

FDR_{MAP} cutoff	p53 untreated IP	P53 untreated Input	p53 HU IP	p53 HU Input	p73 untreated IP	p73 untreated Input	p73 HU IP	p73 HU Input
0.001	575	211	615	81	1006	279	1407	152
0.005	1083	374	1062	84	1359	489	1889	183
0.01	1310	687	1199	136	1555	787	2129	268
0.05	1873	1464	1778	750	2210	1718	2642	985

3.4.2 Validation by qChIP

We performed ChIP and real-time quantitative PCR assays (qChIP) on selected promoters identified by MAP analysis. We first tested the effectiveness of qChIP method on the two positive controls, p21CIP1 and p53R2, by using gene-specific primers spanning the previously characterized p53 response element. Promoter enrichment was calculated in terms of occupancy units as described in Yang et al. (10). Both p21CIP1 and p53R2 promoters are constitutively occupied by both p53 and p73 (not shown). Based on the occupancy units of the negative controls, we defined occupancy units of 2 or greater as positive confirmation (not shown).

To evaluate the accuracy of the MAP analysis, we first performed qChIP to scan across a selected chromosome region of a candidate promoter. We found that OU correlates quite well with the window scores; in other words, peak region identified by MAP shows the highest OU over adjacent regions (Figure 3-3). We next performed qChIP to empirically determine the false discovery rate of the Chip-chip experiments. The procedure for qPCR verification and primer design is shown in Figure 3-4A.

According to the suitability of the primer design, we selected 20 promoters with FDR_{MAP} <0.05 in the IP channel and FDR_{MAP} > 0.8 in the input channel across all four experiments. Primers used for validation were designed to span the maximum window score window (Figure 3-4A; right schematic). Selected promoters and their occupancy units expressed in a log2 scale in all 4 conditions are shown in Figure 3-4B. As negative controls, we also performed qPCR with DNA amplified from non-specific IgG samples. No or weak enrichment of these promoters were found in IgG controls (data not shown). As might be expected, different degrees of enrichment were observed among the 20 promoters, indicating that p53 or p73 have different DNA binding affinity for specific targets.

Based on the validation of the 20 selected promoters, we determined the false positive rate for each experiment using a weighted approach as described in Yang et al. (10), to assess the accuracy of the FDR computed by MAP (FDR_{MAP}). Toward this goal, we sorted the candidate binding sites into different bins according to FDR_{MAP} and experimentally determined the false positive rate for each bin. As the result, we found that the FDR_{MAP} calculation was underestimated as compared to the experimentally determined false positive rate. For example, at FDR_{MAP} <0.005, the false positive rate for the two p53 experiments were in fact around 17-25%. At FDR_{MAP} <0.005, the false positive rate for the two p73 experiments were nearly 25-37%. To carry out subsequent analysis with least 60% confidence level, FDR_{MAP} cut off <0.005 in the IP channel and FDR_{MAP} >0.8 in the corresponding input channel were used as selection criteria for statistically significant ChIP-enriched regions in all four experiments. The number of

promoters that passed the defined cutoff in each experiment is summarized in Table 3-2 (highlighted in yellow).

3.4.3 Comparison of p53 and p73 promoter occupancy profiles at steady state and following HU treatment

Using the FDR cutoff defined as above, we identified 201 p53-bound promoters and 360 p73-bound promoters at steady state. Interestingly, we found that the promoter scores of p53 bound promoters and p73 bound promoters in p53(-HU) and p73 (-HU) experiments are correlated, with a Pearson correlation coefficient (r) of 0.3 and 0.5, respectively (Figure 3-5A). Following HU treatment, we identified 216 p53-bound promoters and 526 p73-bound promoters. The promoter scores of p53 bound promoters in p53 (+HU) and p73 (+HU) experiment are also moderately correlated with a Pearson correlation coefficient r= 0.4, suggesting that p53-bound promoters exhibit some degree of similarity with p73-bound promoters following HU treatment (Figure 3-5B; left scatter plot). In contrast, the promoter scores of p73 bound promoters in p53 (+HU) and p73 (+HU) experiments are weakly correlated (r=0.07), which suggests that p73 binding profile differs from p53 following HU treatment (Figure 3-5B; right scatter plot). Representative examples of novel p53 and p73 overlapping and p53-specific and p73-specific promoters in –HU and +HU conditions are shown in Table 3-2

3.4.4 The effect of HU on the promoter occupancy profiles of p53 and p73

To investigate the effect of HU on the promoter occupancy profiles of p53 and p73, we next examined the degree of overlap between the promoters identified in –HU and +HU conditions. We found that the promoter scores of p53-bound promoters

between –HU and +HU conditions are moderately correlated, with a correlation coefficient of 0.58 (Figure 3-5C; left scatter plot). The promoter scores of p53 (+HU) bound promoters in p53 (–HU) and p53 (+HU) experiments are also correlated, with a correlation coefficient of 0.44 (Figure 3-5C; right scatter plot), which suggests that p53 exhibits a similar promoter occupancy profile following HU treatment. Similarly, the promoter scores of p73 (-HU) bound promoters in p73 (-HU) and p73 (+HU) experiments are also correlated with a similar degree correlation as p53. (Figure 3-5D; left scatter plot). However, the promoter scores of p73 (+HU) bound promoters in p73 (-HU) and p73 (+HU) experiments are less correlated (r=0.11), implying that HU has a different effect on p73 promoter occupancy profile than p53 (Figure 3-5D; right scatter plot).

3.4.5 p53 and p73 associate with the same genomic region of DNA

It has been shown that p53 requires both p63 and p73 for stable binding at apoptotic promoters in response to doxorubicin (19). However, the mechanism by which the p53 family members cooperate to induce apoptosis upon DNA damage remains to be elucidated. Two models for the cooperation of the p53 family members at the promoter level have been proposed by Urist et al. (20). Presumably, if the p53 family members can bind to the same response element, it is conceivable that p63 and p73 have an indirect role in the stabilization of p53 tetramers at the promoter through interaction with other co-activators since wild-type p53 cannot form co-tetramers with p63 or p73 *in vivo* (21) (Figure 1-2). Alternatively, p53 and p63/p73 cooperate by binding to discrete sites in the target gene promoter (Figure 1-2). To address how p53 and p73 interact at the promoter level, we selected promoters that are bound by both p53 and p73 in either –HU or + HU condition and identified peak regions for p53 and p73 (Figure 3-6B). We reasoned that if

p53 and p73 bind to the same DNA region within a target gene promoter, their peaks should reside in windows that are close in vicinity (Figure 3-6A; SR or OR). In both –HU and +HU conditions, we found that over 80% of p53- and p73-bound promoters contain peaks either in the same or neighboring windows (SR or OR), which suggests that p53 and p73 bind to the same region of DNA (Figure 3-6C). Interestingly, at steady state, <10% of p53- and p73–bound promoters contain peaks in non-overlapping windows (DR), suggesting that a relatively small percentage of promoters may contain discrete binding sites for p53 and p73 (Figure 3-6C; top panel). Following HU treatment, 23% of p53- and p73-bound promoters contain peaks in different genomic regions (DR), suggesting that p53 and p73 may bind to different regions of promoters in response to HU (Figure 3-6C; bottom panel). Taken together, our data supports the model that p53 and p73 are likely to associate with the same genomic region in the majority of their overlapping promoters.

3.4.6 Motif Search

Previous studies have suggested that the promoter-proximal region does not constitute the majority of binding sites of p53 or p63 (9, 10). Therefore, it is likely that p53/p63 may bind to distant (enhancer) sites and cooperate with other transcription factors in the proximal region via DNA looping. Typically, p53 transactivates its target genes through binding to two or more tandem repeats of the 10-bp half-site PuPuPu CA/TA/TG PyPyPy, where Pu and Py stands for purine and pyrimidine, respectively. The length of spacer between the repeats can be variable, ranging from 0-13 bases (22). Sequence degeneracy, variability in the number of p53 half-sites, and difference in the linker length may account for the versatility of functions mediated by p53. Although it

remains unknown whether p73 has a DNA sequence selectivity in binding, *in vitro* studies have shown that p53 and p73 exhibit similar sequence-specific affinity for the p53 response element (23, 24). Due to the degeneracy of the p53 consensus motif, we implemented the motif search program CLOVER (25) to search for imperfect p53 consensus sequence matches in each of the promoters identified from the four experiments by using a p53 weight matrix (Figure 3-7A; sequence logo). Considering the possible impreciseness of peak-finding algorithms, we extended our search to also include 500 bp up- and downstream form the 1.5 kb promoter region (Figure 3-7A; top schematic). Consistent with the fact that many experimentally determined transcription factor binding sites from ChIP-chip studies lack canonical motifs (8, 26), we found that a very small percentage (<5%) of p53 and p73-bound promoters contain a full p53 consensus site with $p<0.01$ (Figure 3-7B). We reasoned that a subset of these promoters contain non-canonical p53 sequence or even non-p53 response element, which may not be detected by standard algorithms. Since the spacer between the half-sites in target promoters can be highly variable, we also scanned p53- and p73-specific promoters for any putative 10-bp p53 half-sites in the peak regions. The two most predominant types of p53 half-sites present in the candidate promoters are: PuPuPuCA/TA/TGPyPyPy (forward) or PyPyPyCA/TA/TGPuPuPu (inverted). Since p21 has an 18/20 bp match to the consensus sequence, we allowed at most one base deviation from the consensus p53 half site in the forward orientation or inverted orientation to be called putative p53 half sites. Interestingly, we found that ~ 50% of p53 or p73 specific promoters from all 4 experiments harbor either one or more matches to the p53 half-site sequence in either the forward or inverted orientation allowing one mismatch in the sequence (Figure 3-7B and

Table 3-10). Taken together, our p53 motif search suggests that p53/p73 can bind to non-canonical p53 response elements in their target promoters.

It has been reported that p53 can physically interact with TBP (27) and EGR1 (28), as well as CREB1 (29). Given that some ChIP-enriched regions do not contain recognizable p53 consensus motifs (Figure 3-7B), it is likely that p53/p73 can interact with non-consensus p53 motif and/or other transcription factor binding sites via protein-protein interactions. To ask whether p53- and p73-bound promoters contain any overrepresented motif sequences, we performed a motif search against JASPAR transcription factor database that contains 123 non-redundant and experimentally defined transcription factor binding motifs. Interestingly, we found that p53 and p73-bound promoters are statistically enriched with sequence motifs for C2H2 zinc finger proteins (i.e. sp1, snail) and basic helix-loop-helix transcription factors (Figure 3-7C). Previous findings have shown that p53 and sp1 can be physically associated and function cooperatively to regulate gene expression of p21 (30) and Bax (31). p73 can also interact with sp1 to mediate repression of cyclin B1 transcription (32). Consistent with these findings, we found sp1 (pval=0) is highly overrepresented in p53- and p73 –bound promoters in all 4 experiments (Figure 3-7C). These promoters are also enriched with sequences motifs for Snail family of zinc finger transcription factors (pval=0), which are shown to be involved in cell movement in developmental processes. Interestingly, we have also identified overrepresented motifs that are unique to p73, such as PAX4 (pval=0), which is a transcriptional repressor involved in early pancreatic development. Taken together, our motif search implies that p53/p73 may interact indirectly with

proximal promoter elements through secondary interaction with other transcription factors.

3.4.7 Functional classification of p53 and p73 targets

To compare the biological functions of p53 and p73, we assigned functional categories to each candidate promoter using the DAVID GO term analysis program. The significance of each identified category is provided by a p-value that measures the likelihood of finding the identified category by random chance. We ranked the categories by p-value and highly represented categories (>5%) from each experiment were selected using a p-value cutoff <0.01. As expected, more than 50% of the p53 targets fell into the same functional categories as the p73 targets, suggesting that p53 and p73 share common physiological functions in the absence of cellular stress (Table 3-7). The top overrepresented GO terms include glycoprotein, signal, and disease mutation. We also performed functional classification on p53 and p73 bound promoters in +HU condition. Similarly, we found that p53- and p73-bound promoters have both common and distinct Go terms following HU treatment. (Table 3-8 and Table 3-9). Interestingly, we found that p53 and p73 co-occupied promoters in both –HU and +HU conditions are significantly enriched in signal transduction pathways, suggesting that p53 and p73 may mediate biological responses via regulation of genes encoding various signaling components (Table 3-10). Taken together, functional classification of p53 and p73 target genes revealed that p53 and p73 can mediate both common and unique biological processes.

3.4.8 Relationship between p53/p73 binding and gene expression

To determine the transcriptional effects of p53 and p73 binding, we performed a gene expression profile in untreated and HU-treated cells depleted for both p53 and p73 via transient transfection of siRNA (Figure 3-8). Similar to what Yang et al. (10) reported, we also found that only 10-20% of p53 and p73 bound genes exhibit significant changes in mRNA expression in p53/p73 siRNA double knockdown versus control cells (Table 3-4). In other words, p53/p73 binding to a promoter does not guarantee direct regulation of its expression. Double knockdown of both p53 and p73 can either decrease or increase the transcript levels of several p53 and p73 co-occupied promoters, supporting the notion that p53 and p73 can both repress and activate a common set of genes (Table 3-5 and Table 3-6).

3.5 Discussion

Several ChIP-based approaches have successfully applied to map p53 and p63 binding sites (8-10, 33-35). The structural similarity between p53 and p63/p73 suggests that they can regulate common set of genes. It has also been shown biochemically that the core DNA-binding domains of p53 and p73β exhibit similar sequence preference both *in vitro* and *in vivo* (36). The idea that p53 and p63 bind a common set of promoters has been demonstrated by two recent ChIP-chip studies (9, 35). However, to date, a direct comparison of *in vivo* binding sites of p53 and its family members has not yet been performed. In this study, we compared promoter occupancy profiles of p53 and p73 in the same cellular context using ChIP combined with DNA microarray analysis. The

range for the number of promoters identified in our study (~100-500) is in accord with Yang et al. (10), in which they found that 400 out of 5800 p63 binding sites are located within 5kb upstream to 1kb downstream relative to well-characterized genes. Of the 24,135 human promoters surveyed in this study, we found that: (1) p53 and p73 have overlapping and distinct promoter occupancy profiles, both at steady state and following HU treatment. (2) Detailed mapping shows that p53 and p73 occupy the same region of DNA in their overlapping promoters. (3) Following HU treatment, we found no major change in the overall promoter occupancy profile of p53, where the promoter scores of p53 bound promoters in untreated and HU-untreated conditions remain correlated. Consistent with our finding, a CGI ChIP-chip study (37) has shown that p53 binds to the same set of promoters during hypoxia and DNA damage, suggesting that p53 promoter occupancy profile is not stress-dependent. In contrast, we found that HU alters the promoter occupancy profile of p73 more than that of p53. The physiological significance of the differential effects of HU on p53 and p73 promoter occupancy profiles awaits further investigation.

We found that 51 of the 541 high-confidence p53 binding sites identified by Wei et al. (9) in a ChIP-PET study were mapped within the promoter-proximal region covered by the 1.5 kb NimbleGen promoter array used in this study. Of these 51 sites, 4-20% overlap with the p53 or p73 sites identified in our study (Figure 3-8). Comparisons of ChIP-PET and ChIP-chip on ER (38) and STAT1 (39) targets revealed differential binding site discovery between the two technologies, suggesting that these two methods are complementary for the identification of transcription factor binding sites at the genome-wide level. Out of the 5807 p63 binding sites identified by Yang et al. (10), we

found that 407 of these sites were mapped within the proximal promoter region covered by the 1.5 kb NimbleGen promoter array. Our MAP analysis suggests that 6-14% of these sites overlap with the p53 or p73 sites identified in our study (Figure 3-9). Differences in the experimental conditions and methodologies between the two studies may account for the minimal overlap of targets

The crystallographic analyses of p53 suggests that the tetrameric structure of p53 binds to DNA as a dimer of dimers, with each monomeric subunit interacting with a quarter site (40, 41). *In vitro* studies have shown that one dimer within the tetramer is sufficient for binding to one half-site in DNA. Concurrent interaction of the second dimer with a second half-site in DNA enhances binding affinity by at least 50 fold (42). Our p53 motif search revealed cases where ChIP-enriched regions contain single p53 half sites. We speculate that one of the p53 dimers bind to the half-site while the other dimer may stabilize protein-DNA interaction without directly contacting DNA. Alternatively, synergism between proximal and distal p53 binding as seen in the MCK promoter (43), may also provide explanation for the presence of single p53 half sites in some promoters.

Our current study suggests that the majority of p53 binding sites do not contain p53 consensus binding sites in the proximal promoter region. The lack of a p53 consensus binding motif may be explained by a number of reasons: First, p53-DNA interactions in the promoter–proximal region may be a result of secondary interactions mediated by other proteins. Hence it is likely that p53 and p73 may modulate constitutive gene expression through long-distance interaction via a DNA looping mechanism, which can be examined by a 3D chromosome capture assay (44) . A similar mechanism has been proposed for SUZ12, a subunit of the polycomb group proteins (45). Second,

cooperative interactions between multiple transcription factors could alter the binding preference of an individual transcription factor thus reduce the requirement for a consensus site. Alternatively, p53/p73 can also bind to as of yet unidentified noncanonical p53 consensus sites or nontransactivating regulatory elements to regulate other processes such as DNA repair and recombination (46).

Our present study helps to address several questions in the functional interaction between p53 and p73: First, we show that p53 and p73 can occupy distinct promoters and regulate a subset of these target genes. Therefore, p53 and p73 can function independently of each other in regulating the expression of some target genes. Second, since no evidence has demonstrated the direct association between the full length p73 and wild type p53 (47), the mechanism by which p53 cooperates with p73 in transactivating a subset of genes remains to be elucidated. Based on our results, we found that p53 and p73 can bind to the same genomic region in their target promoters. Nevertheless, it remains unknown whether p53 and p73 can simultaneously occupy the same sequence, or whether p53 and p73 can associate with the same sequence in different DNA molecules. Quantitative sequential ChIP can be used to distinguish between these two possibilities (48). In addition, a higher resolution mapping of these promoters is required to determine whether p53 and p73 bind to the same sequence in their common target promoters. Gel shift experiments have shown that p73α can compete with p53 for the same DNA sequence in an ovarian cancer cell line overexpressing p73 (49). If this were true in other cancer types, p73 might function as an oncogene by attenuating p53 functions in tumors with overexpression of p73, which would be against current thoughts on p73 as a help of

p53. Consistent with this idea, a recent study also showed that p73 can replace p53 in the suppression of genetic instability (50).

The mechanism of how promoter specificity is achieved among the p53 family is unclear. It has been shown that the target specificity of p53 and p63 may be attributed to the differential recognition of the p53 response element (51), which can be explained by their biochemical differences in terms of their interactions with *in vitro* DNA binding sites (36). While p53 preferentially binds to CATG-containing sequences rather than CGTG-containing sequences, TAp63γ can bind to both CATG- and CGTG-containing sequences with similar affinities (51). Detailed biochemical studies are required to address how functional differences among the p53 family members may be due, in part, to the differential recognition and DNA binding affinity for the p53 response element.

Consistent with the notion that DNA binding does not directly result in transcriptional activation (52), our data suggests that only ~10% of p53/p73 bound gene loci are associated with expression changes. This can be accounted by the fact that although p53/p73 can bind to their target sites under both activating and non-activating conditions, p53/p73 may regulate transcription only under specific contexts and/or may require combined functions of multiple transcription regulators. Alternatively, a subset of p53 or p73 binding targets is likely to be regulated at a post-DNA binding step and may involve complex control beyond transcriptional regulation, such as regulation of chromatin structure. Moreover, p53/p73 can regulate secondary targets via regulatory cascades, therefore, differentially expressed genes identified from siRNA expression profiling can include indirect targets whose expression may be not affected by the deletion of p53 and p73. Since siRNA expression profiling was performed at one time

point, the dynamics of gene expression changes associated with p53/p73 binding may have been missed.

In conclusion, our findings suggest that p53 and p73 can bind both common and non-overlapping promoters in the absence of cellular stress and following HU treatment. Furthermore, their differential promoters occupy profiles in response to HU implies that they might regulate distinct biological responses to genotoxic stress. A high resolution mapping of binding sites combined with expression and epigenetic studies would provide keys to the understanding of the diverse functions of the p53 family.

3.6 Acknowledgements

Chapter 3, in part, is a reprint of the material as it appears in a manuscript, "Interactions of p53 and p73 with Human Promoters." Huang, V., Lu, X., Jiang, Y., and Wang, J.Y.J. The dissertation author was the primary investigator and author of this publication.

3-1A)

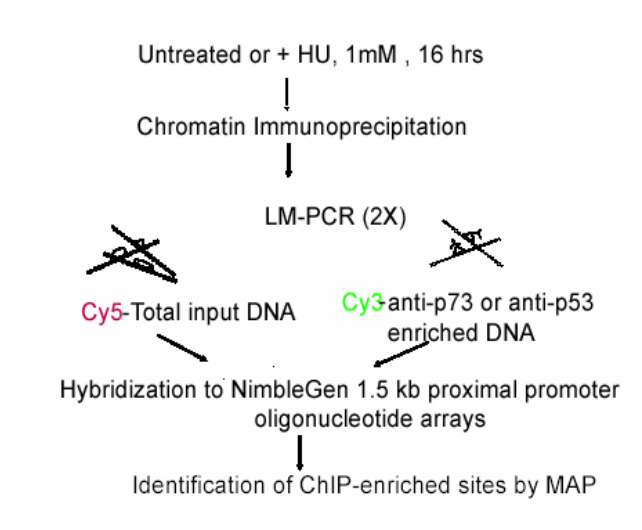

3-1B)

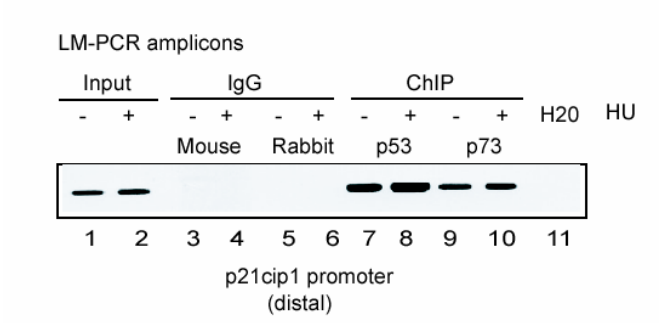

Figure 3-1. ChIP-chip analysis of p53 and p73 promoter occupancy profiles
(A) Scheme for ChIP-chip analysis. (B) Confirmation of ChIP and LM-PCR amplified amplicons. Enrichment of the p21cip1 distal promoter region was used to check the specificity of the samples prior to hybridization. p53 and p73 ChIP (lanes 7-10) and a nonspecific IgG control (lanes 3-6) were performed as described in Figure 2-3A. M: Mouse IgG, R: Rabbit IgG. Total input DNA (lanes 1,2) was used as a positive control.

3-2A)

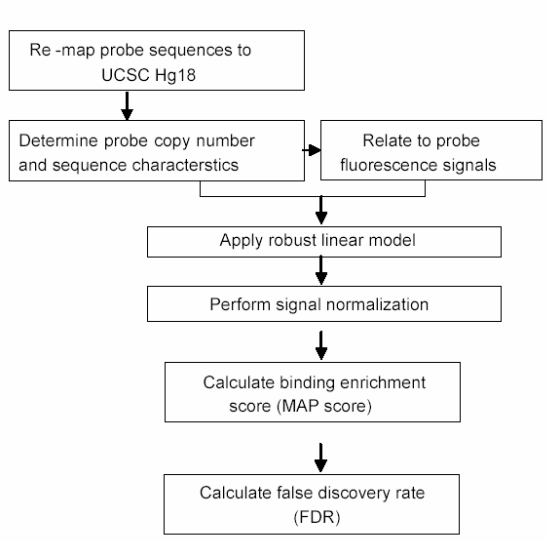

3-2B)

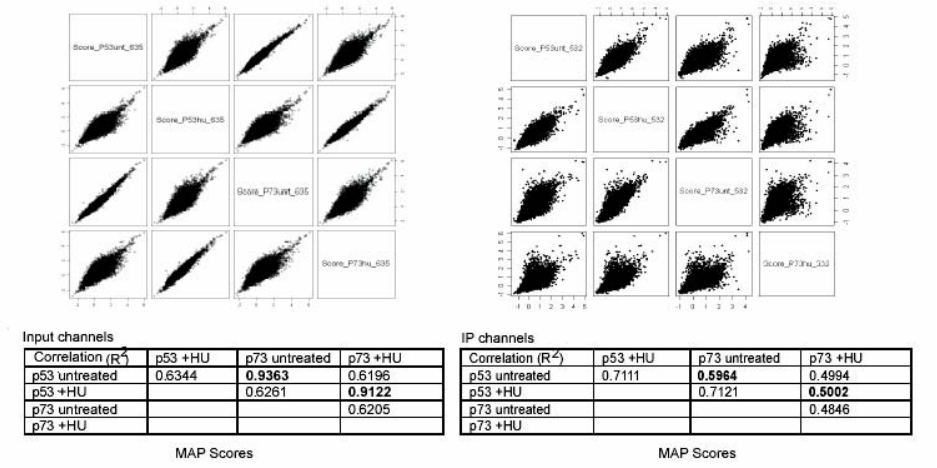

Input channels

Correlation (R^2)	p53 +HU	p73 untreated	p73 +HU
p53 untreated	0.6344	**0.9363**	0.6196
p53 +HU		0.6261	**0.9122**
p73 untreated			0.6205
p73 +HU			

MAP Scores

IP channels

Correlation (R^2)	p53 +HU	p73 untreated	p73 +HU
p53 untreated	0.7111	**0.5964**	0.4994
p53 +HU		0.7121	**0.5002**
p73 untreated			0.4846
p73 +HU			

MAP Scores

Figure 3-2. Identification of p53 and p73 ChIP-enriched promoters by MAP
(A) Flowchart of MAP algorithm for the identification of ChIP-enriched promoter region. (B) Pair-wise scatter plots of the promoter scores for the 4 input channels (left) and the 4 IP channels (right). The R^2 value for each pair of conditions is summarized in the bottom table.

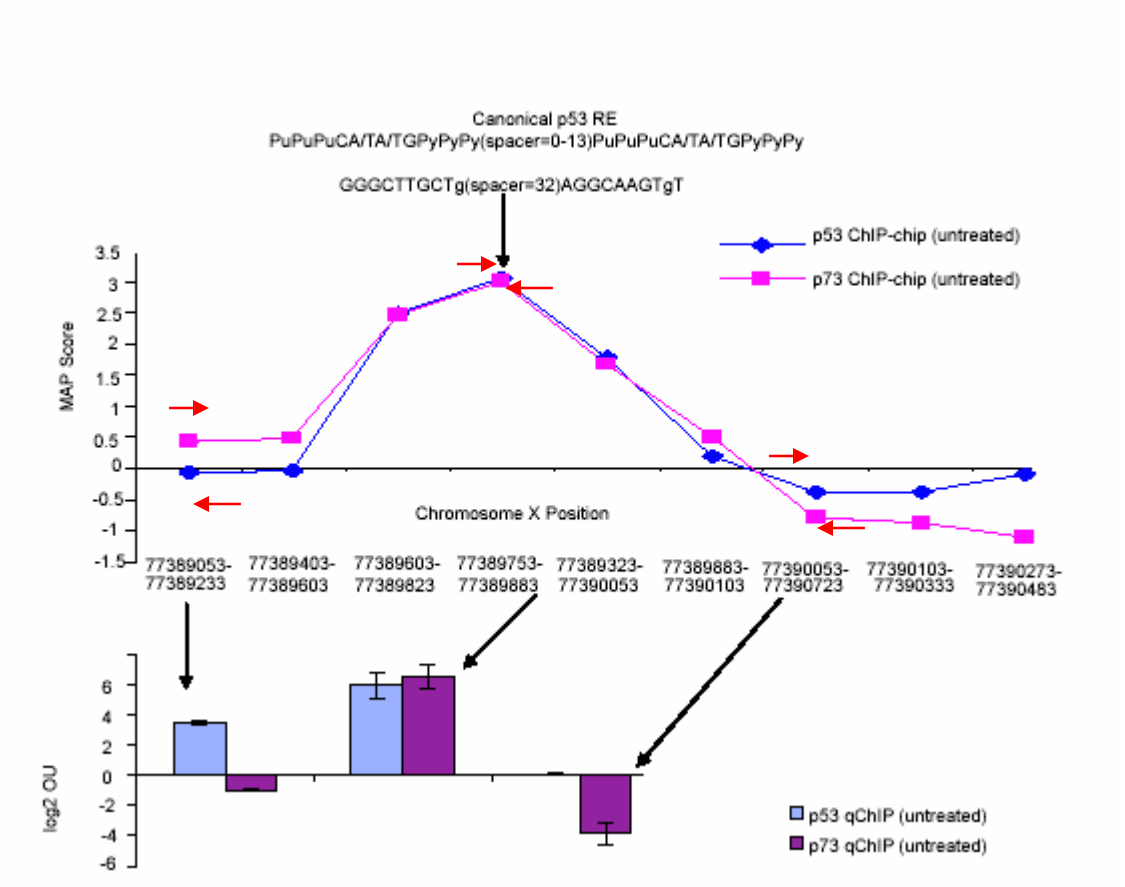

Figure 3-3. qChIP validation of MAP window scores
qChIP scanning of p53 and p73 across a representative promoter region. Window scores across the indicated chromosome regions (top) and the log2 OU of selected chromosome regions determined by qChIP are shown in the bottom histogram. *contains a non-canonical p53 consensus sequence: GGGCTTGCTg(spacer=32)AGGCAAGTgT (capital letters represent perfect match to the consensus sequence). Primers pairs used for qPCR scanning designed within the indicated window region are shown as red arrows.

3-4A)

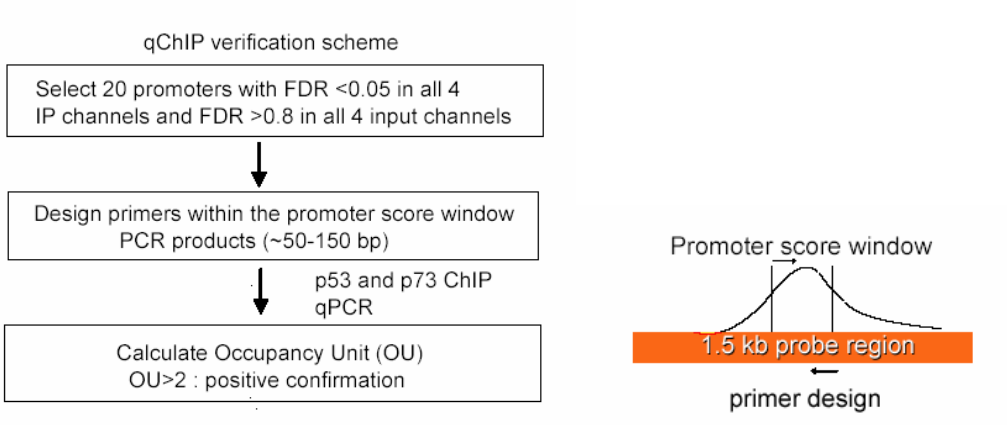

3-4B)

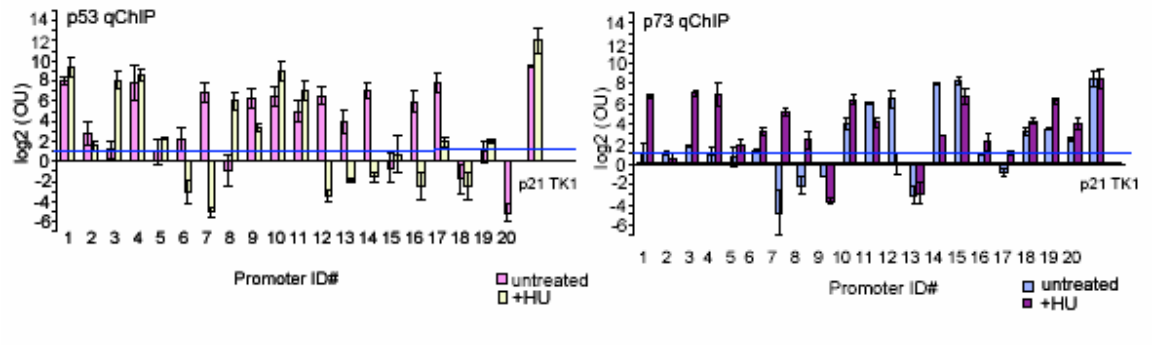

Figure 3-4. Summary of qChIP validation

(A)Outline of the verification strategy used for ChIP-chip validation. Primer design is depicted on the right. (B) Summary of qChIP verification of the 20 selected promoters. Two independent ChIPs were performed (–HU and +HU conditions) using the indicated antibodies. Input and ChIP DNA were amplified by LM-PCR. Enrichment was expressed in terms of occupancy units (OU). OU values of the 20 qChIP-validated promoters for the 4 experiments are presented in a logarithmic-scale (log2). p21cip1 and TK1 were used as controls for the calculation. Log2 (OU) > 1 is considered positive confirmation (indicated by the blue line).

Figure 3-5. Comparison of p53 and p73 promoter occupancy profiles at steady state and following HU treatment

(A) Correlation of the promoter scores between p53 (-HU) and p73 (-HU) experiments using p53 (-HU) bound promoters (left) and p73 (-HU) bound promoters (right). (B) Correlation of the promoter scores between p53 (+HU) and p73 (+HU) experiments using p53 (+HU) bound promoters (left) and p73 (+HU) bound promoters (right). (C) Correlation of the promoter scores between p53 (-HU) and p53 (+HU) experiments using p53 (-HU) bound promoters (left) and p53 (+HU) bound promoters (right). (D)Correlation of the promoter scores between p73 (-HU) and p73 (+HU) experiments using p73 (-HU) bound promoters (left) and p73 (+HU) bound promoters (right).

3-5A)

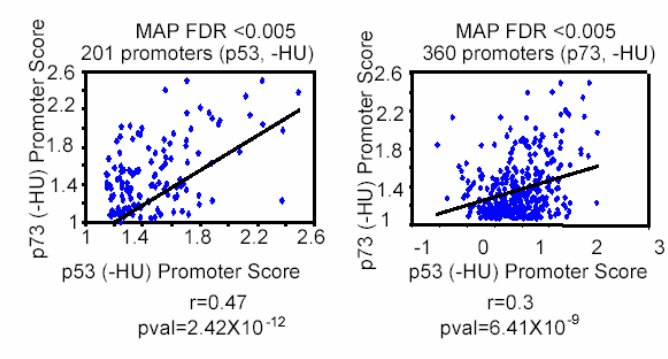

3-5B)

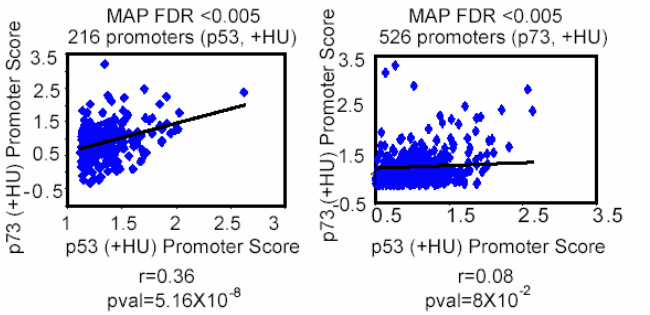

3-5C)

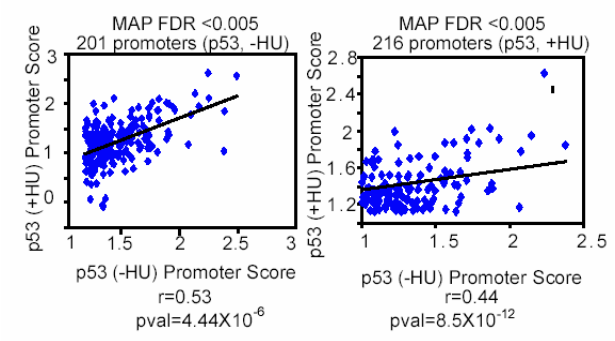

3-5D)

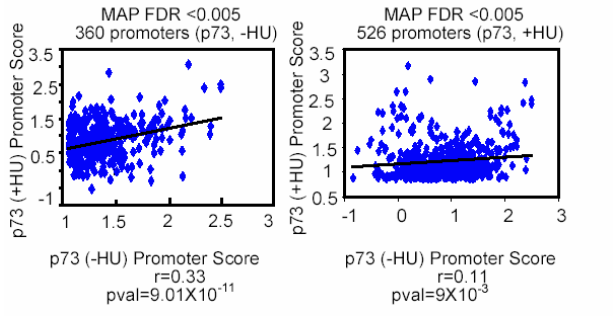

Figure 3-6. Interactions of p53 and p73 with their common promoters
(A) Three possible scenarios for the interactions of p53 and p73 with their overlapping promoters. (B) Flowchart for the analysis. Identify peak regions for promoters that are bound by both p53 and p73 in –HU and +HU experiments. (C) The number of p53- and p73-bound promoters with maximum binding in the same window (same genomic region SR), overlapping windows (overlapping genomic region OR), or different windows (different genomic region DR) are summarized in histograms (top: -HU, bottom: +HU).

3-6A)

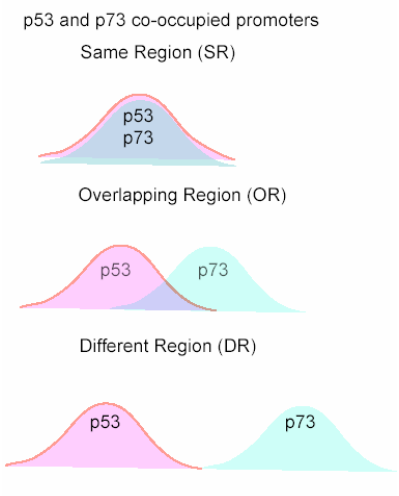
p53 and p73 co-occupied promoters
Same Region (SR)
p53
p73
Overlapping Region (OR)
p53
p73
Different Region (DR)
p53
p73

3-6B)

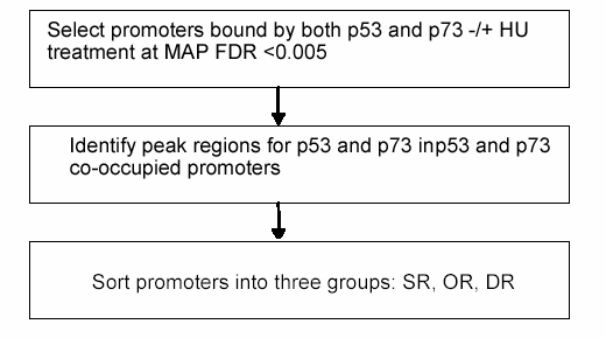
Select promoters bound by both p53 and p73 -/+ HU treatment at MAP FDR <0.005
Identify peak regions for p53 and p73 inp53 and p73 co-occupied promoters
Sort promoters into three groups: SR, OR, DR

3-6C)

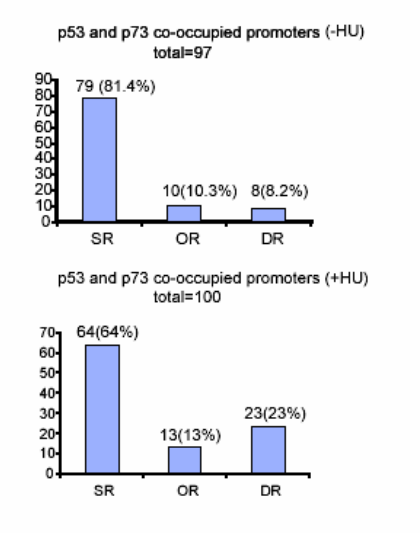
p53 and p73 co-occupied promoters (-HU)
total=97
79 (81.4%)
10(10.3%)
8(8.2%)
SR
OR
DR
p53 and p73 co-occupied promoters (+HU)
total=100
64(64%)
13(13%)
23(23%)
SR
OR
DR

Figure 3-7. Motif analysis
(A)Outline of motif search for p53 and p73-bound promoters. (B) Summary of p53 consensus motif search. Pie charts represent the percentage of promoters containing p53 consensus binding sites in the 2.5 kb query region as shown in schematic in (A) from each experiment with pval <0.01 and motif score >6 . The percentage of promoters containing p53 half-site in the peak region is also shown. (C) Overrepresented JASPAR motifs in p53 and p73-bound promoters. The sequence logo of the JASPAR motif represents the frequency of occurrence in the binding-site matrix. A motif that is overrepresented with pval <0.001 in the experimental set is marked by X. P-values are calculated to indicate the degree of overrepresentation of each PSSM in target versus background sequences randomly selected from 1000 human promoters. Motifs found in all four experiments are highlighted in yellow.

3-7A)

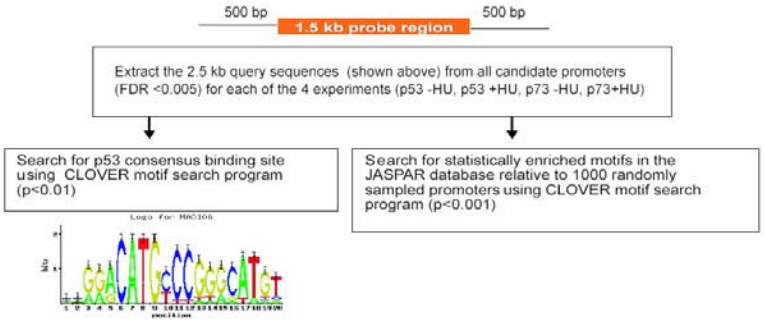

3-7B)

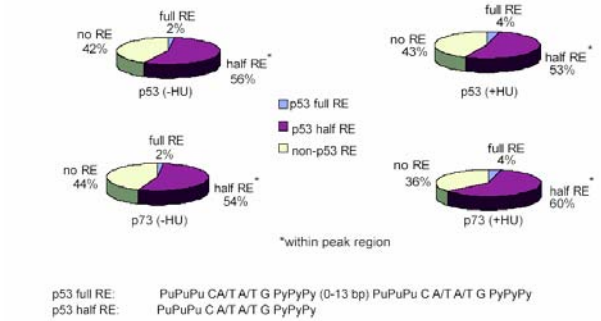

p53 full RE: PuPuPu CA/T A/T G PyPyPy (0-13 bp) PuPuPu C A/T A/T G PyPyPy
p53 half RE: PuPuPu C A/T A/T G PyPyPy

3-7C)

p<0.001			Experiment				
JASPAR Motif ID	Motif name	Motif type	Motif Logo	p53 -HU	p53+HU	p73 -HU	p73 +HU
MA0010	Broad-complex_1	C2H2 ZN-FINGER					X
MA0013	Broad-complex_4	C2H2 ZN-FINGER		X	X	X	X
MA0039	Gklf	C2H2 ZN-FINGER				X	
MA0041	HFH-2	FORKHEAD				X	X
MA0045	HMG-IY	HMG				X	X
MA0049	Hunchback	C2H2 ZN-FINGER		X	X	X	X
MA0055	Myf	bHLH			X	X	X
MA0056	MZF_1-4	C2H2 ZN-FINGER		X	X	X	X
MA0068	Pax-4	PAIRED-HOMEO				X	X
MA0073	RREB-1	C2H2 ZN-FINGER		X	X	X	
MA0079	SP1	C2H2 ZN-FINGER		X	X	X	X
MA0082	SQUA	MADS		X		X	X
MA0086	Snail	C2H2 ZN-FINGER		X	X	X	X

3-8A)

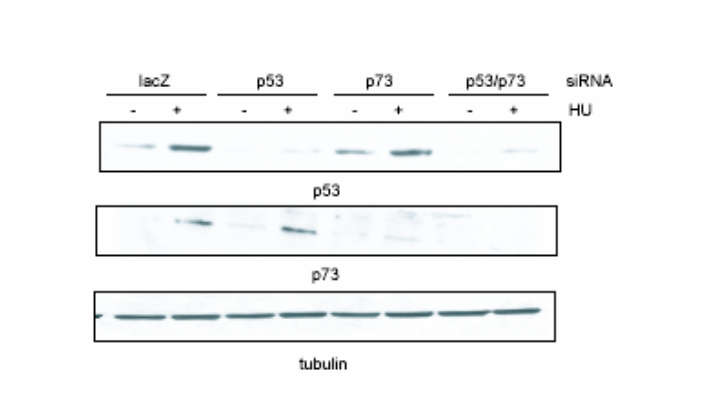

3-8B)

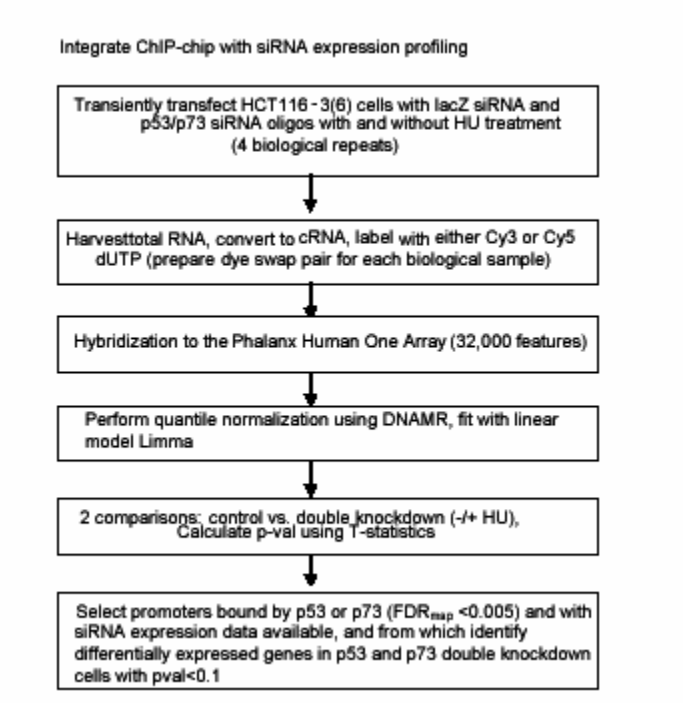

Figure 3-8. Transcriptional profiling in HCT116-3(6) cells deleted for both p53 and p73

(A) The efficacy of transient siRNA-mediated single knockdown of p53 or p73, or double knockdown of p53 and p73 in HCT16-3(6) cells. Immunoblot of lysates from untreated of HU-treated HCT116-3(6) cells following transfection with chemically synthesized siRNA oligos against p53, p73, p53/p73, or lacZ (B) Flow chart for the integrated analysis of ChIP-chip with siRNA expression profiling.

3-9A)

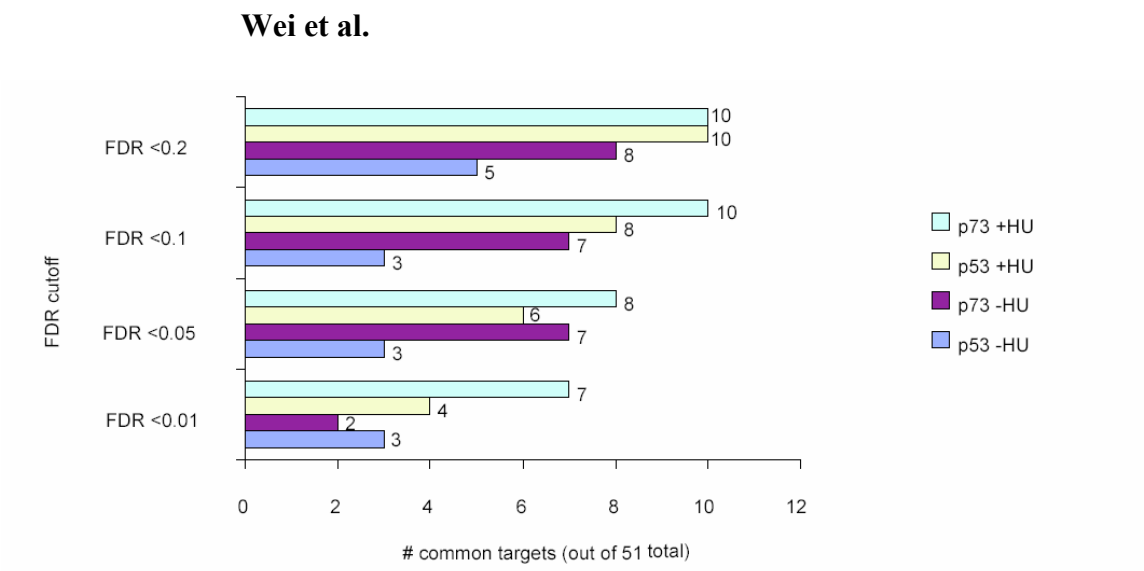

3-9B)

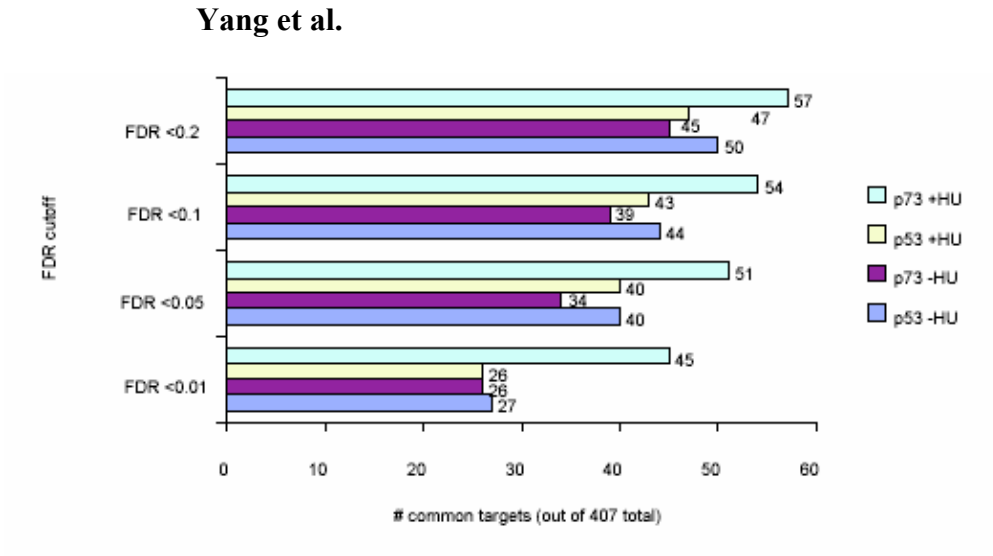

Figure 3-8. Comparisons of p53 and p73 binding sites with Wei et al. and Yang et al. (A)Overlap of the binding sites identified in this study and p53 ChIP-PET study(9). The number of common sites at different FDR_{MAP} cutoff from each experiment is shown. (B) Overlap of the binding sites identified in this study and p63 ChIP-chip study(10). The number of common sites at different FDR_{MAP} cutoff from each experiment is shown.

Table 3-2. Summary of verification experiments

p53 (-HU)

FDR_{MAP} [a]	Promoter Score Range	#false/# assayed[b]	qChIP FDR[c]	# promoters in bin[d]
0-0.005	1.22-2.15	2/12	0.17	201
0.005-0.01	1.11-1.14	1/3	0.33	65
0.01-0.05	0.96-0.99	3/5	0.60	183

p73 (-HU)

FDR_{MAP} [a]	Promoter Score Range	#false/# assayed[b]	qChIP FDR[c]	# promoters in bin[d]
0-0.005	1.08-2.41	7/19*	0.37	360

p53 (+HU)

FDR_{MAP} [a]	Promoter Score Range	# false/# assayed[b]	qChIP FDR[c]	# promoters In bin[d]
0-0.005	1.14-2.03	6/16	0.37	216
0.01-0.05	0.98-1.01	2/4	0.50	173

p73 (+HU)

FDR_{MAP} [a]	Promoter Score Range	# false/# assayed[b]	qChIP FDR[c]	# promoters in bin[d]
0-0.005	0.89-2.13	4/19*	0.21	526

[a]Breakdown of MAP computed FDR. *Note: 1/20 selected p73-bound promoters fell between FDR range 0.01-0.05 and was not included in the FDR calculation.
[b] # false= # promoters with O.U <2
[c] $qPCR_{FDR}$ = # false/total number of promoters assayed
[d] The number of promoters identified by MAP within the specified FDR range

Table 3-3. p53 and p73 occupy common and distinct promoters

Category I: p53 specific promoters (-HU)

Promoter			p53 (-HU)		p73 (-HU)		p53 (+HU)		p73 (+HU)	
NimbleGen Probe ID	Gene ID	Gene Name	log2 OU	MAP FDR	log2 OU	MAP FDR	log2 OU	MAP FDR	log2 OU	MAP FDR
HSAP0406S00016860	NM_006378	SEMA4D	**5.7±2.77**	**0.002**	**2.45±1.41**	**0.026**	-0.20±0.32	0.023	n/a	0.93
HSAP0406S00023356	AK127211	cDNA FLJ45278	**6.9±0.74**	**0.008**	**2.67±1.47**	**0.013**	-2.28±0.50	0.062	1.20±0.66	0.37

Category II: p53 specific promoters (+HU)

Promoter			p53 (+HU)		p73 (+HU)		p53 (-HU)		p73 (-HU)	
NimbleGen Probe ID	Gene ID	Gene Name	log2 OU	MAP FDR	log2 OU	MAP FDR	log2 OU	MAP FDR	log2 OU	MAP FDR
HSAP0406S00013662	NM_021223	MYL7	**6.34±3.74**	**0.005**	**-6.74±0.31**	**0.299**	-1.99±1.24	0.008	3.44±0.28	0.005
HSAP0406S00031561	NM_005583	LYL1	**4.82±3.67**	**0.000**	**0.37±0.76**	**0.932**	3.30±1.03	0.033	4.36±0.07	0.026

Category III: p73 specific promoters (-HU)

Promoter			p73-HU		p53-HU		p53+		p73+HU	
NimbleGen Probe ID	Gene ID	Gene Name	log2 OU	FDR	log2 OU	FDR	log2 OU	FDR	log2 OU	FDR
HSAP0406S0006063	NM_024080	TRPM8	**4.95±0.91**	**0.000**	**n/a**	**0.936**	-1.2±2.2	0.938	-1.1±1.01	0.932
HSAP0406S00019480	NM_053017	ART5	**3.89±0.24**	**0.001**	**-1.8**±0.41	**0.936**	2.1±0.3	0.938	1.7±0.38	0.932

Category IV: p73 specific promoters (+HU)

Promoter			p73 (+HU)		p53 (+HU)		p53 (-HU)		p73 (-HU)	
NimbleGen Probe ID	Gene ID	Gene Name	log2 OU	MAP FDR	log2 OU	MAP FDR	log2 OU	MAP FDR	log2 OU	MAP FDR
HSAP0406S00025741	AB032525	NKCC2	**3.75±0.1**	**0.000**	**-3.64±0.95**	**0.134**	3.18±0.96	0.736	-1.08±0.40	0.346
HSAP0406S00022455	AK094261	cDNA FLJ36942	**3.96±0.67**	**0.000**	**-2.63±0.25**	**0.938**	4.65±0.65	0.397	-0.69±0.86	0.932
HSAP0406S00034475	NM_058186	FAM3B	**1.18±0.31**	**0.000**	**-4.99±1.43**	**0.445**	4.9±0.27	0.04	4.17±0.24	0.095

Category V: p53 and p73 constitutively bound promoters (-HU/+HU)

Promoter			p53 (-HU)		p53 (+HU)		p73 (-HU)		p73 (+HU)	
NimbleGen Probe ID	Gene ID	Gene Name	log2 OU	MAP FDR	log2 OU	MAP FDR	log2 OU	MAP FDR	log2 OU	MAP FDR
HSAP0406S00027218	AJ223280	pp36	**8.02±0.45**	**0**	**9.35±1.02**	**0**	**1.16±1.02**	**0**	**6.48±0.23**	**0**
HSAP0406S00034186	AK127768	cDNA FLJ45869	**6.51±0.94**	**0.003**	**8.96±1.02**	**0**	**3.94±0.54**	**0**	**6.36±0.41**	**0**
HSAP0406S00034239	NM_005286	GPR8	**5.00±1.01**	**0.003**	**7.01±0.93**	**0.01**	**6.03±0.09**	**0**	**4.11±0.38**	**0**

n/a: CT values fall below the detection threshold
Bold: log2 OU of representative promoters that fit category description are highlighted

Table 3-4. Summary of the relationship between p53/p73 binding and gene expression

p53 (-HU) MAP FDR cutoff	Promoters covered by expression array[2]	Expression affected by p53/p73 siRNAs[3]	Down[4]	Up[5]
0.005	102/201	9 (9%)	4	5
0.01	138/266	13 (9.4%)	5	8
0.05	244/449	18(7.4%)	8	10

p73 (-HU) MAP FDR cutoff	Promoters covered by expression array[2]	Expression affected by p53/p73 siRNAs[3]	Down[4]	Up[5]
0.005	196/360	11(5.7%)	5	6
0.01	138/266	13 (9.4%)	5	8
0.05	244/449	18 (7.4%)	8	10

p53 (+HU) MAP FDR cutoff	Promoters covered by expression array[2]	Expression affected by p53/p73 siRNAs[3]	Down[4]	Up[5]
0.005	118/216	11 (9.3%)	8	3
0.01	139/250	12 (8.6%)	7	5
0.05	192/423	25 (13%)	12	13

p73 (+HU) MAP FDR cutoff	Promoters covered by expression array[2]	Expression affected by p53/p73 siRNAs[3]	Down[4]	Up[5]
0.005	292/526	36 (12.3%)	19	17
0.01	344/620	44 (12.8%)	23	21
0.05	466/827	63 (13.5%)	28	35

[1] # promoters that passed defined FDR cutoff and with siRNA expression data available.
[2] # genes identified as differentially expressed in p53/p73 double knockdown cells, pval <0.1.
[4] # genes whose expression is higher in p53/p73 double knockdown cells than that of control cells.
[5] # genes whose expression is lower in p53/p73 double knockdown cells than that of control cells.

Table 3-5. Relationship between p53/p73 binding and gene expression at steady state

p53-bound promoters (FDR_{MAP}<0.005)

Gene ID	Gene Name	siRNA effect[1]	MAP FDR p53 (-HU)	p53 (+HU)	p73 (-HU)	p73 (+HU)
NM_001959	EEF1B2	down	0.002	0.038	0.017	0.932
NM_000040	APOC3	down	0.000	0.000	0.000	0.000
NM_002362	MAGEA4	down	0.003	0.002	0.000	0.770
NM_000674	ADORA1	down	0.000	0.000	0.000	0.000
NM_006144	GZMA	up	0.000	0.000	0.000	0.000
NM_002426	MMP12	up	0.003	0.587	0.526	0.021
AJ238395	RPGR	up	0.002	0.064	0.682	0.932
BC043528	FLJ31978	up	0.003	0.000	0.000	0.003
AB029488	C11orf21	up	0.001	0.216	0.031	0.000

p73-bound promoters (FDR_{MAP} <0.005)

Gene ID	Gene Name	siRNA effect[1]	MAP FDR p53 (-HU)	p53 (+HU)	p73 (-HU)	p73 (+HU)
NM_024059	MGC5356	down	0.077	0.003	0.000	0.264
NM_000040	APOC3	down	0.000	0.000	0.000	0.000
NM_002362	MAGEA4	down	0.003	0.002	0.000	0.770
NM_000674	ADORA1	down	0.000	0.000	0.000	0.000
AK090478	FLJ00400	down	0.018	0.003	0.000	0.000
NM_006144	GZMA	up	0.000	0.000	0.000	0.000
NM_007253	CYP4F9	up	0.069	0.019	0.000	0.000
BC043528	FLJ31978	up	0.003	0.000	0.000	0.003
AL713776	cDNA DKFZ434L192	up	0.000	0.001	0.000	0.000
AK091509	FLJ34190 fis	up	0.008	0.000	0.000	0.000
NM_153699	GSTA5	up	0.936	0.938	0.000	0.932

[1]Gene expression in p53/p73 double knockdown cells relative to control knockdown cells, pval <0.1.

Table 3-6. Relationship between p53 binding and gene expression following HU treatment

p53 occupied promoters (FDR_{MAP} <0.005)

Gene ID	Gene Name	siRNA effect[1]	MAP FDR p53 (-HU)	p53 (+HU)	p73 (-HU)	p73 (+HU)
NM_024296	MGC1203	down	0.002	0.000	0.932	0.867
NM_000040	APOC3	down	0.000	0.000	0.000	0.000
NM_014415	ZBTB11	down	0.018	0.001	0.000	0.001
NM_002362	MAGEA4	down	0.003	0.002	0.000	0.770
AK055975	cDNA FLJ31413	down	0.003	0.001	0.002	0.000
NM_032488	CNFN	down	0.000	0.000	0.000	0.003
NM_021574	BCR	down	0.002	0.000	0.002	0.052
NM_006843	SDS	down	0.816	0.005	0.202	0.002
NM_020795	NLGN2	up	0.277	0.002	0.568	0.932
AK124614	cDNA FLJ42623	up	0.227	0.005	0.932	0.932
AB033092	KIAA1266	up	0.445	0.004	0.030	0.565

[1]Gene expression in p53/p73 double knockdown cells relative to control knockdown cells, pval <0.1

Table 3-6. Relationship between p53 binding and gene expression following HU treatment, Continued

p73 occupied promoters (FDR_{MAP} <0.005)

Gene ID	Gene Name	siRNA effect[1]	MAP FDR p53 (-HU)	p53 (+HU)	p73 (-HU)	p73 (+HU)
BC062347	KIAA1404	down	0.042	0.213	0.932	0.000
NM_020801	ARRDC3	down	0.936	0.938	0.932	0.000
NM_003473	STAM	down	0.817	0.770	0.932	0.000
NM_001004311	FIGLA	down	0.183	0.216	0.002	0.003
AK128127	cDNA FLJ46248	down	0.350	0.220	0.000	0.001
NM_000040	APOC3	down	0.000	0.000	0.000	0.000
NM_013448	BAZ1A	down	0.936	0.938	0.932	0.000
AB007942	KIAA0473	down	0.103	0.938	0.384	0.001
BC014269	ETF1	down	0.936	0.938	0.932	0.002
NM_021175	HAMP	down	0.000	0.000	0.000	0.000
AK055975	cDNA FLJ31413	down	0.003	0.001	0.002	0.000
NM_032488	CNFN	down	0.000	0.000	0.000	0.003
BC036704	TWIST1	down	0.936	0.938	0.932	0.001
NM_006843	SDS	down	0.816	0.005	0.202	0.002
NM_001004051	GPRASP2	down	0.216	0.001	0.000	0.000
NM_032328	MGC12458	down	0.000	0.001	0.363	0.000
NM_001492	GDF1	down	0.727	0.150	0.587	0.001
NM_019098	CNGB3	down	0.936	0.938	0.932	0.001
NM_025227	BPIL1	up	0.116	0.000	0.000	0.000
NM_024644	C14orf169	up	0.936	0.938	0.932	0.003
AK024267	cDNA FLJ14205	up	0.936	0.938	0.932	0.000
BC062320	HAPLN3	up	0.004	0.030	0.012	0.000
AK096466	cDNA FLJ39147	up	0.498	0.725	0.007	0.000
NM_006563	KLF1	up	0.842	0.938	0.006	0.004
NM_004962	GDF10	up	0.489	0.048	0.300	0.002
AB029488	C11orf21	up	0.001	0.216	0.031	0.000
AF286696	olfactory receptor sdolf mRNA	up	0.345	0.515	0.587	0.002
NM_005547	IVL	up	0.936	0.256	0.058	0.000
NM_002373	MAP1A	up	0.433	0.938	0.482	0.003
NM_002444	MSN	up	0.302	0.269	0.024	0.001
NM_145180	C21orf94	up	0.915	0.938	0.738	0.001
L22650	EPAG mRNA	up	0.868	0.133	0.299	0.000
NM_006144	GZMA	up	0.000	0.000	0.000	0.000
NM_207338	KLPH	up	0.936	0.938	0.858	0.000
NM_178570	RTN4RL2	up	0.936	0.938	0.932	0.000
AK055830	cDNA FLJ31268	up	0.304	0.522	0.230	0.000

1Gene expression in p53/p73 double knockdown cells relative to control knockdown cells, pval <0.1

Table 3-7. Go term distribution of p53 and p73 occupied promoters (-HU)
*Categories represented <5% of the total number of genes were excluded from the analysis.
p53 occupied promoters (FDR_{MAP} <0.005)

Category	Term	Count	%*	PValue
SP_PIR_KEYWORDS	Glycoprotein	38	18.27%	5.28E-04
SP_PIR_KEYWORDS	alternative splicing	40	19.23%	8.67E-04
SP_PIR_KEYWORDS	Phosphorylation	25	12.02%	0.001015
GOTERM_BP_ALL	Organismal physiological process	33	15.87%	0.001111
SP_PIR_KEYWORDS	Signal	30	14.42%	0.00118
SP_PIR_KEYWORDS	Transmembrane	39	18.75%	0.001598
SP_PIR_KEYWORDS	disease mutation	17	8.17%	0.001962
SP_PIR_KEYWORDS	Membrane	39	18.75%	0.002351

Table 3-7. Go term distribution of p53 and p73 occupied promoters (-HU), Continued

*Categories represented <5% of the total number of genes were excluded from the analysis.

p73 occupied promoters (FDR_{MAP} <0.005)

Category	Term	Count	%*	PValue
SP_PIR_KEYWORDS	Glycoprotein	81	21.26%	4.96E-10
SP_PIR_KEYWORDS	Transmembrane	77	20.21%	8.60E-07
SP_PIR_KEYWORDS	Membrane	78	20.47%	9.63E-07
UP_SEQ_FEATURE	glycosylation site:N-linked (GlcNAc...)	79	20.73%	1.28E-06
SP_PIR_KEYWORDS	Signal	57	14.96%	3.62E-06
GOTERM_CC_ALL	plasma membrane	47	12.34%	1.83E-04
SP_PIR_KEYWORDS	Receptor	40	10.50%	2.15E-04
UP_SEQ_FEATURE	transmembrane region	73	19.16%	3.54E-04
GOTERM_CC_ALL	integral to plasma membrane	35	9.19%	5.73E-04
GOTERM_CC_ALL	intrinsic to plasma membrane	35	9.19%	6.43E-04
GOTERM_BP_ALL	cell communication	72	18.90%	7.30E-04
SP_PIR_KEYWORDS	disease mutation	27	7.09%	9.13E-04
SP_PIR_KEYWORDS	alternative splicing	65	17.06%	0.001488
UP_SEQ_FEATURE	signal peptide	57	14.96%	0.002579
GOTERM_MF_ALL	transmembrane receptor activity	34	8.92%	0.002635
GOTERM_BP_ALL	intracellular signaling cascade	29	7.61%	0.002964
GOTERM_BP_ALL	signal transduction	64	16.80%	0.004194
GOTERM_MF_ALL	signal transducer activity	59	15.49%	0.006339
GOTERM_MF_ALL	rhodopsin-like receptor activity	20	5.25%	0.007057
GOTERM_MF_ALL	G-protein coupled receptor activity	22	5.77%	0.008211
GOTERM_MF_ALL	protein binding	78	20.47%	0.009625

Table 3-8. Go term distributions of p53 occupied promoters (+HU)
*Categories represented <5% of the total number of genes were excluded from the analysis.
p53 occupied promoters (FDR_{MAP} <0.005)

Category	Term	Count	%*	PValue
SP_PIR_KEYWORDS	Glycoprotein	52	23.53%	4.30E-09
SP_PIR_KEYWORDS	Signal	42	19.00%	3.57E-08
SP_PIR_KEYWORDS	Membrane	48	21.72%	8.30E-06
SP_PIR_KEYWORDS	Transmembrane	47	21.27%	1.11E-05
UP_SEQ_FEATURE	signal peptide	42	19.00%	6.95E-05
UP_SEQ_FEATURE	glycosylation site:N-linked (GlcNAc…)	48	21.72%	7.76E-05
SP_PIR_KEYWORDS	alternative splicing	44	19.91%	1.35E-04
SP_PIR_KEYWORDS	g-protein coupled receptor	16	7.24%	1.62E-04
GOTERM_BP_ALL	G-protein coupled receptor protein signaling pathway	22	9.95%	1.94E-04
GOTERM_MF_ALL	G-protein coupled receptor activity	19	8.60%	2.13E-04
GOTERM_MF_ALL	transmembrane receptor activity	26	11.76%	2.23E-04
GOTERM_BP_ALL	cell surface receptor linked signal transduction	28	12.67%	2.57E-04
SP_PIR_KEYWORDS	Transducer	16	7.24%	3.09E-04
SP_PIR_KEYWORDS	Receptor	25	11.31%	8.00E-04
GOTERM_MF_ALL	receptor activity	32	14.48%	8.35E-04
SP_PIR_KEYWORDS	disease mutation	18	8.14%	0.001205
GOTERM_CC_ALL	integral to membrane	54	24.43%	0.001632
GOTERM_CC_ALL	intrinsic to membrane	54	24.43%	0.001715
UP_SEQ_FEATURE	transmembrane region	45	20.36%	0.001959
GOTERM_MF_ALL	signal transducer activity	40	18.10%	0.002179
GOTERM_MF_ALL	rhodopsin-like receptor activity	15	6.79%	0.002835
GOTERM_CC_ALL	Membrane	65	29.41%	0.003218
GOTERM_BP_ALL	cell communication	43	19.46%	0.003606
GOTERM_BP_ALL	signal transduction	40	18.10%	0.004641
UP_SEQ_FEATURE	disulfide bond	33	14.93%	0.008226
GOTERM_BP_ALL	cell adhesion	13	5.88%	0.009469

Table 3-9. Go term distributions of p73 occupied promoters (+HU)
*Categories represented <5% of the total number of genes were excluded from the analysis.
p73 occupied promoters (FDR_{MAP} <0.005)

Category	Term	Count	%*	PValue
SP_PIR_KEYWORDS	Glycoprotein	126	23.46%	1.99E-17
SP_PIR_KEYWORDS	Signal	93	17.32%	5.40E-12
UP_SEQ_FEATURE	glycosylation site:N-linked (GlcNAc...)	125	23.28%	1.26E-11
SP_PIR_KEYWORDS	Transmembrane	114	21.23%	9.15E-10
SP_PIR_KEYWORDS	Membrane	115	21.42%	1.54E-09
SP_PIR_KEYWORDS	g-protein coupled receptor	35	6.52%	6.03E-07
GOTERM_MF_ALL	G-protein coupled receptor activity	42	7.82%	1.26E-06
GOTERM_BP_ALL	cell surface receptor linked signal transduction	65	12.10%	1.50E-06
SP_PIR_KEYWORDS	Transducer	35	6.52%	2.29E-06
UP_SEQ_FEATURE	signal peptide	93	17.32%	2.88E-06
GOTERM_MF_ALL	rhodopsin-like receptor activity	37	6.89%	3.70E-06
GOTERM_BP_ALL	cell communication	111	20.67%	6.68E-06
GOTERM_MF_ALL	transmembrane receptor activity	57	10.61%	7.67E-06
SP_PIR_KEYWORDS	alternative splicing	100	18.62%	9.93E-06
GOTERM_MF_ALL	signal transducer activity	99	18.44%	1.36E-05
GOTERM_BP_ALL	G-protein coupled receptor protein signaling pathway	46	8.57%	2.13E-05
UP_SEQ_FEATURE	transmembrane region	108	20.11%	2.63E-05
SP_PIR_KEYWORDS	Receptor	56	10.43%	3.88E-05
GOTERM_BP_ALL	signal transduction	100	18.62%	6.56E-05
GOTERM_CC_ALL	plasma membrane	62	11.55%	1.45E-04
INTERPRO_NAME	IPR000276:Rhodopsin-like GPCR superfamily	33	6.15%	1.59E-04
GOTERM_CC_ALL	intrinsic to plasma membrane	47	8.75%	2.46E-04
GOTERM_CC_ALL	intrinsic to membrane	126	23.46%	2.92E-04
SP_PIR_KEYWORDS	disease mutation	37	6.89%	3.33E-04
GOTERM_CC_ALL	extracellular region	48	8.94%	3.74E-04
GOTERM_CC_ALL	integral to membrane	125	23.28%	4.13E-04
GOTERM_CC_ALL	integral to plasma membrane	46	8.57%	4.16E-04
UP_SEQ_FEATURE	disulfide bond	78	14.53%	5.07E-04
GOTERM_MF_ALL	receptor activity	67	12.48%	0.00112
SP_PIR_KEYWORDS	direct protein sequencing	55	10.24%	0.00264
GOTERM_BP_ALL	Development	57	10.61%	0.005173
GOTERM_BP_ALL	organismal physiological process	72	13.41%	0.005911

Table 3-10. Go term distribution of p53 and p73 co-occupied promoters
*Categories represented <5% of the total number of genes were excluded from the analysis.

-HU, FDR_{MAP} <0.005

Category	Term	Count	%*	PValue
SP_PIR_KEYWORDS	phosphorylation	15	15.62%	0.001596
SP_PIR_KEYWORDS	glycoprotein	21	21.88%	0.00195
SP_PIR_KEYWORDS	signal	17	17.71%	0.003175
GOTERM_MF_ALL	protein binding	27	28.12%	0.003473
SP_PIR_KEYWORDS	serine/threonine-protein kinase	6	6.25%	0.005521
SP_PIR_KEYWORDS	alternative splicing	21	21.88%	0.006196
SP_PIR_KEYWORDS	disease mutation	10	10.42%	0.006314
UP_SEQ_FEATURE	binding site:ATP	7	7.29%	0.008279

+HU, FDR_{MAP} <0.005

Category	Term	Count	%*	Pvalue
SP_PIR_KEYWORDS	glycoprotein	27	27.27%	1.26E-05
SP_PIR_KEYWORDS	signal	22	22.22%	3.91E-05
GOTERM_BP_ALL	cell surface receptor linked signal transduction	17	17.17%	3.15E-04
GOTERM_MF_ALL	G-protein coupled receptor activity	12	12.12%	5.37E-04
GOTERM_BP_ALL	G-protein coupled receptor protein signaling pathway	13	13.13%	7.77E-04
SP_PIR_KEYWORDS	g-protein coupled receptor	10	10.10%	7.94E-04
SP_PIR_KEYWORDS	transducer	10	10.10%	0.001211
GOTERM_MF_ALL	transmembrane receptor activity	15	15.15%	0.001351
UP_SEQ_FEATURE	signal peptide	22	22.22%	0.00162
UP_SEQ_FEATURE	glycosylation site:N-linked (GlcNAc...)	25	25.25%	0.001629
GOTERM_MF_ALL	rhodopsin-like receptor activity	10	10.10%	0.002525
GOTERM_MF_ALL	signal transducer activity	23	23.23%	0.002927
SP_PIR_KEYWORDS	transmembrane	23	23.23%	0.003128
GOTERM_MF_ALL	receptor activity	18	18.18%	0.003405
GOTERM_BP_ALL	cell communication	24	24.24%	0.003554
SP_PIR_KEYWORDS	membrane	23	23.23%	0.004078
GOTERM_BP_ALL	signal transduction	22	22.22%	0.006506
SP_PIR_KEYWORDS	alternative splicing	22	22.22%	0.007254
GOTERM_BP_ALL	organismal physiological process	18	18.18%	0.009652

Table 3-11. p53 half-site search

p53 (-HU)[1] unique	# Promoters[a] (Forward)	% Total # promoters scanned[b]	# Promoters[c] (Forward)	% Total # promoters scanned[d]
Perfect	3	4.11	3	4.11
1 mismatch	12	16.44	23	31.51
Total	15	20.55	26	35.62

p73 (-HU)[2] unique	# Promoters[a] (Forward)	% Total # promoters scanned[b]	# Promoters[c] (Forward)	% Total # promoters scanned[d]
Perfect	2	2.86	4	5.71
1 mismatch	17	24.29	15	21.43
Total	19	27.14	19	27.14

p53 (+HU)[3] unique	# Promoters[a] (Forward)	% Total # promoters scanned[b]	# Promoters[c] (Forward)	% Total # promoters scanned[d]
Perfect	1	1.43	5	7.14
1 mismatch	13	18.57	17	24.29
Total	14	20.55	22	31.43

p73 (+HU)[4] unique	# Promoters[a] (Forward)	% Total # promoters scanned[b]	# Promoters[c] (Forward)	% Total # promoters scanned[d]
Perfect	4	5.71	4	5.71
1 mismatch	18	25.71	16	22.86
Total	22	31.43	20	28.57

[1] A total of 70 p53 specific promoters (-HU, FDR_{MAP} <0.005) were scanned for p53 half-sites in MAP score window.
[2] A total of 70 p73 specific promoters (-HU, FDR_{MAP} <0.005) were scanned for p53 half-sites in MAP score window.
[3] A total of 70 p53 occupied promoters (+HU, FDR_{MAP} <0.005) were scanned for p53 half-sites in their MAP score window.
[4] A total of 70 p53 occupied promoters (+HU, FDR_{MAP} <0.005) were scanned for p53 half-sites in their MAP score window.

aThe number of promoters with p53 half-site in forward orientation PuPuPu**CA/TA/TG**PyPyPy
b % Total # promoters scanned=# promoter with p53 half-site/70 X 100
cThe number of promoters with p53 half-site in inverted orientation PyPyPy**CA/TA/TG**PuPuPu
d % Total # promoters scanned (inverted) =# promoter with p53 half-site (inverted) /70 X 100
e Perfect match to the p53 half-site sequence
f p53 half-site containing 1 mismatch in the sequence surrounding the core sequence
bold: core sequence

Table 3-12. Primer sequences for qChIP verification

NimbleGen Seq ID	Gene Acession ID	Validation ID	Forward	Reverse	Verification on gel
HSAP0406S00027218	AJ223280	1	TCTTGCACCCCGTCTTCAC	CCAGAGCCCTGAGGAATGAC	Yes
HSAP0406S00021203	NM_000040	2	GCCTGCCTGGATTGAAACC	GCACAGAAGACCAGGCATCA	Yes
HSAP0406S00024903	AB007865	3	AGTCATCACCTCTACCTTGAAACTAGTCT	ACACTGCTGAATCCACTCAATCA	Yes
HSAP0406S00001733	AY129015	4	GCCAGAGGTTTAAAAAGGTTAAGATTT	GCGGCAGGACAACATGGT	Yes
HSAP0406S00032402	NM_032488	5	AGACCAGCCTGGGCAACA	CCCGGCTAATTCTATTTGTATTTTTT	Yes
HSAP0406S00002422	M26316	6	AGAAAGACCACGAAGACCACCTAA	GCTGCTCCTCACAGTGCTTACA	Yes
HSAP0406S00003249	NM_014002	7	CCCAGCTGCCCATCAAGAT	GCCACAGAGAAGCCAGGAACT	Yes
HSAP0406S00019175	NM_014661	8	CACACCGGACCCATTCTTTT	GAGCGAGCTGTAGTGTGAAAGGA	Yes
HSAP0406S00036295	AL831883	9	TCTGGGTCTGACATCAACCATTT	TGTTTCAGAAAGATAGGAGATAGCTCTGT	Yes
HSAP0406S00034186	AK127768	10	GCTTACAACTGGTGTGTGTCTTAGG	TGCTCTCAAAGGCGGAACA	Yes
HSAP0406S00034239	NM_005286	11	CCAGTGCTTCGAGTCCAGAAG	GACTGCCTGTACTGGCCAAAA	Yes
HSAP0406S00036196	NM_006639	12	CTGGAATGACTGGGCTTGCT	CTTGCCTGATCCCCCAAAT	Yes
HSAP0406S00027800	AK122592	13	GTAAAGTCCCCCAAACCAAAGTT	CGACTTAGCAACCACCTCATAGG	Yes
HSAP0406S00018051	AK025655	14	ACAGGGAGTGCAGTCTTAAATGG	AAAAAATGCAACCACAGCTATCC	Yes
HSAP0406S00017623	AK124271	15	GCAGCGGTACCTGACCAGAA	CTTCCTGTGCTTCCTACAACTTTTC	Yes
HSAP0406S00008775	BC026264	16	GCTGTAATTCAGCTAATATCAATGATCTTG	TGCTACTCTTATGCACACTATTCTGAAA	Yes
HSAP0406S00016016	AF370371	17	TTGTTCTGTTGGTGCCATGAG	TCATGTCTGGAGGCTGAGGTT	Yes
HSAP0406S00009756	AK124770	18	AGAAGGATAGAAATTGGGTTTGTAGAAT	AAAACTGCGGGCTCTGACA	Yes
HSAP0406S00004567	NM_138938	19	TAGCTCCTCCCTGGGTCTCA	ACCATATCCCACCAGAGAGGTAAG	Yes
HSAP0406S00011489	NM_000410	20	TCCCCTCCCAACTGCTAATG	CCTAACCCCAGACACACTGATTT	Yes
p21cip1	NM_078467	n/a	AGCCTCCCTCCATCCCTATG	TTCTATGCCAGAGCTCAACATGTT	Yes
TK1	NM_003258	n/a	AGTCCCTCCCTGCAATCCA	TGGGTTTCCCAAGCAAGGT	Yes

Table 3-12. Primer sequences for qChIP verification, Continued
For verification in Table 3-5.

NimbleGen Seq ID	Gene Acession ID	Forward	Reverse
HSAP0406S00013662	NM_021223	CAGGGCCCAGCCTCCTT	TCCTCTCCTTATTTGGACCTTCAG
HSAP0406S00031561	NM_005583	TGCCACCCACTTGTGATACTCA	GCTCTTGCAGTTGCCCAGAT
HSAP0406S00025741	AB032525	CGAGGCATGGACCTGAAAAC	TCTTCCTTGGATTCCCTATTGC
HSAP0406S00022455	AK094261	GGCTACTGCTGCTTCAAGACAGT	TCACCAGCGCTCCTGACA
HSAP0406S00034475	NM_058186	ACTGTTCTGGAGGAAGCAAAGAA	CAAGTTCGCCGTCCATGTC
HSAP0406S00016860	NM_006378	AGACCTGCCCCAGGAAGTG	TTTATTGTCCTTTCAGGACACCAA
HSAP0406S00023356	AK127211	ACTTCTCCCCCTTCCAGAACTC	GTCGCCGTAGCAGGTCAGA
HSAP0406S00006063	NM_024080	GAAAGTTGCCCACTGACAATTG	TGTCCCCTTTAAACTACACTTTGGA
HSAP0406S00019480	NM_053017	CGTCAGAGGTCATGGGAGAAG	CTCTGGCTGCTAGGAAGCTCTT

3.7 References

1. Harms, K., Nozell, S., and Chen, X. (2004) The common and distinct target genes of the p53 family transcription factors. *Cell Mol Life Sci* 61, 822-842

2. Donehower, L. A., Harvey, M., Slagle, B. L., McArthur, M. J., Montgomery, C. A., Jr., Butel, J. S., and Bradley, A. (1992) Mice deficient for p53 are developmentally normal but susceptible to spontaneous tumours. *Nature* 356, 215-221

3. Yang, A., Schweitzer, R., Sun, D., Kaghad, M., Walker, N., Bronson, R. T., Tabin, C., Sharpe, A., Caput, D., Crum, C., and McKeon, F. (1999) p63 is essential for regenerative proliferation in limb, craniofacial and epithelial development. *Nature* 398, 714-718

4. Yang, A., Walker, N., Bronson, R., Kaghad, M., Oosterwegel, M., Bonnin, J., Vagner, C., Bonnet, H., Dikkes, P., Sharpe, A., McKeon, F., and Caput, D. (2000) p73-deficient mice have neurological, pheromonal and inflammatory defects but lack spontaneous tumours. *Nature* 404, 99-103

5. Flores, E. R., Sengupta, S., Miller, J. B., Newman, J. J., Bronson, R., Crowley, D., Yang, A., McKeon, F., and Jacks, T. (2005) Tumor predisposition in mice mutant for p63 and p73: evidence for broader tumor suppressor functions for the p53 family. *Cancer Cell* 7, 363-373

6. Fontemaggi, G., Kela, I., Amariglio, N., Rechavi, G., Krishnamurthy, J., Strano, S., Sacchi, A., Givol, D., and Blandino, G. (2002) Identification of direct p73 target genes combining DNA microarray and chromatin immunoprecipitation analyses. *J Biol Chem* 277, 43359-43368

7. Kim, T. H., and Ren, B. (2006) Genome-Wide Analysis of Protein-DNA Interactions. *Annu Rev Genomics Hum Genet* 7, 81-102

8. Cawley, S., Bekiranov, S., Ng, H. H., Kapranov, P., Sekinger, E. A., Kampa, D., Piccolboni, A., Sementchenko, V., Cheng, J., Williams, A. J., Wheeler, R., Wong, B., Drenkow, J., Yamanaka, M., Patel, S., Brubaker, S., Tammana, H., Helt, G., Struhl, K., and Gingeras, T. R. (2004) Unbiased mapping of transcription factor binding sites along human chromosomes 21 and 22 points to widespread regulation of noncoding RNAs. *Cell* 116, 499-509

9. Wei, C. L., Wu, Q., Vega, V. B., Chiu, K. P., Ng, P., Zhang, T., Shahab, A., Yong, H. C., Fu, Y., Weng, Z., Liu, J., Zhao, X. D., Chew, J. L., Lee, Y. L., Kuznetsov, V. A., Sung, W. K., Miller, L. D., Lim, B., Liu, E. T., Yu, Q., Ng, H. H., and Ruan, Y. (2006) A global map of p53 transcription-factor binding sites in the human genome. *Cell* 124, 207-219

10. Yang, A., Zhu, Z., Kapranov, P., McKeon, F., Church, G. M., Gingeras, T. R., and Struhl, K. (2006) Relationships between p63 binding, DNA sequence, transcription activity, and biological function in human cells. *Mol Cell* 24, 593-602

11. Shang, Y., Hu, X., DiRenzo, J., Lazar, M. A., and Brown, M. (2000) Cofactor dynamics and sufficiency in estrogen receptor-regulated transcription. *Cell* 103, 843-852

12. Ren, B., Cam, H., Takahashi, Y., Volkert, T., Terragni, J., Young, R. A., and Dynlacht, B. D. (2002) E2F integrates cell cycle progression with DNA repair, replication, and G(2)/M checkpoints. *Genes Dev* 16, 245-256

13. Johnson, W. E., Li, W., Meyer, C. A., Gottardo, R., Carroll, J. S., Brown, M., and Liu, X. S. (2006) Model-based analysis of tiling-arrays for ChIP-chip. *Proc Natl Acad Sci U S A* 103, 12457-12462

14. Vlieghe, D., Sandelin, A., De Bleser, P. J., Vleminckx, K., Wasserman, W. W., van Roy, F., and Lenhard, B. (2006) A new generation of JASPAR, the open-access repository for transcription factor binding site profiles. *Nucleic Acids Res* 34, D95-97

15. Chau, B. N., Chen, T. T., Wan, Y. Y., DeGregori, J., and Wang, J. Y. (2004) Tumor necrosis factor alpha-induced apoptosis requires p73 and c-ABL activation downstream of RB degradation. *Mol Cell Biol* 24, 4438-4447

16. Smyth, G. K. (2004) Linear models and empirical bayes methods for assessing differential expression in microarray experiments. *Stat Appl Genet Mol Biol* 3, Article3

17. Barrera, L. O., and Ren, B. (2006) The transcriptional regulatory code of eukaryotic cells--insights from genome-wide analysis of chromatin organization and transcription factor binding. *Curr Opin Cell Biol* 18, 291-298

18. Storey, J. D., and Tibshirani, R. (2003) Statistical significance for genomewide studies. *Proc Natl Acad Sci U S A* 100, 9440-9445

19. Flores, E. R., Tsai, K. Y., Crowley, D., Sengupta, S., Yang, A., McKeon, F., and Jacks, T. (2002) p63 and p73 are required for p53-dependent apoptosis in response to DNA damage. *Nature* 416, 560-564

20. Urist, M., and Prives, C. (2002) p53 leans on its siblings. *Cancer Cell* 1, 311-313

21. Gaiddon, C., Lokshin, M., Ahn, J., Zhang, T., and Prives, C. (2001) A subset of tumor-derived mutant forms of p53 down-regulate p63 and p73 through a direct interaction with the p53 core domain. *Mol Cell Biol* 21, 1874-1887

22. el-Deiry, W. S., Kern, S. E., Pietenpol, J. A., Kinzler, K. W., and Vogelstein, B. (1992) Definition of a consensus binding site for p53. *Nat Genet* 1, 45-49

23. Lokshin, M., Li, Y., Gaiddon, C., and Prives, C. (2007) p53 and p73 display common and distinct requirements for sequence specific binding to DNA. *Nucleic Acids Res* 35, 340-352

24. Mondal, N., and Parvin, J. D. (2005) The tumor suppressor protein p53 functions similarly to p63 and p73 in activating transcription in vitro. *Cancer Biol Ther* 4, 414-418

25. Frith, M. C., Hansen, U., and Weng, Z. (2001) Detection of cis-element clusters in higher eukaryotic DNA. *Bioinformatics* 17, 878-889

26. Bieda, M., Xu, X., Singer, M. A., Green, R., and Farnham, P. J. (2006) Unbiased location analysis of E2F1-binding sites suggests a widespread role for E2F1 in the human genome. *Genome Res* 16, 595-605

27. Martin, D. W., Munoz, R. M., Subler, M. A., and Deb, S. (1993) p53 binds to the TATA-binding protein-TATA complex. *J Biol Chem* 268, 13062-13067

28. Liu, J., Grogan, L., Nau, M. M., Allegra, C. J., Chu, E., and Wright, J. J. (2001) Physical interaction between p53 and primary response gene Egr-1. *Int J Oncol* 18, 863-870

29. Van Orden, K., Giebler, H. A., Lemasson, I., Gonzales, M., and Nyborg, J. K. (1999) Binding of p53 to the KIX domain of CREB binding protein. A potential link to human T-cell leukemia virus, type I-associated leukemogenesis. *J Biol Chem* 274, 26321-26328

30. Koutsodontis, G., Tentes, I., Papakosta, P., Moustakas, A., and Kardassis, D. (2001) Sp1 plays a critical role in the transcriptional activation of the human cyclin-dependent kinase inhibitor p21(WAF1/Cip1) gene by the p53 tumor suppressor protein. *J Biol Chem* 276, 29116-29125

31. Thornborrow, E. C., and Manfredi, J. J. (2001) The tumor suppressor protein p53 requires a cofactor to activate transcriptionally the human BAX promoter. *J Biol Chem* 276, 15598-15608

32. Innocente, S. A., and Lee, J. M. (2005) p53 is a NF-Y- and p21-independent, Sp1-dependent repressor of cyclin B1 transcription. *FEBS Lett* 579, 1001-1007

33. Hearnes, J. M., Mays, D. J., Schavolt, K. L., Tang, L., Jiang, X., and Pietenpol, J. A. (2005) Chromatin immunoprecipitation-based screen to identify functional genomic binding sites for sequence-specific transactivators. *Mol Cell Biol* 25, 10148-10158

34. Jen, K. Y., and Cheung, V. G. (2005) Identification of novel p53 target genes in ionizing radiation response. *Cancer Res* 65, 7666-7673

35. Vigano, M. A., Lamartine, J., Testoni, B., Merico, D., Alotto, D., Castagnoli, C., Robert, A., Candi, E., Melino, G., Gidrol, X., and Mantovani, R. (2006) New p63 targets in keratinocytes identified by a genome-wide approach. *Embo J* 25, 5105-5116

36. Lokshin, M., Li, Y., Gaiddon, C., and Prives, C. (2006) p53 and p73 display common and distinct requirements for sequence specific binding to DNA. *Nucleic Acids Res*

37. Krieg, A. J., Hammond, E. M., and Giaccia, A. J. (2006) Functional analysis of p53 binding under differential stresses. *Mol Cell Biol* 26, 7030-7045

38. Lin, C. Y., Vega, V. B., Thomsen, J. S., Zhang, T., Kong, S. L., Xie, M., Chiu, K. P., Lipovich, L., Barnett, D. H., Stossi, F., Yeo, A., George, J., Kuznetsov,

V. A., Lee, Y. K., Charn, T. H., Palanisamy, N., Miller, L. D., Cheung, E., Katzenellenbogen, B. S., Ruan, Y., Bourque, G., Wei, C. L., and Liu, E. T. (2007) Whole-Genome Cartography of Estrogen Receptor alpha Binding Sites. *PLoS Genet* 3, e87

39. Euskirchen, G. M., Rozowsky, J. S., Wei, C. L., Lee, W. H., Zhang, Z. D., Hartman, S., Emanuelsson, O., Stolc, V., Weissman, S., Gerstein, M. B., Ruan, Y., and Snyder, M. (2007) Mapping of transcription factor binding regions in mammalian cells by ChIP: comparison of array- and sequencing-based technologies. *Genome Res* 17, 898-909

40. Kitayner, M., Rozenberg, H., Kessler, N., Rabinovich, D., Shaulov, L., Haran, T. E., and Shakked, Z. (2006) Structural basis of DNA recognition by p53 tetramers. *Mol Cell* 22, 741-753

41. Cho, Y., Gorina, S., Jeffrey, P. D., and Pavletich, N. P. (1994) Crystal structure of a p53 tumor suppressor-DNA complex: understanding tumorigenic mutations. *Science* 265, 346-355

42. McLure, K. G., and Lee, P. W. (1998) How p53 binds DNA as a tetramer. *Embo J* 17, 3342-3350

43. Jackson, P., Mastrangelo, I., Reed, M., Tegtmeyer, P., Yardley, G., and Barrett, J. (1998) Synergistic transcriptional activation of the MCK promoter by p53: tetramers link separated DNA response elements by DNA looping. *Oncogene* 16, 283-292

44. Carroll, J. S., Liu, X. S., Brodsky, A. S., Li, W., Meyer, C. A., Szary, A. J., Eeckhoute, J., Shao, W., Hestermann, E. V., Geistlinger, T. R., Fox, E. A., Silver, P. A., and Brown, M. (2005) Chromosome-wide mapping of estrogen receptor binding reveals long-range regulation requiring the forkhead protein FoxA1. *Cell* 122, 33-43

45. Kirmizis, A., Bartley, S. M., Kuzmichev, A., Margueron, R., Reinberg, D., Green, R., and Farnham, P. J. (2004) Silencing of human polycomb target genes is associated with methylation of histone H3 Lys 27. *Genes Dev* 18, 1592-1605

46. Gatz, S. A., and Wiesmuller, L. (2006) p53 in recombination and repair. *Cell Death Differ* 13, 1003-1016

47. Davison, T. S., Vagner, C., Kaghad, M., Ayed, A., Caput, D., and Arrowsmith, C. H. (1999) p73 and p63 are homotetramers capable of weak heterotypic interactions with each other but not with p53. *J Biol Chem* 274, 18709-18714

48. Geisberg, J. V., and Struhl, K. (2004) Quantitative sequential chromatin immunoprecipitation, a method for analyzing co-occupancy of proteins at genomic regions in vivo. *Nucleic Acids Res* 32, e151

49. Vikhanskaya, F., D'Incalci, M., and Broggini, M. (2000) p73 competes with p53 and attenuates its response in a human ovarian cancer cell line. *Nucleic Acids Res* 28, 513-519

50. Talos, F., Nemajerova, A., Flores, E. R., Petrenko, O., and Moll, U. M. (2007) p73 suppresses polyploidy and aneuploidy in the absence of functional p53. *Mol Cell* 27, 647-659

51. Osada, M., Park, H. L., Nagakawa, Y., Yamashita, K., Fomenkov, A., Kim, M. S., Wu, G., Nomoto, S., Trink, B., and Sidransky, D. (2005) Differential recognition of response elements determines target gene specificity for p53 and p63. *Mol Cell Biol* 25, 6077-6089

52. Beima, K. M., Miazgowicz, M. M., Lewis, M. D., Yan, P. S., Huang, T. H., and Weinmann, A. S. (2006) T-bet binding to newly identified target gene promoters is cell type-independent but results in variable context-dependent functional effects. *J Biol Chem* 281, 11992-12000

Chapter 4:
Conclusions and Future Perspectives

The work described in chapter 2 and 3 of this dissertation presents the first direct comparison of p53 and p73 promoter occupancy profiles in a human colon cancer cell line by combining chromatin immunoprecipitation with promoter arrays, or ChIP-chip. This final chapter touches upon some of the unresolved issues in the biological functions of the p53 family as well as some technical issues that need to be considered when interpreting ChIP-chip data.

4.1 Unsolved mystery in the functions of the p53 family

Our results confirm the genetic data and in vitro data that the p53 family members have both overlapping and differential functions in terms of DNA binding and target selection. One of the long-standing questions in the p53 field that remains to be addressed in the future is how p63 and p73 modulate promoter choice by p53 in governing life and death decisions (i.e. choice between activation of pro-apoptotic genes versus cell-cycles arrest genes).

The tumors suppressor gene p53 is known to elicit both apoptotic death and cell cycle arrest in response to cellular stress through its ability to recognize and bind specific DNA sequences and to recruit both general and specialized transcriptional co-regulators. Multiple interactions with co-activators and co-repressors as well as with the components of the general transcriptional machinery allow p53 to activate/repress specific sets of genes. In addition, a growing number of proteins that act as transcriptional cofactors by selectively stabilization the interaction of p53 and or its family members with specific promoters have been identified (1-3). A recent study by Tanaka et al. have shown that target gene selectivity of p53 is also likely to be orchestrated at the level of gene-specific chromatin modifications (4). Using a multifaceted experimental approach that couples

ChIP with size-fractionation by sucrose gradient ultracentrifugation and mass spectrometry, they identified hCAS/CSE1L, as a component of p53 transcriptional complexes on the chromatin of promoters of several proapoptotic genes. It has also been shown that p63 and/or p73 are constitutively associated with apoptotic promoters, and are required for recruitment of p53 to those sites in response to stress in a cell-context dependent manner (5). Consistent with this finding, our study showed that p53 and p73 bind to the same genomic region. Nevertheless, the mechanism for the requirement of p63/p73 in the recruitment of p53 to apoptotic promoters remains to be elucidated. It would be of interest to determine if there is any connection between hCAS/CSE1L and p63/p73 in the regulation of p53-dependent apoptotic response.

Our study suggests that p53 and p73 exhibit both common and differential promoter occupancy profiles, both at steady state and following HU treatment. It appears that the difference in target selection can be explained at the DNA level. There are several reports showing that promoter topology contributes to differential target selection. For example, the arrangement of the decamers is important for the differential regulation of IGFBP3 by the p53 family(6). Moreover, the spacing between the decamers may also influence the choice between apoptosis and cell-cycle arrest genes. Cell cycle arrest genes do not contain interspersed sequences between the two decamers whereas proapoptotic genes do (7). One might speculate that p53 family members might have different requirements for the spacer sequences.

The differential promoter occupancy profiles between p53 and p73 may also be accounted by the fact that p53/p73 have differential affinities toward different p53REs, which may also affect promoter specificity. High affinity sites are generally associated

with growth arrest-related genes while low affinity sites are found in proapoptotic genes (8). Differential activation of p53 target genes may also be attributed to the nucleosome occupancy states. p53 can bind to promoters with constitutively open chromatin state (such as GADD45 or mdm2) with higher affinity. Therefore, p53-interacting proteins that can affect the level or covalent modification of p53, which in turn can influence the DNA binding affinity, can have a profound effect on its promoter selectivity. *In vitro* studies have shown that the DNA binding domain of p53 exhibits similar sequence preference as that of p73β(9). The binding site preference for p63 remains controversial, with at least three studies reporting different consensus motifs. Osada et al. (10) reported that p63 has higher specificity for the core sequence CGTG than CATG. Similar to the findings from Osada et al (10), Perez et al (11) reported that p63 and p53 display a different nucleotide preference for the fifth and sixteenth position of the core sequence and a different nucleotide bias at the tenth and eleventh position. In contrast, Sinha et al. (12) concluded that similar to p53, the optimal p63 DNA-binding motif contains a half-site with central core sequence CATG, but differs by having AT-rich 5' and 3' flanking sequences. In the p63 ChIP-chip study by Yang et al (13), two direct repeats resembling the p53 consensus sequence but of slight different sequence composition were identified as p63 consensus sequence. Due the degenerate nature of the consensus sequence for p53, further biochemical studies need to be followed up to address whether sequence discrimination can contribute to target gene selection for all three p53 family members.

4.2 ChIP-chip and future challenge

ChIP-chip has become a powerful tool to study protein-DNA interactions in many fundamental biological processes in mammalian cells, including transcription factor

binding dynamics (13-15), general transcription (16), chromatin structure and histone modifications(17-19), and more recently, nucleosome occupancy (20).

In chapter 2 and 3 of this dissertation, I have discussed two ChIP-chip studies carried out via different microarray platforms aimed to understand the interactions of p53 and p73 with promoters in a human colon cancer cell line. Due to the complexity and background noise in the ChIP-chip experiments, much effort has been devoted to develop computational methods to extract useful information in order to identify true binding events. The basis of these model-based algorithms is to identify binding sites by modeling key aspects of ChIP-chip experiments. Although several model-based algorithms have been successfully applied on ChIP-chip to identify ChIP-enriched sites with high accuracy, such as Mpeak (16), MAT (21), and JBD (22), and MAP (described in chapter 3 of this dissertation), improvements in ChIP-chip data analysis along with other experimental issues remain to be considered when performing ChIP-chip analysis.

There are fundamental issues involved in the data analysis part of ChIP-chip experiment, including background subtraction, probe standardization, and other statistical problems in handling large set of data points. Therefore, quality control tests must performed on the ChIP samples by checking the enrichment of known binding sites. Regardless, one challenge in the ChIP-chip data analysis is high background noise caused by experimental variation. There are several key steps in the ChIP-chip procedure during which variation may arise: The time of duration for formaldehyde crosslinking, random nature of chromatin shearing, non-specific binding during the immunoprecipitation step, intrinsic noise from microarray synthesis and hybridization, and bias introduced in DNA amplification and labeling. Current amplification protocols, which include linear

amplification (23), whole-genome amplification(24), and ligation-mediated PCR (LM-PCR)(25) may generate some degree of variation in ChIP-chip experiments. In addition, constraints on probe design in certain genomic regions (i.e. repetitive sequences) remains an intrinsic limitation for ChIP-chip studies. The emergence of cost-effective sequencing technologies can remedy some of these issues arise from using ChIP-chip (26).

There are several different mechanisms by which a factor can be recruited to the DNA and be identified in a ChIP–chip experiment. Three possible scenarios for the interactions between a transcription factor and its binding site on DNA: (I) direct binding of a transcription factor to its consensus site; (II) Indirect binding via protein–protein interactions with a protein that directly interacts with the DNA; (III) A transcription factor directly binds to a low affinity binding site on DNA but specificity is achieved via cooperative interaction with another nearby factor bound to a specific motif. Integration of computational and bioinformatic tools with ChIP-chip would be required to identify combinatorial transcriptional interactions and to construct gene regulatory networks (27).

Other than overcoming technical issues mentioned above, there are also experimental issues that need to be addressed, such as fixation, antibody specificity and epitope accessibility, and microarray design and coverage. Among many, one major limiting step in the ChIP-chip procedure is the poor cross-linking efficiency of formaldehyde. Typically, only ~1-2% crosslinking efficiency is achieved by formaldehyde, thus a large amount of input material is required for ChIP experiments. A modified crosslinking procedure such as the combined use of a protein-protein crosslinking reagent (i.e. dimethyl adipimidate) in addition to formaldehyde has been proposed to improve the crosslinking efficiency in ChIP experiments (28). Another issue

worth noting is the targets identified from ChIP-chip can result from both direct and indirect binding since it is unclear whether the majority of the crosslinks formed by formaldehyde are protein-protein or protein-DNA. The efficiency of crosslinking of proteins to their sites of DNA interaction also varies from protein to protein (29).

ChIP-based technology requires a highly specific antibody against the protein of interest, which is often a liming factor since not all antibodies can recognize the epitope in the context of crosslinked-chromatin. As an alternative to ChIP-chip, technology such as DamID (30) has been developed to get around the use of antibody to identify sites of DNA interaction. Here, a transcription factor of interest is fused to DNA adenine methyltransferase (Dam). When this fusion protein is expressed *in vivo*, Dam will be targeted to the native binding sites of its fusion partner and it will mark the position of DNA-protein interactions by methylating adenines in DNA in the immediate vicinity of the binding sites. To identify these sites, the methylated regions are purified or selectively amplified from genomic DNA, fluorescently labeled and hybridized to a microarray (Figure 1-3). However, DamID is not suitable for detection of post-translational modifications, such as histone modifications. Although side-by-side comparisons have revealed that the two methods can yield very similar results, the resolution of DamID is less precise than of ChIP-chip (31).

In conclusion, ChIP-chip integrated with other genomics analyses, such as gene expression analysis and DNase hypersensitive site (HS) mapping (32), can be further expanded to other aspects of biology to greatly enhance our understanding in the molecular basis of human diseases in the future.

4.3 References

1. Sullivan, A., and Lu, X. (2007) ASPP: a new family of oncogenes and tumour suppressor genes. *Br J Cancer* 96, 196-200

2. Brown, L., Boswell, S., Raj, L., and Lee, S. W. (2007) Transcriptional targets of p53 that regulate cellular proliferation. *Crit Rev Eukaryot Gene Expr* 17, 73-85

3. Strano, S., Monti, O., Pediconi, N., Baccarini, A., Fontemaggi, G., Lapi, E., Mantovani, F., Damalas, A., Citro, G., Sacchi, A., Del Sal, G., Levrero, M., and Blandino, G. (2005) The transcriptional coactivator Yes-associated protein drives p73 gene-target specificity in response to DNA Damage. *Mol Cell* 18, 447-459

4. Tanaka, T., Ohkubo, S., Tatsuno, I., and Prives, C. (2007) hCAS/CSE1L Associates with Chromatin and Regulates Expression of Select p53 Target Genes. *Cell* 130, 638-650

5. Flores, E. R., Tsai, K. Y., Crowley, D., Sengupta, S., Yang, A., McKeon, F., and Jacks, T. (2002) p63 and p73 are required for p53-dependent apoptosis in response to DNA damage. *Nature* 416, 560-564

6. Harms, K. L., and Chen, X. (2005) The C terminus of p53 family proteins is a cell fate determinant. *Mol Cell Biol* 25, 2014-2030

7. Qian, H., Wang, T., Naumovski, L., Lopez, C. D., and Brachmann, R. K. (2002) Groups of p53 target genes involved in specific p53 downstream effects cluster into different classes of DNA binding sites. *Oncogene* 21, 7901-7911

8. Inga, A., Storici, F., Darden, T. A., and Resnick, M. A. (2002) Differential transactivation by the p53 transcription factor is highly dependent on p53 level and promoter target sequence. *Mol Cell Biol* 22, 8612-8625

9. Lokshin, M., Li, Y., Gaiddon, C., and Prives, C. (2007) p53 and p73 display common and distinct requirements for sequence specific binding to DNA. *Nucleic Acids Res* 35, 340-352

10. Osada, M., Park, H. L., Nagakawa, Y., Yamashita, K., Fomenkov, A., Kim, M. S., Wu, G., Nomoto, S., Trink, B., and Sidransky, D. (2005) Differential recognition of response elements determines target gene specificity for p53 and p63. *Mol Cell Biol* 25, 6077-6089

11. Perez, C. A., Ott, J., Mays, D. J., and Pietenpol, J. A. (2007) p63 consensus DNA-binding site: identification, analysis and application into a p63MH algorithm. *Oncogene*

12. Ortt, K., and Sinha, S. (2006) Derivation of the consensus DNA-binding sequence for p63 reveals unique requirements that are distinct from p53. *FEBS Lett* 580, 4544-4550

13. Yang, A., Zhu, Z., Kapranov, P., McKeon, F., Church, G. M., Gingeras, T. R., and Struhl, K. (2006) Relationships between p63 binding, DNA sequence, transcription activity, and biological function in human cells. *Mol Cell* 24, 593-602

14. Bieda, M., Xu, X., Singer, M. A., Green, R., and Farnham, P. J. (2006) Unbiased location analysis of E2F1-binding sites suggests a widespread role for E2F1 in the human genome. *Genome Res* 16, 595-605

15. Boyer, L. A., Lee, T. I., Cole, M. F., Johnstone, S. E., Levine, S. S., Zucker, J. P., Guenther, M. G., Kumar, R. M., Murray, H. L., Jenner, R. G., Gifford, D. K., Melton, D. A., Jaenisch, R., and Young, R. A. (2005) Core transcriptional regulatory circuitry in human embryonic stem cells. *Cell* 122, 947-956

16. Kim, T. H., Barrera, L. O., Zheng, M., Qu, C., Singer, M. A., Richmond, T. A., Wu, Y., Green, R. D., and Ren, B. (2005) A high-resolution map of active promoters in the human genome. *Nature* 436, 876-880

17. Garcia-Bassets, I., Kwon, Y. S., Telese, F., Prefontaine, G. G., Hutt, K. R., Cheng, C. S., Ju, B. G., Ohgi, K. A., Wang, J., Escoubet-Lozach, L., Rose, D. W., Glass, C. K., Fu, X. D., and Rosenfeld, M. G. (2007) Histone methylation-dependent mechanisms impose ligand dependency for gene activation by nuclear receptors. *Cell* 128, 505-518

18. Heintzman, N. D., Stuart, R. K., Hon, G., Fu, Y., Ching, C. W., Hawkins, R. D., Barrera, L. O., Van Calcar, S., Qu, C., Ching, K. A., Wang, W., Weng, Z., Green, R. D., Crawford, G. E., and Ren, B. (2007) Distinct and predictive chromatin signatures of transcriptional promoters and enhancers in the human genome. *Nat Genet* 39, 311-318

19. Bernstein, B. E., Kamal, M., Lindblad-Toh, K., Bekiranov, S., Bailey, D. K., Huebert, D. J., McMahon, S., Karlsson, E. K., Kulbokas, E. J., 3rd, Gingeras, T. R., Schreiber, S. L., and Lander, E. S. (2005) Genomic maps and comparative analysis of histone modifications in human and mouse. *Cell* 120, 169-181

20. Peckham, H. E., Thurman, R. E., Fu, Y., Stamatoyannopoulos, J. A., Noble, W. S., Struhl, K., and Weng, Z. (2007) Nucleosome positioning signals in genomic DNA. *Genome Res* 17, 1170-1177

21. Johnson, W. E., Li, W., Meyer, C. A., Gottardo, R., Carroll, J. S., Brown, M., and Liu, X. S. (2006) Model-based analysis of tiling-arrays for ChIP-chip. *Proc Natl Acad Sci U S A* 103, 12457-12462

22. Qi, Y., Rolfe, A., MacIsaac, K. D., Gerber, G. K., Pokholok, D., Zeitlinger, J., Danford, T., Dowell, R. D., Fraenkel, E., Jaakkola, T. S., Young, R. A., and Gifford, D. K. (2006) High-resolution computational models of genome binding events. *Nat Biotechnol* 24, 963-970

23. Liu, C. L., Schreiber, S. L., and Bernstein, B. E. (2003) Development and validation of a T7 based linear amplification for genomic DNA. *BMC Genomics* 4, 19

24. O'Geen, H., Nicolet, C. M., Blahnik, K., Green, R., and Farnham, P. J. (2006) Comparison of sample preparation methods for ChIP-chip assays. *Biotechniques* 41, 577-580

25. Ren, B., and Dynlacht, B. D. (2004) Use of chromatin immunoprecipitation assays in genome-wide location analysis of mammalian transcription factors. *Methods Enzymol* 376, 304-315

26. Margulies, M., Egholm, M., Altman, W. E., Attiya, S., Bader, J. S., Bemben, L. A., Berka, J., Braverman, M. S., Chen, Y. J., Chen, Z., Dewell, S. B., Du, L., Fierro, J. M., Gomes, X. V., Godwin, B. C., He, W., Helgesen, S., Ho, C. H., Irzyk, G. P., Jando, S. C., Alenquer, M. L., Jarvie, T. P., Jirage, K. B., Kim, J. B., Knight, J. R., Lanza, J. R., Leamon, J. H., Lefkowitz, S. M., Lei, M., Li, J., Lohman, K. L., Lu, H., Makhijani, V. B., McDade, K. E., McKenna, M. P., Myers, E. W., Nickerson, E., Nobile, J. R., Plant, R., Puc, B. P., Ronan, M. T., Roth, G. T., Sarkis, G. J., Simons, J. F., Simpson, J. W., Srinivasan, M., Tartaro, K. R., Tomasz, A., Vogt, K. A., Volkmer, G. A., Wang, S. H., Wang, Y., Weiner, M. P., Yu, P., Begley, R. F., and Rothberg, J. M. (2005) Genome sequencing in microfabricated high-density picolitre reactors. *Nature* 437, 376-380

27. Kato, M., Hata, N., Banerjee, N., Futcher, B., and Zhang, M. Q. (2004) Identifying combinatorial regulation of transcription factors and binding motifs. *Genome Biol* 5, R56

28. Kurdistani, S. K., Tavazoie, S., and Grunstein, M. (2004) Mapping global histone acetylation patterns to gene expression. *Cell* 117, 721-733

29. Solomon, M. J., and Varshavsky, A. (1985) Formaldehyde-mediated DNA-protein crosslinking: a probe for in vivo chromatin structures. *Proc Natl Acad Sci U S A* 82, 6470-6474

30. van Steensel, B., and Henikoff, S. (2000) Identification of in vivo DNA targets of chromatin proteins using tethered dam methyltransferase. *Nat Biotechnol* 18, 424-428

31. Holland, S., Ioannou, D., Haines, S., and Brown, W. R. (2005) Comparison of Dam tagging and chromatin immunoprecipitation as tools for the identification of the binding sites for S. pombe CENP-C. *Chromosome Res* 13, 73-83

32. Xi, H., Shulha, H. P., Lin, J. M., Vales, T. R., Fu, Y., Bodine, D. M., McKay, R. D., Chenoweth, J. G., Tesar, P. J., Furey, T. S., Ren, B., Weng, Z., and Crawford, G. E. (2007) Identification and Characterization of Cell Type-Specific and Ubiquitous Chromatin Regulatory Structures in the Human Genome. *PLoS Genet* 3, e136